Eur. Phys. J. C (2026) 86:483
https://doi.org/10.1140/epjc/s10052-025-15264-w

THE EUROPEAN PHYSICAL JOURNAL C

Regular Article - Experimental Physics

Measurement of the W-boson angular coefficients and transverse momentum in pp collisions at $\sqrt{s} = 13$ TeV with the ATLAS detector

ATLAS Collaboration[⋆]

CERN, 1211 Geneva 23, Switzerland

Received: 18 September 2025 / Accepted: 27 December 2025

Abstract The angular distributions of Drell–Yan lepton pairs provide sensitive probes of the underlying dynamics of quantum chromodynamics (QCD) effects in vector-boson production. This paper presents for the first time the measurement of the full set of angular coefficients together with the differential cross-section as a function of the transverse momentum of the W boson, in the full phase space of the decay leptons. The measurements are performed separately for the W^- and W^+ channels. The analysis uses proton–proton collision data recorded by the ATLAS experiment at the Large Hadron Collider in 2017 and 2018, during special low-luminosity runs with a reduced number of interactions per bunch crossings (pile-up). The data correspond to an integrated luminosity of 338 pb^{-1} at a centre-of-mass energy of $\sqrt{s} = 13$ TeV. The low pile-up environment provides excellent experimental conditions for high-precision measurements of W-boson production. All results agree with theoretical predictions incorporating finite-order QCD corrections up to order α_S^2.

Contents

⋆ e-mail: atlas.publications@cern.ch

1 Introduction and motivation

The angular distributions of lepton pairs produced in hadron collisions via the Drell–Yan process are governed by the spin correlation effects between the initial-state partons and the final-state leptons, mediated by a spin-1 intermediate state, such as in the case of the process $p_1 + p_2 \to W \to \ell\nu$, where p_1 and p_2, are the incoming partons [1,2]. These spin correlations are described by a set of nine helicity density matrix elements, which can be calculated within the context of the parton model using perturbative quantum chromodynamics (QCD). The full differential cross-section describing the kinematics of the two leptons arising from the decay of a W boson can be decomposed as a sum of harmonic polynomials, which depend on the lepton polar and azimuthal angles, denoted by θ and ϕ, multiplied by the corresponding helicity-dependent cross-sections which depend on the W-boson transverse momentum, p_{T}^W, invariant mass, m^W, and rapidity, y^W. It is a standard convention to factorise out the unpolarised cross-section, denoted by σ^{U+L}, and to present this differential cross-section as an expansion into the nine harmonic polynomials and eight dimensionless angular coefficients A_i [3–5], which represent ratios of helicity cross-sections relative to the unpolarised one, σ^{U+L}.

All eight Z-boson angular coefficients were measured at a centre-of-mass energy of $\sqrt{s} = 8$ TeV by the ATLAS Collaboration as a function of both the Z-boson transverse momentum, p_{T}^Z, and rapidity, y^Z, using $Z \to \ell\ell$ events, where $\ell = \{e, \mu\}$ [6,7]. Other measurements of the Z-boson angular coefficients were also extracted as a function of p_{T}^Z from $Z \to \mu\mu$ events by the LHCb Collaboration [8] and the CMS Collaboration [9], resulting in the extraction of four and five of the eight coefficients, respectively. Prior to these

Published online: 06 May 2026

measurements at the Large Hadron Collider (LHC) [10], four of the eight coefficients as a function of p_{T}^{Z} were measured by the CDF Collaboration at the Tevatron from $Z \to ee$ events [11].

Direct measurements of only two of these angular coefficients for the W boson have previously been performed. The A_2 and A_3 angular coefficients were extracted as a function of p_{T}^{W} by the CDF Collaboration from $W \to \ell\nu$ events, where $\ell = \{e, \mu\}$ [12]. However, other measurements of the W-boson polarisation were previously done by the ATLAS Collaboration [13] and by the CMS Collaboration [14,15]. These polarisation fraction measurements are related to the A_0 and A_4 coefficients and so can be used to probe their values.

The angular coefficients of the W boson are related to the nature of electroweak processes, the W-boson polarisation, and the presence of QCD effects. They are important for modelling QCD effects in the production of W bosons and have a direct impact on the precision of other measurements, such as the determination of the W-boson mass [16]. Currently, the validation of the modelling of these coefficients for the W-mass measurements at the LHC relies on extrapolations from the predictions and measurements of the angular coefficients of the Zboson, thereby contributing to larger uncertainties [17–19]. Precise determinations of the W-boson transverse momentum spectrum and its angular coefficients offer direct experimental insights into the proton structure and parton density and consequently to the production dynamics of the W and enable stringent comparisons with state-of-the-art QCD predictions. This model-independent approach exploits the spin-one nature of the gauge boson and the spin-1/2 nature of the decay leptons, constrained by angular momentum conservation. This method bypasses the need for detailed modelling of the gauge-boson polarisation and decay, and instead isolates the production dynamics. Consequently, it mitigates theory uncertainties associated with spin correlations and the resummation of fiducial power corrections, which can be sizeable [20–23].

This paper presents, for the first time, simultaneous measurements of the full set of W-boson angular coefficients A_i and the differential cross-section $\frac{d\sigma}{dp_T}$ as functions of p_{T}^{W}, performed in the full phase space of the decay leptons using $W^{\pm} \to \ell^{\pm}\nu$ events, where $\ell = \{e, \mu\}$. This represents a complementary approach to previous precise measurements of W-boson differential cross-section [24,25], which were limited to the fiducial phase space. The measurements are based on dedicated proton-proton (pp) collision data samples collected by the ATLAS experiment at the LHC with low instantaneous luminosity at a centre-of-mass energy of $\sqrt{s} = 13\,\mathrm{TeV}$, corresponding to $338\,\mathrm{pb}^{-1}$ of integrated luminosity. The mean number of additional pp interactions per bunch crossing (pile-up events) in the dataset is approximately two. This low pile-up dataset provides excellent experimental conditions for high-precision measurements of W-boson production.

While this analysis is based on the same dataset and systematic uncertainty evaluations as in Refs. [24,25], the use of differential angular distributions introduces additional sensitivity to certain experimental systematic effects. Notably, these angular observables are not directly involved in the detector calibration procedures, thereby providing complementary and independent constraints.

The structure of the paper is as follows: Sect. 2 details the ATLAS detector and Sect. 3 describes the methodology used to extract the angular coefficients and the differential cross-section in the full phase space of the decay leptons. Section 4 outlines the experimental set-up, including the dataset, event selection, and background estimate. The impact of systematic uncertainties in the final results is discussed in Sect. 5. Finally, the results are presented in Sect. 6.

2 ATLAS detector

The ATLAS experiment [26] at the LHC is a multipurpose particle detector with a forward–backward symmetric cylindrical geometry and a near 4π coverage in solid angle.[1] It consists of an inner tracking detector surrounded by a thin superconducting solenoid providing a 2T axial magnetic field, electromagnetic and hadronic calorimeters, and a muon spectrometer. The inner tracking detector covers the pseudorapidity range $|\eta| < 2.5$. It consists of silicon pixel, silicon microstrip, and transition radiation tracking detectors. Lead/liquid-argon (LAr) sampling calorimeters provide electromagnetic (EM) energy measurements with high granularity within the region $|\eta| < 3.2$. A steel/scintillator-tile hadronic calorimeter covers the central pseudorapidity range ($|\eta| < 1.7$). The endcap and forward regions are instrumented with LAr calorimeters for EM and hadronic energy measurements up to $|\eta| = 4.9$. The muon spectrometer surrounds the calorimeters and is based on three large superconducting air-core toroidal magnets with eight coils each. The field integral of the toroids ranges between 2.0 and 6.0 T m across most of the detector. The muon spectrometer includes a system of precision tracking chambers up to $|\eta| = 2.7$ and fast detectors for triggering up to $|\eta| = 2.4$. The luminosity is measured mainly by the LUCID–2 [27] detector, which

[1] ATLAS uses a right-handed coordinate system with its origin at the nominal interaction point (IP) in the centre of the detector and the z-axis along the beam pipe. The x-axis points from the IP to the centre of the LHC ring, and the y-axis points upwards. Polar coordinates (r, ϕ) are used in the transverse plane, ϕ being the azimuthal angle around the z-axis. The pseudorapidity is defined in terms of the polar angle θ as $\eta = -\ln\tan(\theta/2)$ and is equal to the rapidity $y = \frac{1}{2}\ln\left(\frac{E+p_z}{E-p_z}\right)$ in the relativistic limit. Angular distance is measured in units of $\Delta R \equiv \sqrt{(\Delta y)^2 + (\Delta\phi)^2}$.

is located close to the beampipe. A two-level trigger system is used to select events [28]. The first-level trigger is implemented in hardware and uses a subset of the detector information to accept events at a rate close to 100 kHz. This is followed by a software-based trigger that reduces the accepted rate of complete events to 1.25 kHz on average depending on the data-taking conditions. A software suite [29] is used in data simulation, in the reconstruction and analysis of real and simulated data, in detector operations, and in the trigger and data acquisition systems of the experiment.

3 Measurement methodology

This methodology used for this analysis relies on the same formalism already developed and published for the ATLAS extraction of the Z-boson angular coefficients and full phase-space cross-section [7]. The full five-dimensional differential cross-section describing the kinematics of the two Born-level leptons from the W-boson decay can be decomposed as:

$$\begin{aligned}\frac{\mathrm{d}\sigma}{\mathrm{d}p_{\mathrm{T}}^{W}\,\mathrm{d}y^{W}\,\mathrm{d}m^{W}\,\mathrm{d}\cos\theta\,\mathrm{d}\phi} &= \frac{3}{16\pi}\frac{\mathrm{d}\sigma^{U+L}}{\mathrm{d}p_{\mathrm{T}}^{W}\,\mathrm{d}y^{W}\,\mathrm{d}m^{W}} \\ &\Big\{(1+\cos^2\theta)+\frac{1}{2}A_0(1-3\cos^2\theta)+A_1\ \sin 2\theta\ \cos\phi \\ &+\frac{1}{2}A_2\ \sin^2\theta\ \cos 2\phi+A_3\ \sin\theta\ \cos\phi+A_4\ \cos\theta \\ &+A_5\ \sin^2\theta\ \sin 2\phi+A_6\ \sin 2\theta\ \sin\phi+A_7\ \sin\theta\ \sin\phi\Big\}. \quad (1)\end{aligned}$$

The dependence of the differential cross-section on the lepton angular $\cos\theta$ and ϕ distributions in the Collins–Soper (CS) frame [1] is analytical and fully contained in the nine harmonic polynomials $P_i(\cos\theta,\phi)$ given in the equation. On the other hand, the dependence on p_{T}^{W}, y^{W} and m^{W} is entirely contained in the unpolarised cross-section, σ^{U+L}, and in the A_{0-7} angular coefficients. Therefore, all hadronic dynamics from the production mechanism are factorised from the decay kinematics in the W-boson rest frame.

If the W boson is produced with no initial-state radiation, it is polarised along the beam axis, due to the vector minus axial vector, V-A, nature of the weak interaction and helicity conservation. In that case, A_4 is the only non-zero coefficient. If the W boson is produced with non-negligible transverse momentum balanced by the associated production of one or more jets, the A_{0-3} angular coefficients become non-zero and hence the cross-section depends on the azimuthal angle, ϕ, as well. The remaining three angular coefficients, A_{5-7}, are non-zero only if gluon loops of $\mathcal{O}(\alpha_s^2)$ are present in the production of the W boson.

The Lam-Tung relation [30–32], which predicts that $A_0 - A_2 = 0$ is a consequence of the spin-1 nature of the gluon, is expected to hold up to $\mathcal{O}(\alpha_s)$, but can be violated at higher orders. Such violations were experimentally confirmed in Z-boson events [6], while this has yet to be confirmed in W-boson events.

The W-boson kinematic dependence of the coefficients varies strongly with the choice of the spin quantisation axis in the W-boson rest frame (z-axis). In the CS reference frame adopted for this analysis, the z-axis is defined in the W-boson rest frame as the external bisector of the angle between the momenta of the two protons, as is described in more detail in Ref. [6]. The positive direction of the z-axis is defined by the direction of positive longitudinal W-boson momentum in the laboratory frame. At detector level, the directions of the leptons in the CS frame are defined by two angles, θ_{CS} and ϕ_{CS}. The angle θ_{CS} is defined as the angle between the momentum of the negatively charged lepton and the z-axis. In the case of W^+, there is no negatively charged lepton and instead the direction of the neutrino is used [3].

For the leptonic decay modes, W-bosons have the disadvantage relative to Z-bosons that the $\ell\nu$ decay kinematics cannot be completely reconstructed due to the inability to fully reconstruct the longitudinal momentum of the neutrino in a hadron collider. The neutrino transverse components p_x^{ν} and p_y^{ν} are determined from measurable laboratory-frame quantities, while the longitudinal component p_z^{ν} is determined only up to a sign. This twofold sign ambiguity in the reconstruction of the neutrino momentum in the CS frame translates into an ambiguity on the sign of $\cos\theta_{\mathrm{CS}}$, while ϕ_{CS} is determined. This effect dilutes the sensitivity of the measurement to the coefficients that directly depend on $\cos\theta_{\mathrm{CS}}$ namely A_0 and A_4.

3.1 Inferring the neutrino p_z^{ν} information

The unmeasured longitudinal momentum of the neutrino is inferred by assuming that the dilepton system from the Drell–Yan process has an invariant mass equal to the measured mass of the W boson [33]. In the laboratory frame, both the charged lepton and the neutrino are treated as massless particles. By imposing the m_W constraint and expressing the resulting condition in terms of the neutrino's unknown longitudinal component, a quadratic equation is obtained. Solving this equation yields two possible real solutions for the neutrino's longitudinal momentum, p_z^{ν}. For this analysis, one of the two solutions for the neutrino longitudinal momentum is chosen randomly, with equal probability. As an illustration, the resulting rapidity distributions obtained with this random choice are shown in Fig. 1 for the $W^- \to e^-\nu$ and $W^+ \to \mu^+\nu$ channels.

As mentioned already in Sect. 3, the z-axis of the CS frame is defined along the direction of the W-boson's longitudinal momentum, leading to the transformation $\cos\theta_{\mathrm{CS}} \to \cos\theta_{\mathrm{CS}} \times \mathrm{sign}(y^{\ell\nu})$, where $y^{\ell\nu}$ is the W-boson rapidity.

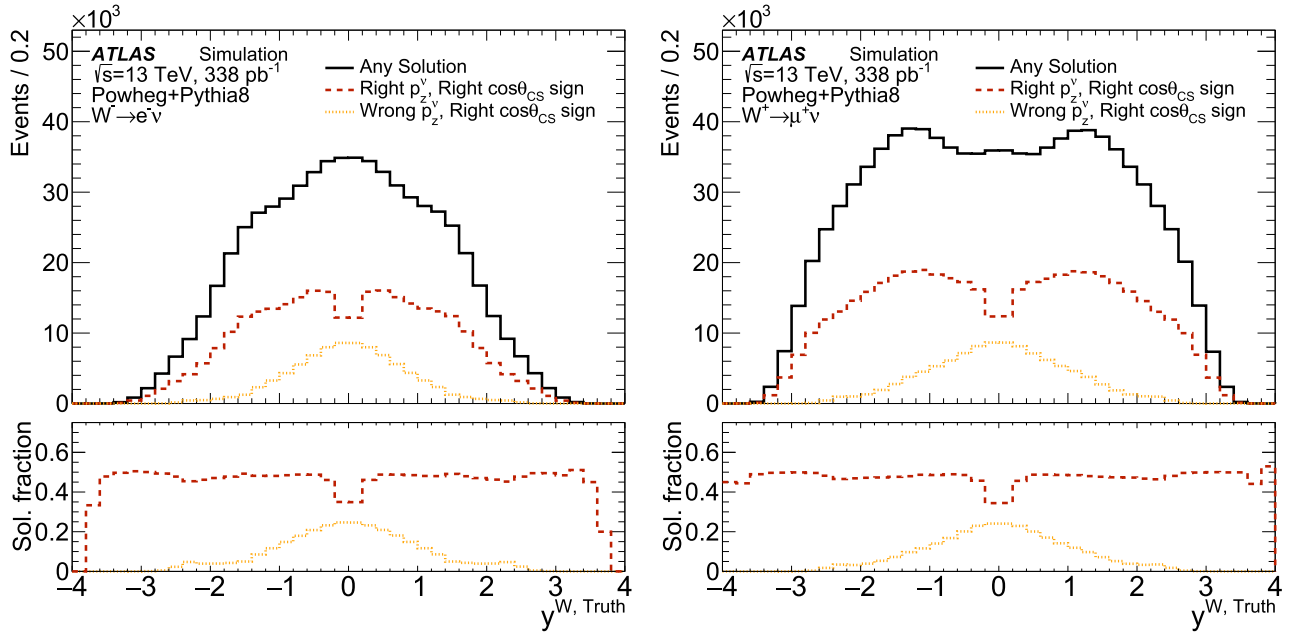

Fig. 1 W-boson rapidity distributions for events reconstructed with the correct or the wrong sign of $\cos\theta_{\mathrm{CS}}$ for the **a** $W^- \to e^-\nu$ and the **b** $W^+ \to \mu^+\nu$ channels. Events with the chosen solution closest to the true p_{z}^{ν} are labelled as *right* p_{z}^{ν}. Events with an unambiguous determination of $\cos\theta_{\mathrm{CS}}$ are labelled as *right* $\cos\theta_{\mathrm{CS}}$ sign. The differences between the electron and muon distributions reflect both the different efficiencies for reconstructing and selecting the two lepton flavours, and the intrinsic kinematic differences between W^- and W^+-boson events. The ratio panel shows the fraction of events with an unambiguous determination of $\cos\theta_{\mathrm{CS}}$ relative to all events with a real-valued solution for p_{z}^{ν}

Under this convention, events for which the two real p_{z}^{ν} solutions yield opposite signs for $y^{\ell\nu}$ correspond to cases where the ambiguity in the sign of $\cos\theta_{\mathrm{CS}}$ cancels, resulting in an unambiguous determination of $\cos\theta_{\mathrm{CS}}$. Nevertheless, an ambiguity in the sign of the W-boson rapidity remains. These events, which predominantly occur at central rapidities (see Fig. 1), allow for the resolution of the $\cos\theta_{\mathrm{CS}}$ sign ambiguity in an additional 25% of the dataset, enabling a direct measurement of the forward–backward asymmetry, associated with the A_4 coefficient, in W-boson production.

Events for which the quadratic equation yields no real solution are still included in the analysis. In these cases, the reconstructed neutrino kinematics are adjusted by applying a momentum imbalance constraint, which modifies the input to ensure a unique, real-valued solution. This approach follows a methodology similar to that described in Ref. [34]. The fraction of events with no real solution increases with the reconstructed transverse momentum of the W boson, $p_{\mathrm{T}}^{\ell\nu}$. It is approximately 15% at low $p_{\mathrm{T}}^{\ell\nu}$ and rises to around 60% for $p_{\mathrm{T}}^{\ell\nu}$ values exceeding 250 GeV. This behaviour is primarily driven by the limited resolution in the reconstruction of the neutrino transverse momentum at detector level, which degrades with increasing $p_{\mathrm{T}}^{\ell\nu}$.

3.2 Extraction of angular coefficients and differential cross-sections

The angular coefficients, A_i, and the differential cross-sections as a function of p_{T}^{W}, $\frac{d\sigma}{dp_T}$, are extracted from the data by performing a template fit to the polynomial terms $P_i(\cos\theta, \phi)$ defined in Eq. (1) to the two-dimensional reconstructed angular distributions, using a binning of 10×8 in the $(\cos\theta_{\mathrm{CS}}, \phi_{\mathrm{CS}})$ plane. This procedure is performed separately for W^- and W^+ candidates. The particle-level distributions are related to the reconstructed angular distributions using a folding procedure, which accounts for detector effects and bin migrations in the $(\cos\theta_{\mathrm{CS}}, \phi_{\mathrm{CS}})$ plane. Compared to the methodology employed in Refs. [6,7], the binning in $\cos\theta_{\mathrm{CS}}$ is modified to account for events without a real solution for p_{z}^{ν}. Events with a real solution, as described in Sect. 3.1, are assigned to one of eight same-size $\cos\theta_{\mathrm{CS}}$ bins, distributed over the range $[-1, 1]$, while events without a real solution are included as overflow in the tenth bin in $\cos\theta_{\mathrm{CS}}$. The ninth $\cos\theta_{\mathrm{CS}}$ bin serves as an empty separator. This approach ensures that events lacking a real p_{z}^{ν} solution contribute to the fit, thereby preserving sensitivity to the ϕ_{CS} distribution and avoiding distortions in the $\cos\theta_{\mathrm{CS}}$ shape.

Each template is normalised by a free parameter for its corresponding polynomial coefficient, A_{0-7}, and by a common parameter representing the unpolarised cross-section, σ^{U+L}. The polynomial $1+\cos^2\theta$ in Eq. (1) is normalised only by the parameter for the unpolarised cross-section. All of the angular coefficients together with the corresponding unpolarised cross-section parameters are measured in each of the analysis bins in the $p_{\mathrm{T}}^{\ell\nu}$ space. The binning in $p_{\mathrm{T}}^{\ell\nu}$ is chosen based on the experimental resolution at low $p_{\mathrm{T}}^{\ell\nu}$ and on the number of events at high $p_{\mathrm{T}}^{\ell\nu}$, and has the following boundaries:

$$p_{\mathrm{T}}^{\ell\nu} = [0, 8, 17, 27, 40, 55, 75, 110, 150, 210, 600]\ \mathrm{GeV}. \tag{2}$$

In the same way as described in Ref. [7], a likelihood is built as a product of Poisson probabilities across all the bins in the reconstructed $\cos\theta_{\mathrm{CS}}$, ϕ_{CS}, and $p_{\mathrm{T}}^{\ell\nu}$ distributions and of auxiliary constraints for each nuisance parameter. A profile likelihood ratio method is used to extract the best fit values of the parameters of interest (POIs) and their uncertainties. The POIs include the angular coefficients, A_{ij}, and the cross-sections, ${\sigma_j}^{U+L}$, in each j-th measurement bin defined in Eq. (2).

4 Analysis

The analysis is performed with leptonically decaying W-boson events, $W \to \ell\nu$, where here the charged lepton refers to electrons and muons, $\ell = e, \mu$. The analysis is carried out separately for positively and negatively charged leptons. The hadronic recoil, $\vec{u}_{\mathrm{T}}$, reconstructed in the plane transverse to the beam using charged-particle tracks and energy deposits is used to infer the transverse momentum of the decay neutrino, p_{T}^{ν}. The extraction of the angular coefficients and the differential cross-section as a function of the W-boson transverse momentum are first performed separately for the electron and muon channels. After confirming the compatibility of the results, the electron and muon channels are combined, taking into account correlations between systematic uncertainties.

In this analysis, the full set of angular coefficients is measured, along with the difference $A_0 - A_2$. Given the level of statistical precision provided by the data, only the coefficients A_0, A_2, A_3, and A_4 are measured to be significantly different from zero. The sensitivity to A_1, the higher-order coefficients A_{5-7}, and the difference $A_0 - A_2$ is limited. Nevertheless, these coefficients are included in the likelihood fit, and the results are reported.

4.1 Data and simulated-event samples

The data were collected by the ATLAS detector in 2017 and 2018 at a centre-of-mass energy of $\sqrt{s} = 13\,\mathrm{TeV}$, and correspond to a total integrated luminosity of $338.1 \pm 3.1\,\mathrm{pb}^{-1}$ [35]. These data were collected during dedicated LHC low pile-up runs, where the average number of additional pp interactions was approximately two, which is about a factor 20 smaller than that of the nominal LHC Run 2 13 TeV operation between 2015 and 2018. To fully exploit these low pile-up conditions, the thresholds applied to suppress noise in the reconstruction of clusters of energy in the calorimeters were lowered, thereby optimising the reconstruction of the hadronic recoil, as is discussed in Ref. [24].

Samples of Monte Carlo (MC) simulated events are used to model the signal and all background processes except for QCD multijet production. All of the samples were processed with the GEANT4-based simulation [36] of the ATLAS detector [37] using settings specific to the low pile-up run conditions. The effects of pile-up collisions in the same or neighbouring bunch crossings were included in the MC simulation by overlaying inelastic pp interactions produced using PYTHIA 8 [38] with the NNPDF2.3LO set of parton distribution functions (PDFs) [39] and the A3 set of parameters (tune) [40].

The main signal event samples for W-boson and for background Z-boson production were generated using the POWHEG event generator at next-to-leading-order (NLO) in QCD [41–44] using the CT10 PDFs [45], interfaced to PYTHIA 8 [46] using the AZNLO tune [47]. These POWHEG+PYTHIA 8 samples were interfaced to PHOTOS++ [48] to simulate the effect of final-state quantum electrodynamics (QED) radiation. The effective sample size is typically 10–20 times larger than the data, to minimise the impact of MC statistical uncertainties.

Alternative signal samples were prepared with SHERPA 2.2.1 [49] using the NNPDF3.0 next-to-next-to-leading-order (NNLO) PDFs [50] and merging matrix element calculations from COMIX [51] and OPENLOOPS [52–54] for vector-boson $V + 0, 1, 2$ partons at NLO accuracy with $V + 3, 4$ partons at leading-order (LO) accuracy in the MEPS@NLO scheme [55–59]. These samples are used to evaluate the uncertainty arising from the choice of the model used to simulate the signal events.

The W-boson samples were normalised to NNLO calculations using the DYTURBO [60–63] program with the MMHT2014 NNLO PDF set [64]. A total uncertainty of $\pm 5\%$ was taken on the predictions normalised using these cross-sections, and accounts for uncertainties in the choice of PDF set and corresponding variations ($3-4\%$), as well as variations in the value of the strong coupling constant α_S ($1-2\%$), and missing higher order corrections (1%).

Backgrounds arising from top-antitop-quark-pair ($t\bar{t}$) production as well as single-top-quark production (Wt associated production, t-channel and s-channel) were generated with POWHEG+PYTHIA 8 [65] and normalised to the NNLO predictions with resummation at next-to-next-to-leading-logarithmic (NNLL) accuracy [66–72]. Diboson production $VV(V = W, Z)$ was generated with SHERPA in all decay channels with at least one real lepton in the final state and is considered as background in this analysis [73].

In addition, two auxiliary MC samples are used to model backgrounds from non-prompt leptons. The first, generated with PYTHIA 8 and EVTGEN1.2.0 [74], simulates b- and c-hadron decays. The second models backgrounds to prompt photon and electron production and includes all tree-level $2 \to 2$ QCD processes, top-quark pair, and weak vector-boson production, generated with PYTHIA 8 using the A14 tune [75] and the NNPDF2.3LO PDF set [39].

4.2 Analysis overview and event selection

The data were collected with triggers that require at least one electron or one muon with transverse momentum $p_{\mathrm{T}}^{e} > 15\,\mathrm{GeV}$ or $p_{\mathrm{T}}^{\mu} > 14\,\mathrm{GeV}$, respectively [28,76,77]. Loose electron and muon identification criteria are applied at the trigger level. Events are selected if they include exactly one electron or muon candidate matched to a corresponding trigger-lepton candidate.

Events are also required to have at least one reconstructed collision vertex with two or more charged-particle tracks [78]. The vertex with the largest sum of squared transverse momenta of its associated tracks is taken as the primary vertex.

Electron candidates are reconstructed from clusters of energy deposited in the electromagnetic calorimeter and associated with at least one track in the inner detector [79]. Electron candidates are required to fall within the coverage of the inner detector and the precision region of the EM calorimeter, namely $|\eta| < 2.47$. Electrons in the transition region between the barrel and endcap calorimeters, $1.37 < |\eta| < 1.52$, are excluded. Electron candidates are required to have $p_{\mathrm{T}} > 25\,\mathrm{GeV}$ and satisfy the *Tight* likelihood identification requirements [79].

Muon reconstruction is first performed independently in the inner detector and in the muon spectrometer. A muon candidate is then formed using the combined information from both detectors [80]. The muon candidates are required to have an absolute pseudorapidity of $|\eta| < 2.4$, a transverse momentum of $p_{\mathrm{T}} > 25\,\mathrm{GeV}$, and to satisfy the *Medium* identification criteria [80].

Both electron and muon candidates are also required to be isolated from nearby activity, as measured by tracks in a cone of size $\Delta R < 0.2$ around the candidate lepton. The scalar sum of the p_{T} of these tracks, $p_{\mathrm{T}}^{\mathrm{cone20}}$, is required to be less than 10% of the lepton p_{T} and may not exceed 5 GeV for leptons with $p_{\mathrm{T}} > 50\,\mathrm{GeV}$, i.e. $p_{\mathrm{T}}^{\mathrm{cone20}}/\min(p_{\mathrm{T}}, 50\,\mathrm{GeV}) < 0.1$.

Dedicated lepton calibrations and efficiency corrections are applied to the reconstructed electron and muon candidates as described in Ref. [24].

The charged-lepton candidates are required to originate from the primary vertex. The track transverse impact parameter significance, $|d_0/\sigma_{d_0}|$, calculated relative to the beam line, must be smaller than three for muons and five for electrons. Furthermore, the longitudinal impact parameter, z_0, which is the difference between the z-coordinate of the point on the track at which d_0 is defined and the longitudinal position of the primary vertex, is required to satisfy $|z_0 \sin\theta| < 0.5$ mm.

The missing transverse momentum, $\vec{p}_{\mathrm{T}}^{\,\mathrm{miss}}$, with its magnitude $E_{\mathrm{T}}^{\mathrm{miss}}$, represents a measure of the transverse momentum of the neutrino. It is defined as $\vec{p}_{\mathrm{T}}^{\,\mathrm{miss}} = -(\vec{p}_{\mathrm{T}} + \vec{u}_{\mathrm{T}})$ using the lepton $\vec{p}_{\mathrm{T}}$ and hadronic recoil $\vec{u}_{\mathrm{T}}$. The hadronic recoil is reconstructed in the plane transverse to the beam using particle-flow objects (PFOs), that combine information from charged-particle tracks in the inner detector and energy deposits in the calorimeter [81,82]. The hadronic recoil is calibrated using $Z \to \ell\ell$ events by comparing u_{T} with $p_{\mathrm{T}}^{\ell\ell}$, the transverse momentum of the dilepton system [24]. The low pile-up datasets used in this analysis significantly improve the resolution of the recoil measurement and therefore the overall resolution of the detector-level measurement of the neutrino-related observables and the reconstructed p_{T}^{W}, referred to in the following as $p_{\mathrm{T}}^{\ell\nu}$.

The background from QCD multijet events is reduced by the requirement $E_{\mathrm{T}}^{\mathrm{miss}} > 25\,\mathrm{GeV}$. Furthermore, the W-boson transverse mass $m_{\mathrm{T}} = \sqrt{2 p_{\mathrm{T}} E_{\mathrm{T}}^{\mathrm{miss}} (1 - \cos\Delta\phi_{\ell\nu})}$ is required to exceed 50 GeV, where $\Delta\phi_{\ell\nu}$ is the azimuthal angle between the lepton $\vec{p}_{\mathrm{T}}$ and $\vec{p}_{\mathrm{T}}^{\,\mathrm{miss}}$.

After all selections, the numbers of $W \to e\nu$ and $W \to \mu\nu$ candidates used in this analysis are approximately 1.95×10^6 and 2.21×10^6, respectively.

In each of the analysis $p_{\mathrm{T}}^{\ell\nu}$ bins defined in Eq. (2), two-dimensional $(\cos\theta_{\mathrm{CS}}, \phi_{\mathrm{CS}})$ angular distributions are measured separately for positively and negatively charged leptons. Those two-dimensional distributions serve as the basis for the simultaneous extraction of all the angular coefficients and of the differential cross-sections, following the methodology described in Sect. 3.2.

4.3 Background estimates

Background contributions from electroweak processes such as single-boson (in this analysis, $W \to \tau\nu$ and Z-boson production $Z \to \tau\tau$ and $Z \to \ell\ell$ are treated as backgrounds) and diboson production, as well as background arising from

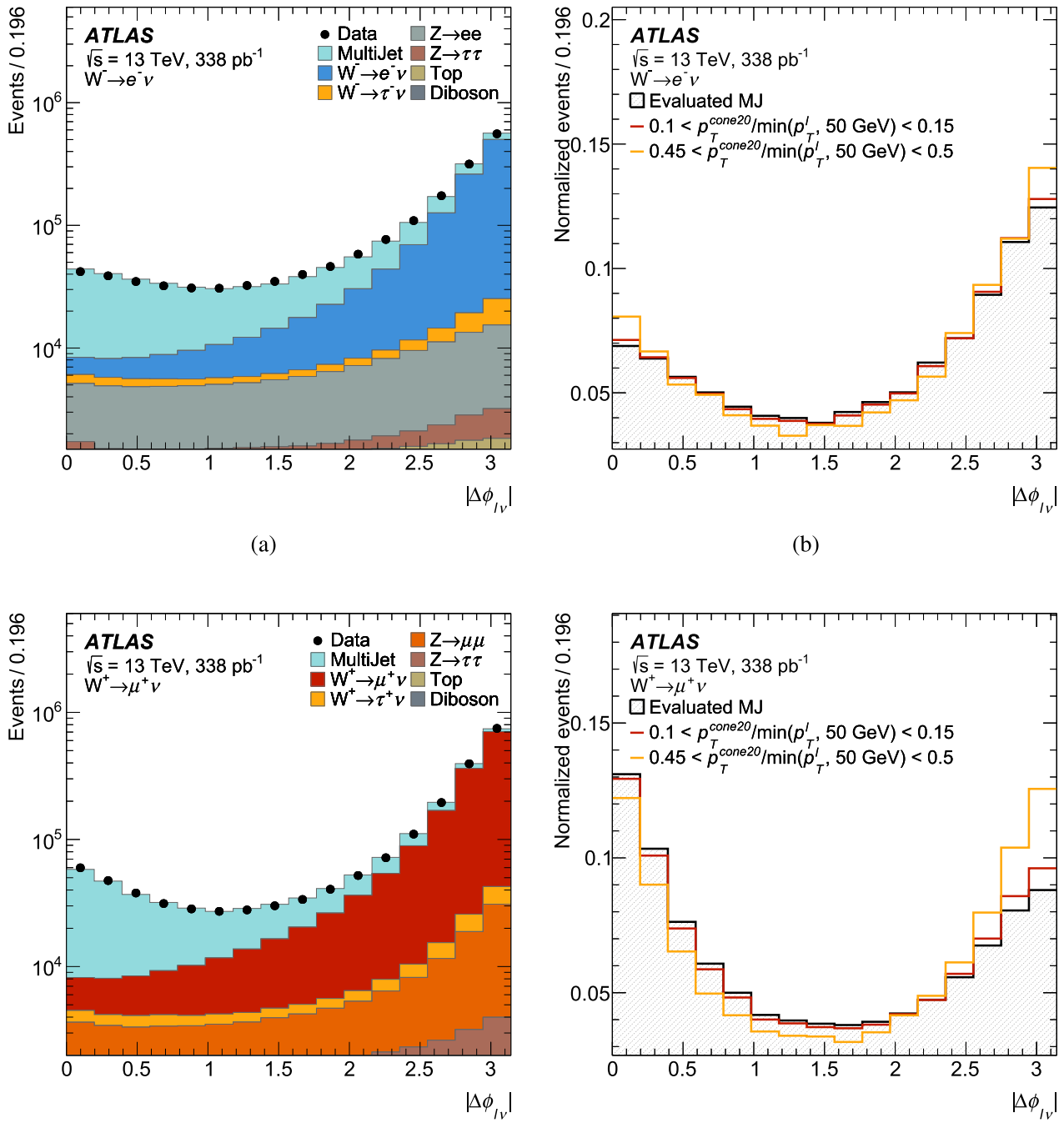

Fig. 2 $|\Delta\phi_{\ell\nu}|$ distribution in the fit region for data, multijet background and for signal and background from simulation in the **a** $W^- \to e^-\nu$ and **c** $W^+ \to \mu^+\nu$ channel. The multijet template shown in the plots is the one obtained from data in the first anti-isolation interval, as an example. Multijet templates for the $|\Delta\phi_{\ell\nu}|$ distribution in the signal region in the **b** $W^- \to e^-\nu$ and **d** $W^+ \to \mu^+\nu$ channel, derived from two anti-isolation intervals and compared with the final multijet template shown in black

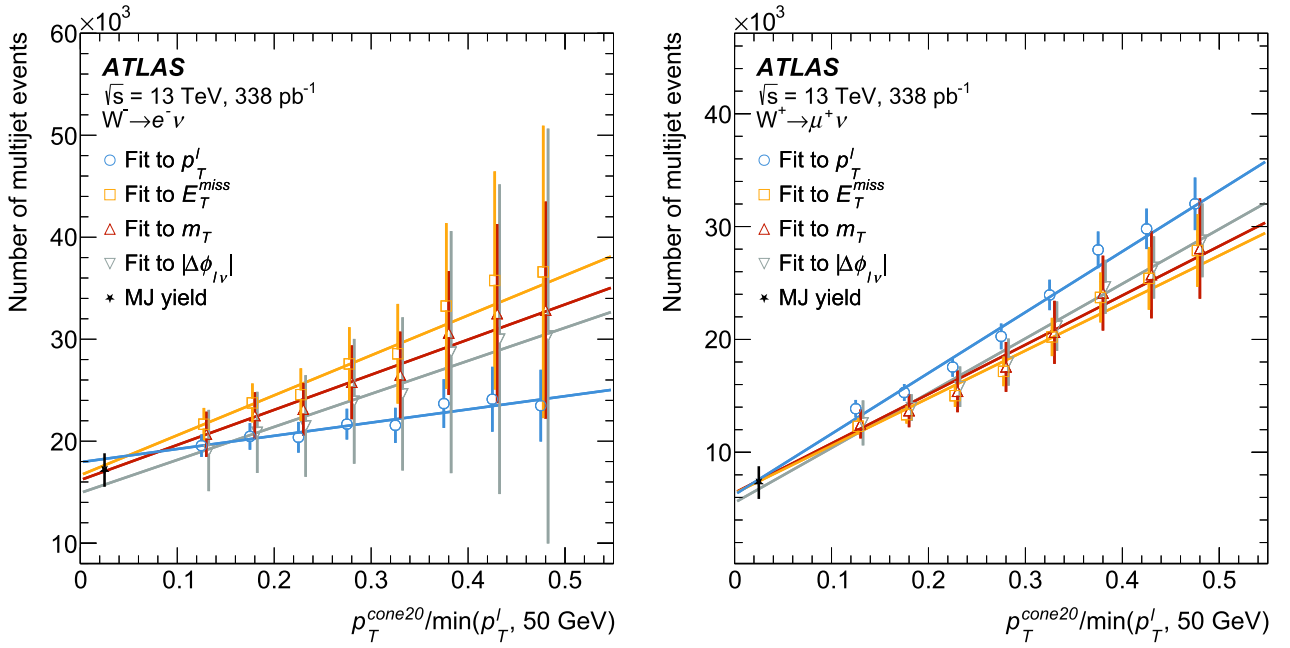

Fig. 3 Examples of multijet event yields extraction procedure from the template fit described in the text as a function of the different anti-isolation regions in $p_{\mathrm{T}}^{\mathrm{cone20}}/\min(p_{\mathrm{T}}, 50\,\mathrm{GeV})$ are shown for the **a** $W^- \to e^-\nu$ and the **b** $W^+ \to \mu^+\nu$ channels. The legend indicates each kinematic distributions used in the fit, as detailed in the text. The black vertical error bar on the extrapolated multijet yield in the isolated region represents the total uncertainty in the signal region

Table 1 Observed and expected event yields for candidate W^- and W^+ events in the electron and muon channels. The uncertainty in the expected event yields includes only the statistical uncertainty of the simulation, whereas the total uncertainty is given for the multijet background

Channel	$W^- \to e^-\nu$	$W^+ \to e^+\nu$	$W^- \to \mu^-\nu$	$W^+ \to \mu^+\nu$
$W \to e\nu$	802370 ± 260	1019420 ± 290	–	–
$W \to \mu\nu$	–	–	893900 ± 270	1153450 ± 310
$W \to \tau\nu$	14950 ± 110	18260 ± 130	14670 ± 110	18210 ± 130
$Z \to ee$	4953 ± 17	5227 ± 17	–	–
$Z \to \mu\mu$	–	–	33469 ± 42	37148 ± 44
$Z \to \tau\tau$	1106 ± 32	1183 ± 32	1705 ± 51	1663 ± 49
Top	11928 ± 47	12372 ± 49	11948 ± 47	12516 ± 49
Diboson	1581 ± 43	1605 ± 46	1617 ± 43	1718 ± 44
Multijet	17200 ± 1600	18600 ± 1900	6800 ± 1300	7400 ± 1400
Total expected	854000 ± 1700	1076600 ± 2000	964100 ± 1400	1232100 ± 1500
Data	857807	1093356	964514	1245755

processes involving the top-quark, such as $t\bar{t}$ and single-top-quark production, are directly estimated from the MC simulation samples described in Sect. 4.1.

The background from QCD multijet (MJ) production cannot be reliably simulated and so is derived from data. Depending on the lepton flavour, the MJ background has significant contributions from leptons produced in semileptonic decays of heavy quarks (beauty or charm), pion and kaon decays, and in the case of electron candidates photon conversions and hadronic activity faking a lepton.

The multijet yields are estimated following an approach similar to that described in Ref. [24], performed separately in the electron and muon channels, as well as for negatively and positively charged W-boson candidates. Differences relative the previous method are discussed below.

As multijet production mainly arises at lower values of p_{T}^{ℓ}, $E_{\mathrm{T}}^{\mathrm{miss}}$, and m_{T} as compared with the signal, this back-

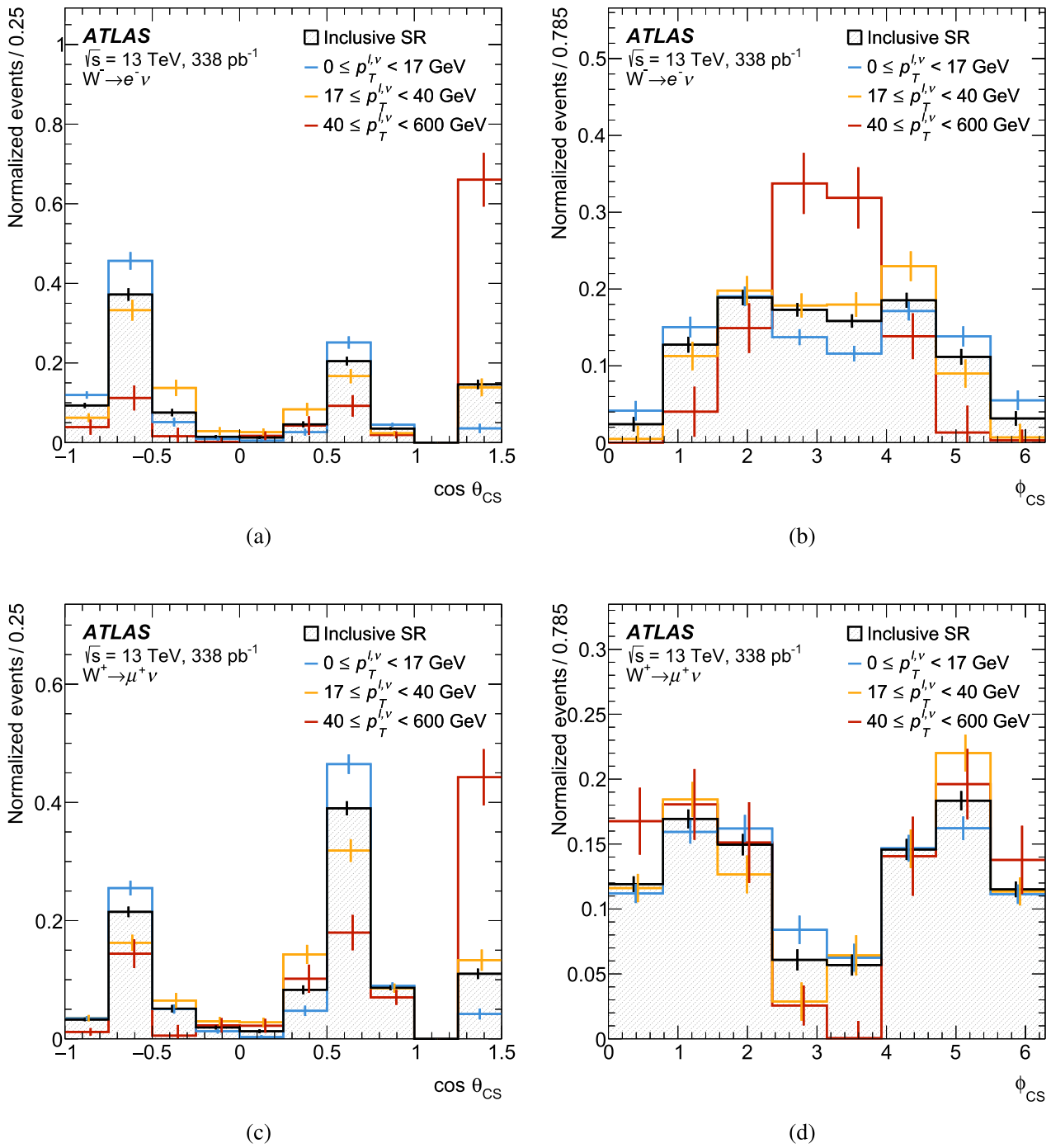

Fig. 4 Examples of one dimensional projections of the normalised angular distributions $\cos\theta_{\mathrm{CS}}$ and ϕ_{CS} of the multijet background for the **a**, **b** $W^- \to e^-\nu$ and **c**, **d** $W^+ \to \mu^+\nu$ channels extracted in the $p_{\mathrm{T}}^{\ell\nu}$-inclusive signal region (black curve) and in three broad $p_{\mathrm{T}}^{\ell\nu}$ intervals [0, 17) GeV, [17, 40) GeV, and [40, 600) GeV (coloured curves). As mentioned in Sect. 3.2, events without a real solution for p_{z}^{ν} are included as overflow in the tenth bin in $\cos\theta_{\mathrm{CS}}$

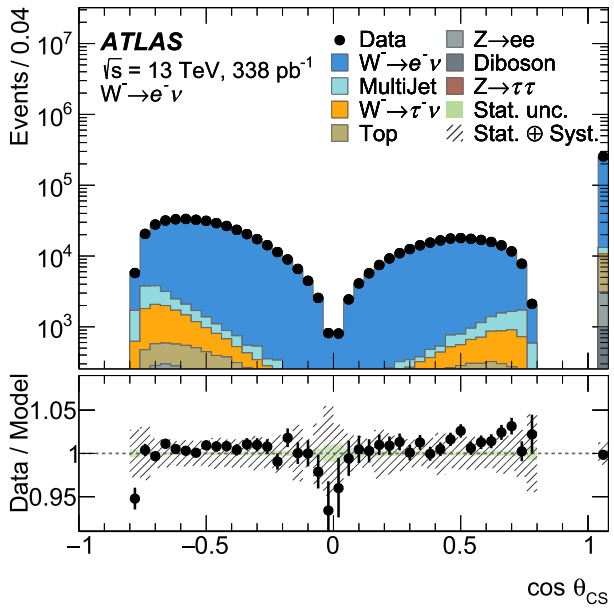

(a)

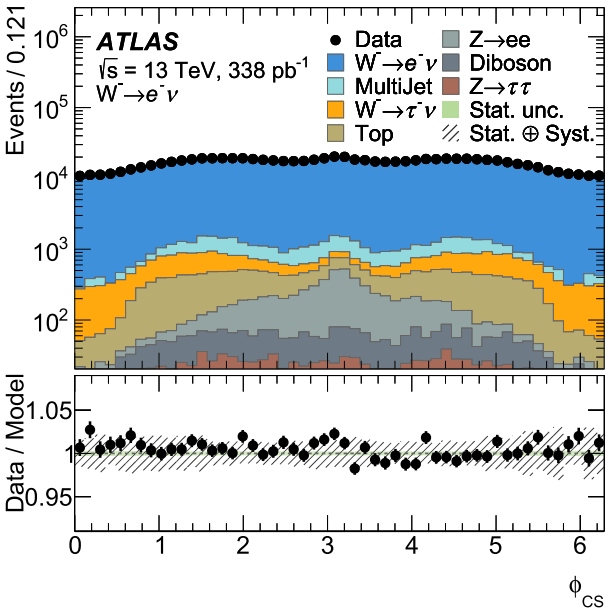

(b)

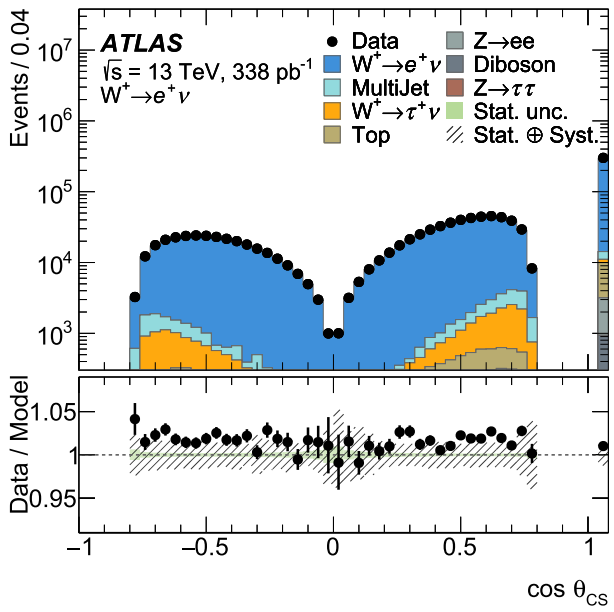

(c)

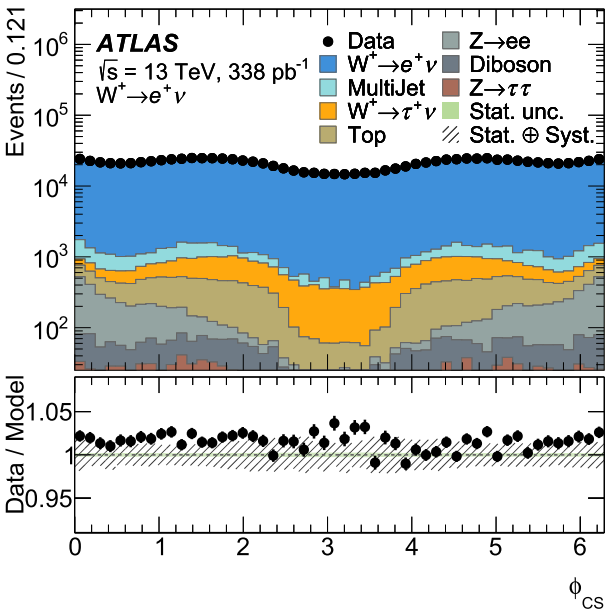

(d)

Fig. 5 The $\cos\theta_{\mathrm{CS}}$ and ϕ_{CS} angular distributions, integrated over $p_{\mathrm{T}}^{\ell\nu}$ for the $W \to e\nu$ channel for **a**, **b** negative and **c**, **d** positive leptons. The expected distributions are shown separately for the signal and the different background sources contributing to each channel. The grey band represents the total experimental uncertainties. Events without a real solution for p_z^{ν} are included as overflow bin in $\cos\theta_{\mathrm{CS}}$ distribution

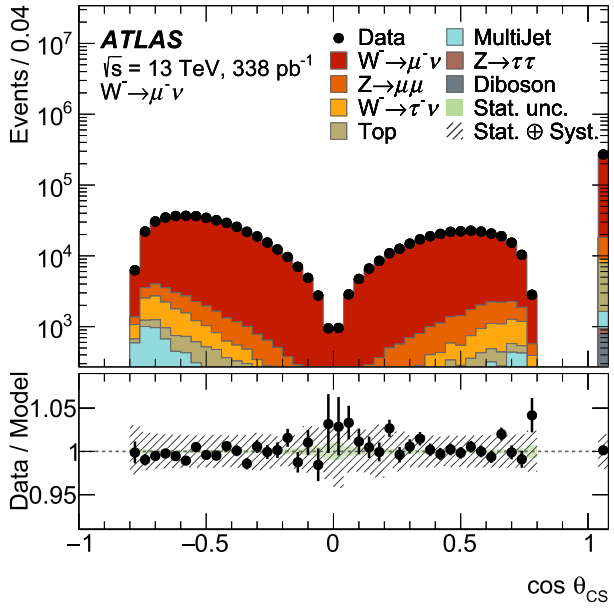

(a)

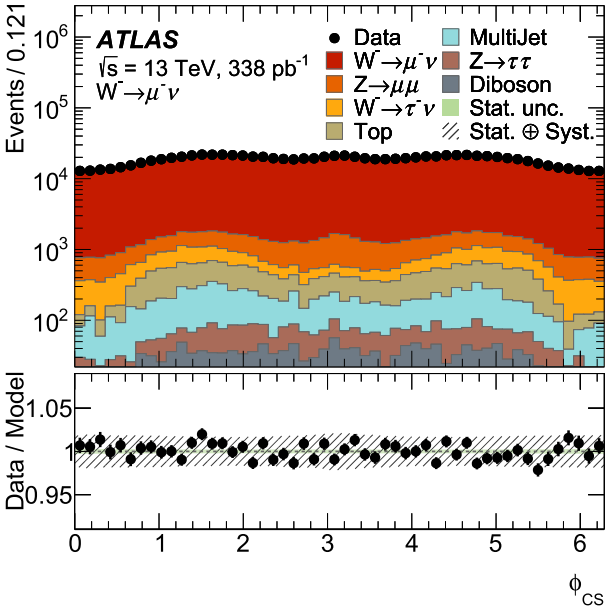

(b)

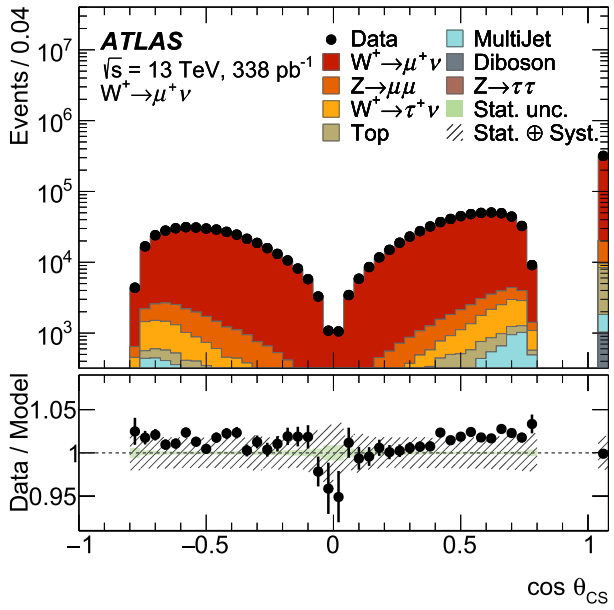

(c)

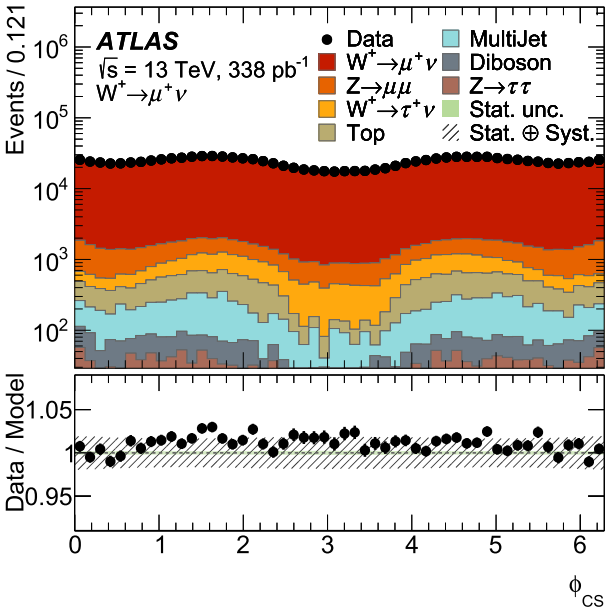

(d)

Fig. 6 The $\cos\theta_{CS}$ and ϕ_{CS} angular distributions, integrated over $p_T^{\ell\nu}$ for the $W \to \mu\nu$ channel for **a**, **b** negative and **c**, **d** positive leptons. The expected distributions are shown separately for the signal and the different background sources contributing to each channel. The grey band represents the total experimental uncertainties. Events without a real solution for p_z^{ν} are included as overflow bin in $\cos\theta_{CS}$ distribution

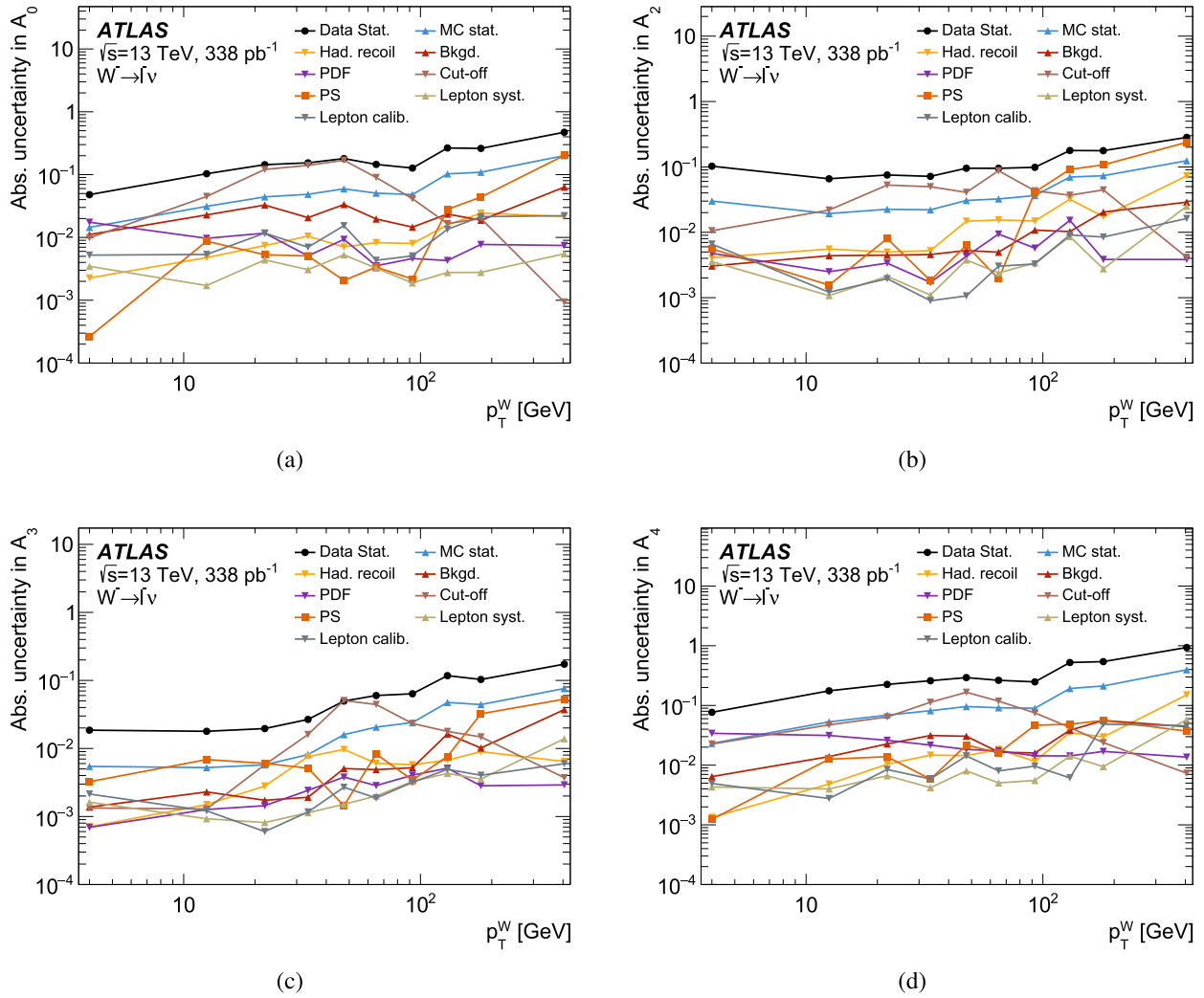

Fig. 7 The breakdown into statistical and systematic components of all the uncertainties for the measured **a** A_0, **b** A_2, **c** A_3 and **d** A_4 angular coefficients as a function of p_{T}^{W} in the $W^- \to \ell^- \nu$ channel, as obtained from the full fit. The values are given as absolute uncertainty

ground is estimated by using a template fit to these three kinematic distributions in the so-called fit region (FR), which is defined as the signal region with the $E_{\mathrm{T}}^{\mathrm{miss}}$ and m_{T} selections removed. As this analysis involves angular observables, the $|\Delta\phi_{\ell\nu}|$ variable is also included. As an example, the distribution of $|\Delta\phi_{\ell\nu}|$ in the fit region is shown in Fig. 2a for $W^- \to e^-\nu$ and in Fig. 2c for $W^+ \to \mu^+\nu$ events where the shape difference between signal and multijet background is clearly visible and exploited in the fit.

The multijet kinematic distributions used in the template fit are derived from data in anti-isolation regions (i.e. regions where the isolation requirement is inverted), after correcting for contamination from the $W \to \ell\nu$ signal and other non-multijet backgrounds using simulation. As shown in Fig. 2b, d, the shape of the multijet templates depends on the value of the isolation criterion. Mutually exclusive intervals in the isolation variable are defined to create statistically independent multijet templates that approach progressively to the signal-candidate selection. Following the procedure described in more detail in Ref. [24], the soft-energy activity in the anti-isolated regions is further corrected to reduce biases in the multijet kinematics arising from the dependence on the anti-isolation requirement.

For each kinematic distribution, the template fit in the fit region is repeated multiple times, each time using a different multijet template. Each multijet yield extracted in this way is then scaled by a transfer factor that corrects for the acceptance of the $E_{\mathrm{T}}^{\mathrm{miss}}$ and m_{T} selections in the signal region. As an example, Fig. 3 shows for the $W^- \to e^-\nu$ and $W^+ \to \mu^+\nu$ channels the variation of the extracted MJ yields as a function of the isolation interval used to define the template, together with a linear fit used to extrapolate to the average isolation value in the signal region. Alternative functional forms were tested for the extrapolation and found to

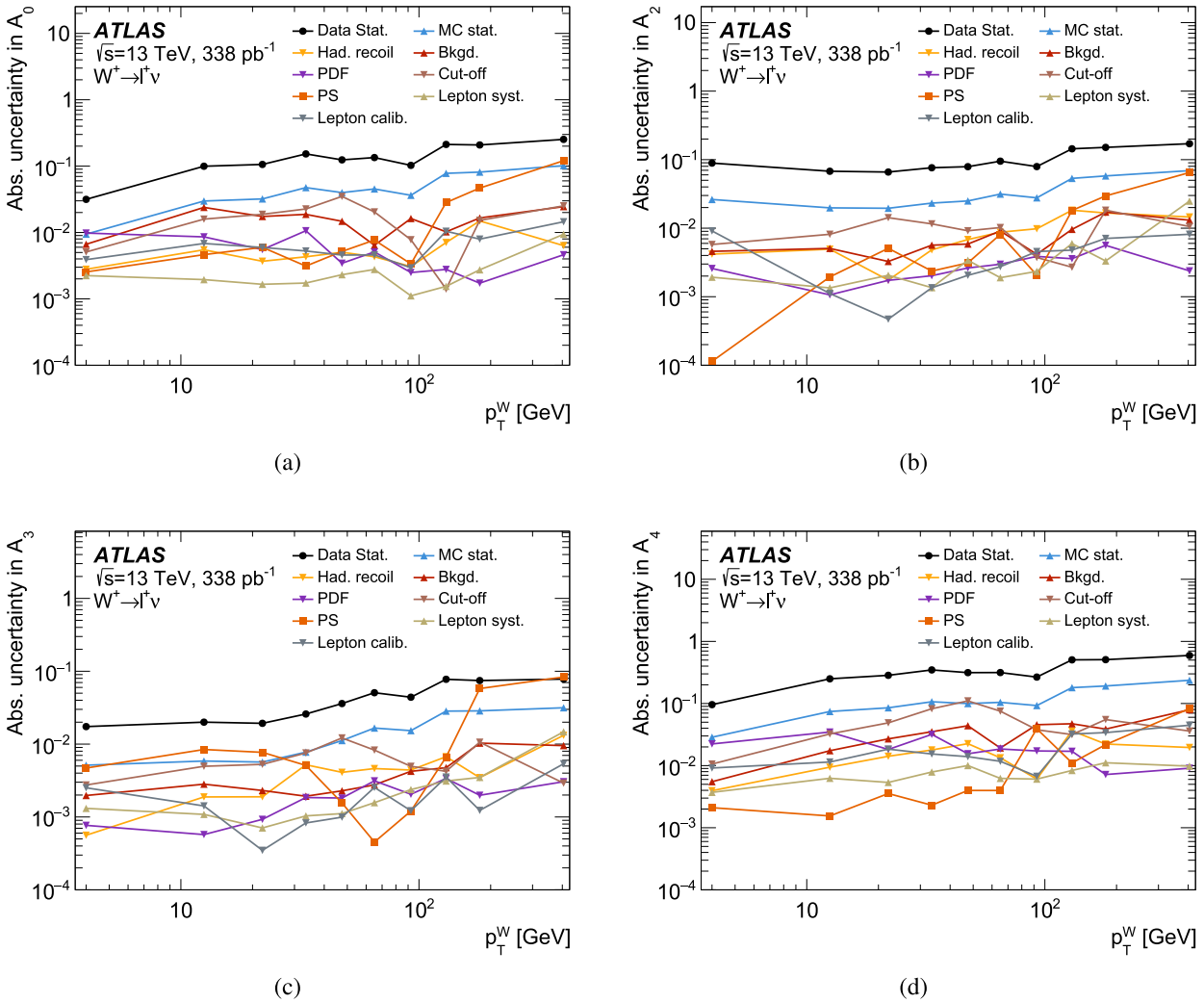

Fig. 8 The breakdown into statistical and systematic components of all the uncertainties for the measured **a** A_0, **b** A_2, **c** A_3 and **d** A_4 angular coefficients as a function of p_{T}^{W} in the $W^+ \to \ell^+\nu$ channel, as obtained from the full fit. The values are given as absolute uncertainty

give consistent results within the associated uncertainties in the yield. The final MJ yield is determined by averaging the extrapolated values from the four kinematic variables. The dominant uncertainties in this procedure arise from the linear extrapolation to the isolated region, the subtraction of signal and other backgrounds contamination in the anti-isolation regions, and the mismodelling of the soft energy activity in the anti-isolated regions. The final uncertainty in the MJ yield is about 10% in the electron channel and around 20% in the muon channel.

Similarly to the yield extraction, the shapes of the MJ kinematic distributions in the signal region are determined by linearly extrapolating the shapes observed in the mutually exclusive anti-isolation intervals into the isolated region, as illustrated by the black histograms in Fig. 2b, d. Additional corrections to the shapes of the angular distributions of the MJ background in the signal region are applied to account for the strong dependence of the two-dimensional ($\cos\theta_{\mathrm{CS}}$, ϕ_{CS}) distributions on $p_{\mathrm{T}}^{\ell\nu}$, as shown in Fig. 4. To derive these corrections, MJ background templates are constructed independently in three broad $p_{\mathrm{T}}^{\ell\nu}$ intervals: $p_{\mathrm{T}}^{\ell\nu} \in [0, 17)$ GeV, $[17, 40)$ GeV, and $[40, 600)$ GeV. Within each $p_{\mathrm{T}}^{\ell\nu}$ interval, acceptance corrections derived from MC simulation are applied to the MJ angular distributions to account for kinematic differences between the broad $p_{\mathrm{T}}^{\ell\nu}$ intervals used in the estimate and the finer binning defined in Eq. (2) for the final measurement. The dominant sources of uncertainty in the corrected multijet angular distributions arise from the limited data statistics in the anti-isolated regions of each $p_{\mathrm{T}}^{\ell\nu}$ interval, the limited size of the MC samples used to derive acceptance corrections, and differences in the modelling of non-prompt lepton backgrounds between data and simulation.

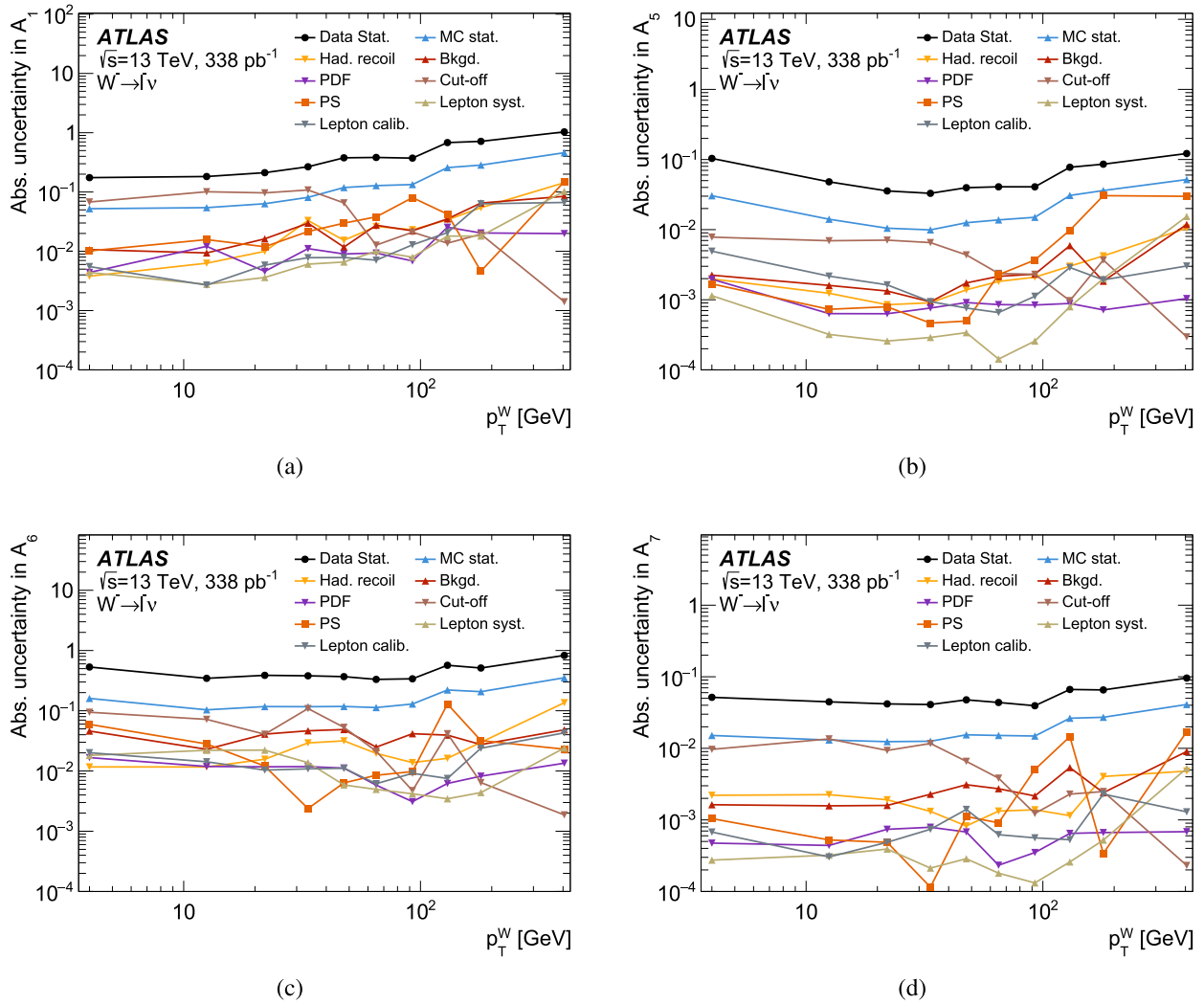

Fig. 9 The breakdown into statistical and systematic components of all the uncertainties for the measured **a** A_1, **b** A_5, **c** A_6 and **d** A_7 angular coefficients as a function of p_{T}^{W} in the $W^- \to \ell^- \nu$ channel, as obtained from the full fit. The values are given as absolute uncertainty

The final multijet background yields, as well as the two-dimensional angular distributions in $(\cos\theta_{\mathrm{CS}}, \phi_{\mathrm{CS}})$, are provided for each $p_{\mathrm{T}}^{\ell\nu}$ bin as input for the likelihood fit described in Sect. 3.2. This information is given separately for W^- and W^+ in each channel. The corresponding uncertainties, both in normalisation and shape, are propagated to the subsequent stages of the analysis.

4.4 Event yields and detector-level distributions

Projections of the detector-level distributions of the angular distributions $\cos\theta_{\mathrm{CS}}$ and ϕ_{CS} integrated over $p_{\mathrm{T}}^{\ell\nu}$ are shown for W^- and W^+ in Fig. 5 for the electron channel and in Fig. 6 for the muon channel.

The differences between the electron and muon distributions reflect the different efficiencies for reconstructing and selecting the two lepton flavours. Intrinsic kinematic differences between W^--boson events and W^+-boson events at $\sqrt{s} = 13\,\mathrm{TeV}$ are also observed when comparing the two charged channels. Overall, good agreement is observed between the data and the expectations in all the kinematic distributions. Small normalisation differences between the data and the MC distributions are observed at the level of a few percent, compatible with the combined uncertainties in the integrated luminosity and signal cross-section. The measurement of the angular coefficients is, however, independent of the normalisation between data and simulation in each measurement bin.

The expected event yields for signal and background processes are shown in Table 1, along with the yields as measured in data. The total MJ background yield and total uncertainty described in Sect. 4.3 are also presented in Table 1. The estimated multijet background fractions represent 2.0% and 0.7% of the total number of observed W^- candidate events

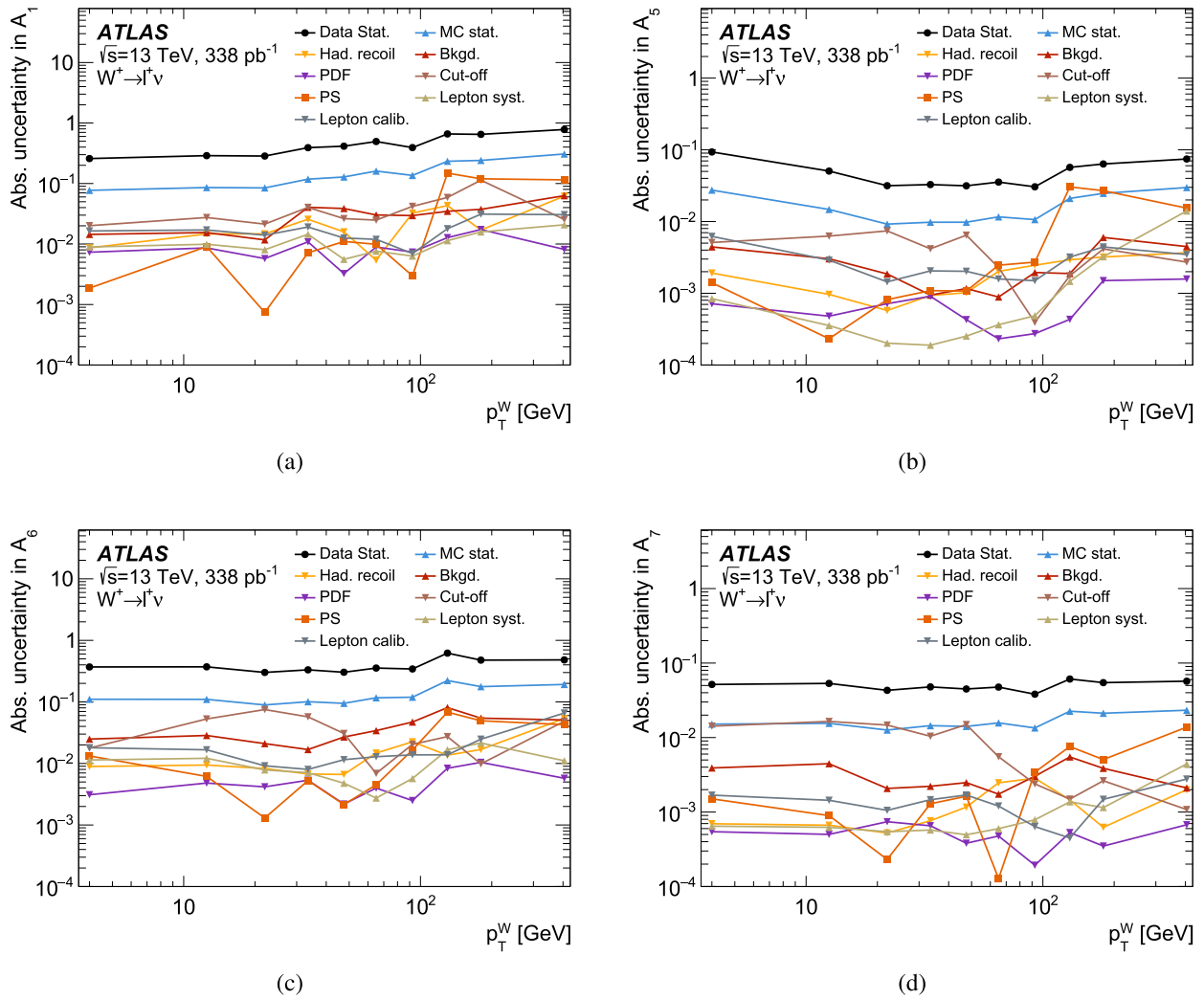

Fig. 10 The breakdown into statistical and systematic components of all the uncertainties for the measured **a** A_1, **b** A_5, **c** A_6 and **d** A_7 angular coefficients as a function of p_{T}^{W} in the $W^+ \to \ell^+\nu$ channel, as obtained from the full fit. The values are given as absolute uncertainty

in the electron and muon channels, respectively. The corresponding numbers for W^+ candidate events are 1.6% and 0.6%, respectively.

5 Systematic uncertainties

Several sources of statistical and systematic uncertainty affect the extraction of the angular coefficients and differential cross-sections presented in this paper. Systematic uncertainties are incorporated into the likelihood fit as constrained nuisance parameters, and their categorisation follows the methodology outlined in Ref. [6]. The overall impact of experimental and theory uncertainties in the values of $A_{0,2-4}$ is illustrated in Figs. 7 and 8 for the W^- and W^+ channels respectively, while the corresponding results for $A_{1,5-7}$ are shown in Figs. 9 and 10. The uncertainties in the $A_{1,5-7}$ coefficients are generally larger than those for $A_{0,2-4}$, due to their suppressed contribution. The dependence of the uncertainties in the differential cross-section, $\frac{d\sigma}{dp_T}$, as a function of p_{T}^{W}, is also shown in Fig. 11 separately for the W^- and W^+ channels. The impact of all uncertainty sources on the final results is evaluated after combining the electron and muon channels (see Sect. 6 for a discussion of their compatibility). A detailed discussion of these uncertainties is presented in this section.

The dominant contribution arises from the statistical uncertainty associated with the limited size of the dataset. Although the harmonic polynomials used in this methodology are completely orthogonal in the full phase space, detector-level resolution and acceptance effects lead to non-zero correlations between the measured coefficients. Due to the limited resolution and the intrinsic twofold ambiguity in

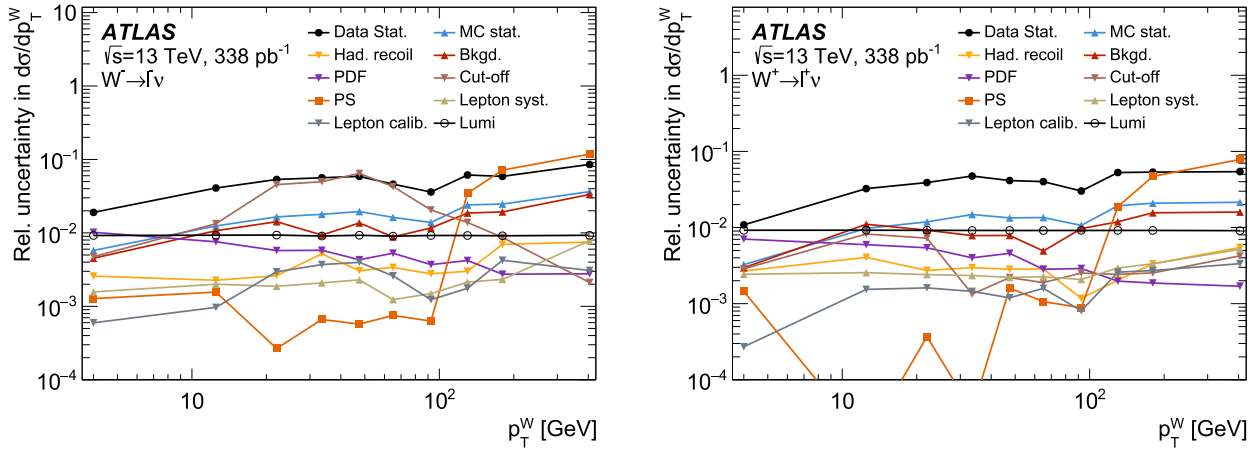

Fig. 11 The breakdown into statistical and systematic components of all the uncertainties for the measured $\frac{d\sigma}{dp_T}$ in the **a** $W^- \to \ell^-\nu$ and **b** $W^+ \to \ell^+\nu$ channel, as obtained from the full fit. The values are given as relative uncertainty. The uncertainty of 0.92% in the integrated luminosity is included

the reconstruction of the neutrino momentum, the templates used to extract the cross-sections and angular distributions measured in bins of (reconstructed) $p_{\mathrm{T}}^{\ell\nu}$ receive contributions from a broad range of (true) p_{T}^{W} values. This migration leads to correlations between the measured coefficients which increase their statistical uncertainties. For the cross-section measurements, the number of data events available is the largest source of uncertainty at large p_{T}^{W} where data statistics are limited, but otherwise the dominant source of uncertainty arises from bin-to-bin migration, making it the leading contributor to the overall statistical uncertainty.

Monte Carlo simulation is used to build the folding templates for the likelihood fit, as described in Sect. 3.2, and for modelling event migration between truth and reconstructed bins. The statistical uncertainty from MC simulation is treated as uncorrelated between each bin of the three-dimensional ($p_{\mathrm{T}}^{\ell\nu}$, $\cos\theta_{\mathrm{CS}}$, ϕ_{CS}) distribution and represents a non-negligible, though subdominant, contribution towards the total uncertainty. To ensure the statistical stability of the folding procedure, a threshold is applied such that templates contributing less than 2% of the expected number of events in a given truth bin are excluded. This *cut-off* value is determined by generating pseudo-data through random fluctuations of the expected MC yields and performing a series of likelihood fits with varying threshold values; the optimal cut-off is defined as the point where the variation in the χ^2 between successive fits is minimised. The systematic uncertainty associated with this choice is quantified separately for the W^- and W^+ channels, by varying the threshold up and down by 50% . The lower variation (1%) corresponds to the minimum value of the cut-off required to remove potential biases in the folded results, while the upper variation (3%) accounts for additional uncertainties arising from the reduced event information in the folding migrations. Both the direct impact on the fit results and the induced uncertainty due to event migration are taken into account. This uncertainty is added post-fit to the total systematic uncertainty. The W^- channel exhibits larger sensitivity to this variation, resulting in a systematic uncertainty that becomes comparable to the statistical uncertainty in the cross-section measurement at intermediate values of p_{T}^{W}.

Experimental systematic uncertainties affect both the $\cos\theta_{\mathrm{CS}}$ and ϕ_{CS} distributions used to construct the templates and the event weights applied to the simulation. The main experimental uncertainties affecting the measurements arise from the hadronic recoil calibration. The uncertainties in the scale and resolution of the hadronic recoil are discussed in greater detail in Ref. [24]. In this analysis, the hadronic recoil systematic uncertainty remains below 1% across the entire p_{T}^{W} range. Lepton-related systematic uncertainties due to energy/momentum scale and resolution as well as reconstruction and selection efficiency corrections are propagated considering the statistical and systematic uncertainties in the procedures, as detailed in Ref. [24]. They have only a small impact on both the A_i and cross-section measurements.

Uncertainties arising from the use of MC simulation to estimate the backgrounds are obtained by independently varying their corresponding cross-sections. An additional uncertainty in the $t\bar{t}$ background is evaluated using alternative MC samples, where the modelling parameter associated with high-p_{T} radiation is varied. This variation impacts both the normalisation and the shape of the $t\bar{t}$ background contribution. Systematic uncertainties affecting both the yield and shape of the multijet background are evaluated separately for

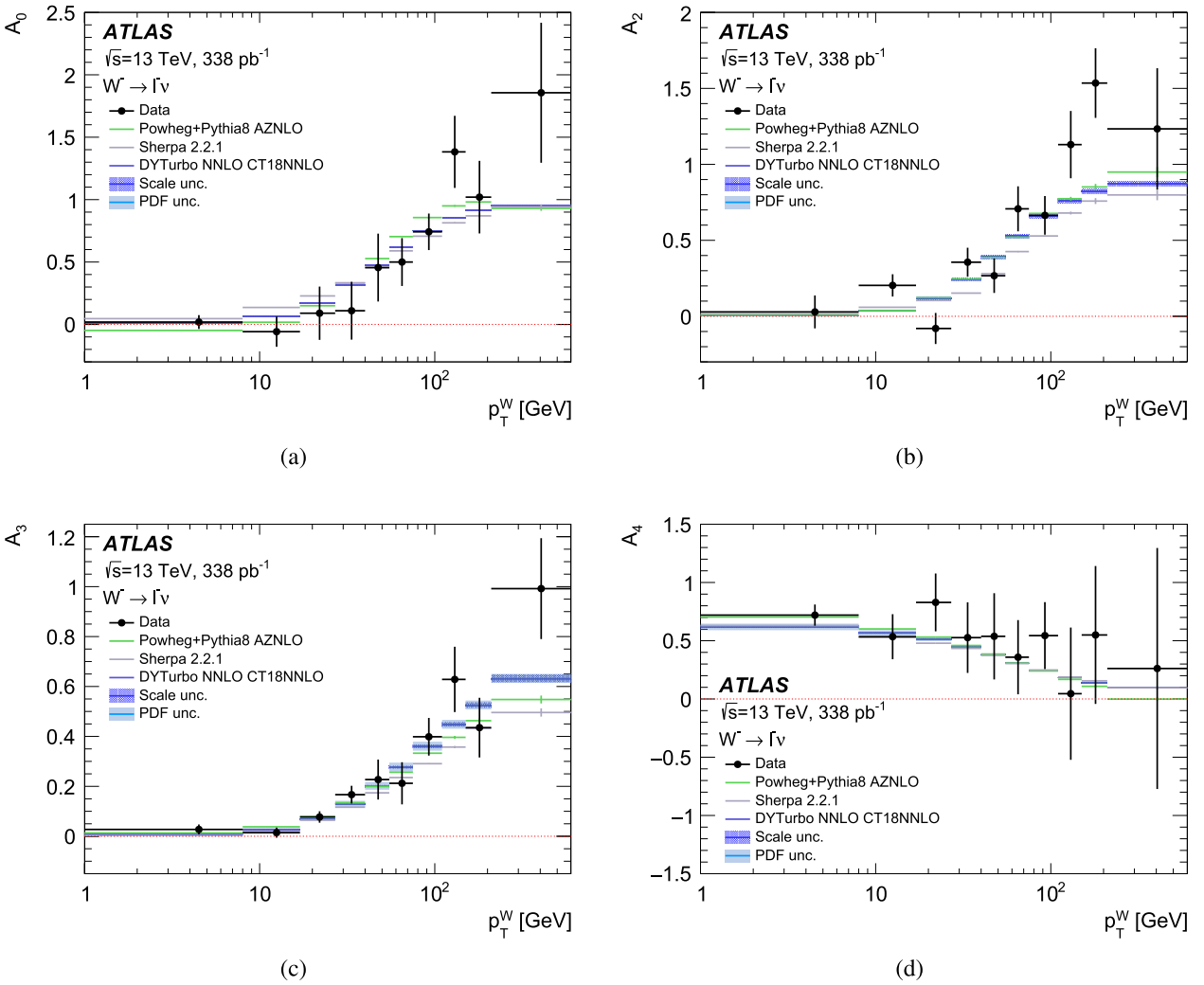

Fig. 12 The measured **a** A_0, **b** A_2, **c** A_3 and **d** A_4 coefficients extracted for the $W^- \to \ell^- \nu$ channel as a function of p_{T}^W with comparison to the predictions from DYTURBO, POWHEG, and SHERPA. The errors on the data points represent the total uncertainty in the measurement. Theory uncertainties in the DYTURBO predictions include variations of the renormalisation and factorisation scales, as well as PDF uncertainties for the CT18NNLO PDF set

W^- and W^+ candidate events, as detailed in Sect. 4.3, and are treated as uncorrelated between the electron and muon channels. This choice is motivated by the use of independent MC samples to correct the acceptance of the angular distribution templates in $p_{\mathrm{T}}^{\ell\nu}$ bins for each lepton flavour. The overall impact of background-related uncertainties in the A_i coefficients is subdominant but for the differential cross-sections, the uncertainty reaches up to 3% for W^- and 2% for W^+ at high p_{T}^W.

The overall uncertainty in the integrated luminosity of the 13 TeV low pile-up datasets is 0.92% [35]. The integrated luminosity uncertainty affects the absolute cross-section measurements, as shown in Fig. 11, but it is negligible in the A_i measurements because the coefficients are effectively cross-section ratios.

Theory systematic uncertainties due to the choice of parton distribution functions, parton shower modelling and the underlying event are also considered. Other theory uncertainties due to QCD renormalisation and factorisation scales, MC event generator modelling, and QED/EW (electroweak) corrections are not considered in this measurement as they were found to contribute negligibly in the previous, more precise, ATLAS measurement of Zangular coefficients [6]. The PDF-related uncertainties are evaluated using the CT10 eigenvector variations after rescaling them by a factor of 1.64 to obtain 68% confidence level (CL) variations. The resulting impact on the angular coefficients is subdominant, and the effect on the differential cross-section remains below $\sim 1\%$. Systematic uncertainties related to the underlying event and parton shower modelling (PS) are evaluated using a dedicated

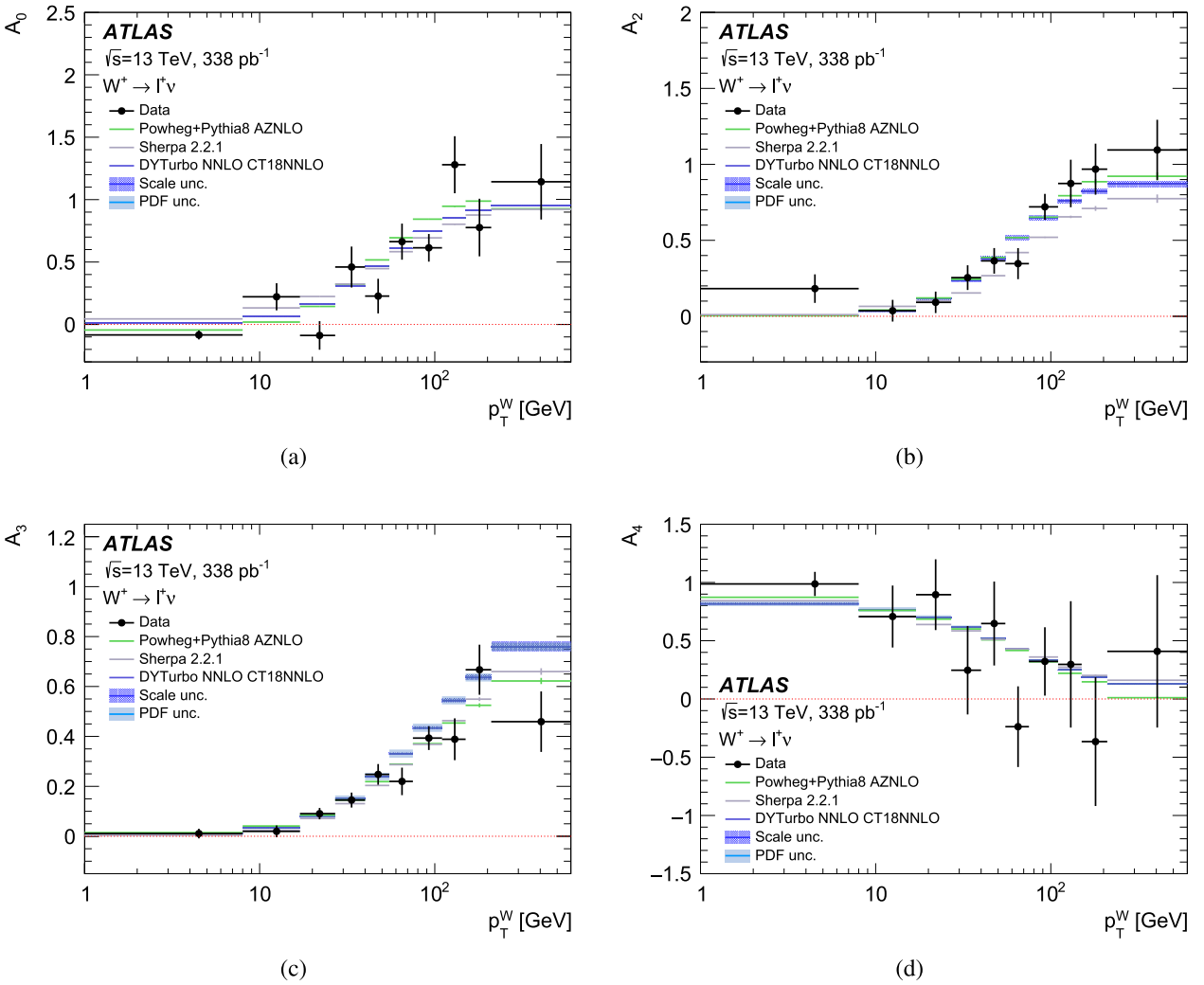

Fig. 13 The measured **a** A_0, **b** A_2, **c** A_3 and **d** A_4 coefficients extracted for the $W^+ \to \ell^+\nu$ channel as a function of p_{T}^W with comparison to the predictions from DYTURBO, POWHEG, and SHERPA. The errors on the data points represent the total uncertainty in the measurement. Theory uncertainties in the DYTURBO predictions include variations of the renormalisation and factorisation scales, as well as PDF uncertainties for the CT18NNLO PDF set

SHERPA sample reweighted to match the W-boson kinematics of the nominal POWHEG prediction. Folding templates derived from the SHERPA sample are used to extract the angular coefficients and differential cross-sections, and the absolute difference relative to the nominal result defines the uncertainty. This uncertainty is evaluated per channel and included post-fit in the total systematic uncertainty. The impact is generally subdominant, except in the highest $p_T^{\ell\nu}$ bin, where it becomes comparable to or exceeds the statistical uncertainty.

6 Results

This section presents the measurements of the full set of angular coefficients, A_{0-7}, together with the differential cross-sections as functions of p_{T}^W in the full phase space of the leptons from W-boson decays, shown separately for W^- and W^+-boson production.

The results are first measured separately in the electron and muon channels with the methodology detailed in Sect. 3.2. The compatibility of the two channels is assessed with a χ^2 test. The results are found to agree within their statistical uncertainties, with compatibility p-values of 0.92 for the W^- channel and 0.98 for the W^+ channel. The electron and muon channels are subsequently combined.

The measured angular coefficients, obtained from the combination of the electron and muon channels, are compared with theory predictions from the POWHEG+PYTHIA and SHERPA MC generators, as well as to fixed-order predictions at $\mathcal{O}(\alpha_s^2)$ in perturbative QCD, calculated with the DYTURBO

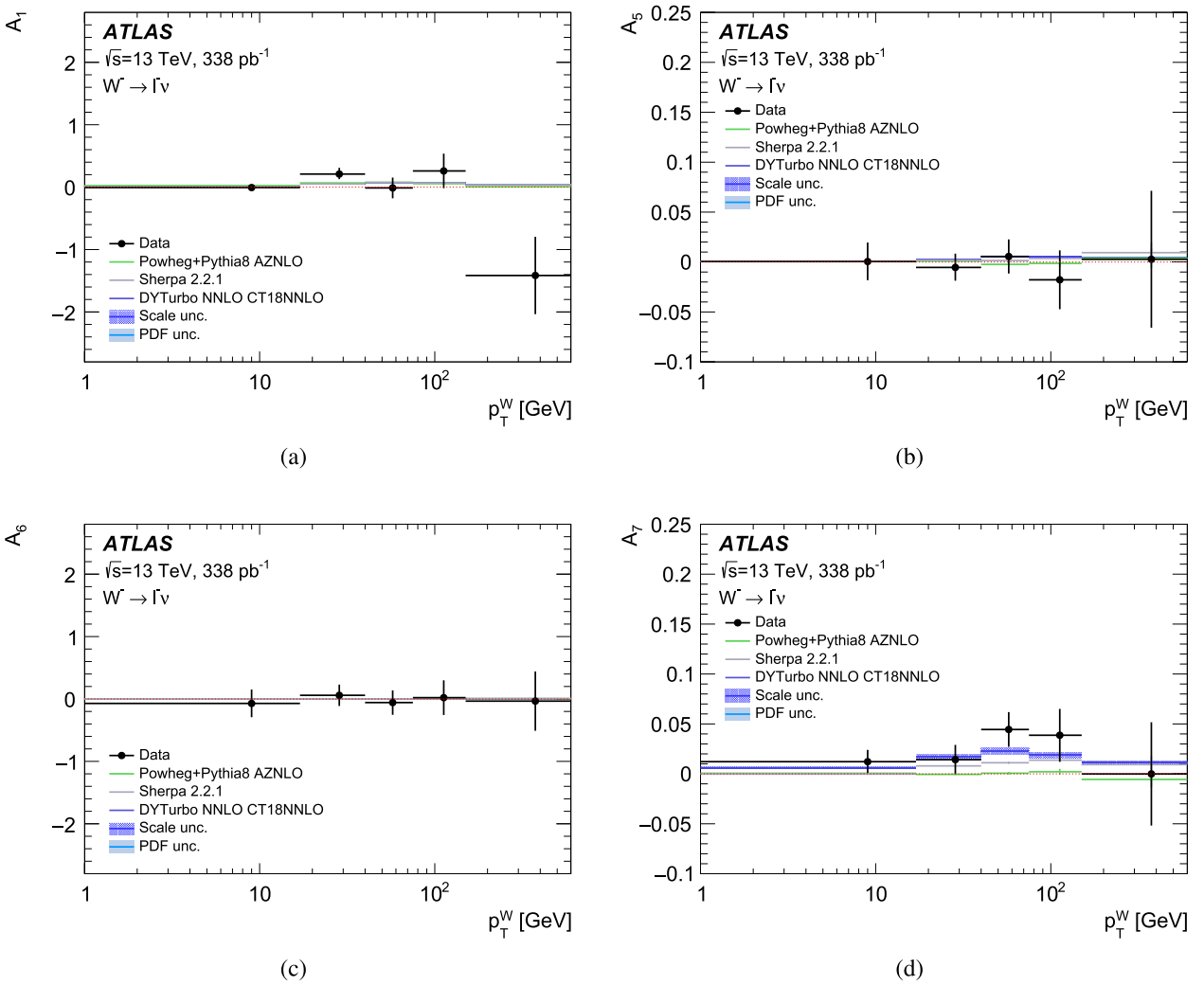

Fig. 14 The **a** A_1, **b** A_5, **c** A_6 and **d** A_7 coefficients extracted for the channel $W^- \to \ell^- \nu$ as a function of p_{T}^W with comparison to the predictions from DYTURBO, POWHEG, and SHERPA. The errors represent the total uncertainty in the measurement. As described in the text, a post-fit rebinning is applied in which two adjacent bins are averaged, effectively reducing the number of bins by a factor of two to mitigate strong bin-to-bin anticorrelations induced by statistical fluctuations. The error bars for the predictions show the total uncertainty for DYTURBO, but only the statistical uncertainties for POWHEG+PYTHIA8 and SHERPA MC generators

program. Theory uncertainties in the DYTURBO predictions are evaluated by varying the nominal factorisation and renormalisation scales independently up and down by a factor of two, excluding variations in opposite directions. In this analysis the theory uncertainties associated with the choice of these scales are varied simultaneously in the numerator and denominator of the cross-section ratios used to define the angular coefficients. The resulting envelope of all variations is taken as the uncertainty. Alternative treatments may yield larger uncertainties as described in Ref. [83]. PDF uncertainties for the CT18NNLO [84] set are evaluated using the standard eigenvector method and combined accordingly.

The results for the leading four angular coefficients, A_0 and A_{2-4} are shown in Figs. 12 and 13. These coefficients are clearly determined and show good agreement with theory predictions. This analysis provides the first direct measurement of the A_0 and A_4 coefficients as a function of p_{T}^W in both W^- and W^+ boson production. The precision achieved in the measurement of the A_3 coefficients exceeds that of any previous measurement. The measurement is intrinsically more sensitive to coefficients that do not depend on $\cos\theta$, as they are less affected by the twofold sign ambiguity in the angular reconstruction of the neutrino momentum. Owing to the statistics-limited nature of the measurement, strong bin-to-bin anticorrelations are present, reaching about 80% negative correlation in the low-p_{T}^W region.

Although the data statistics are not enough to distinguish overall non-zero values for the smaller angular coefficients,

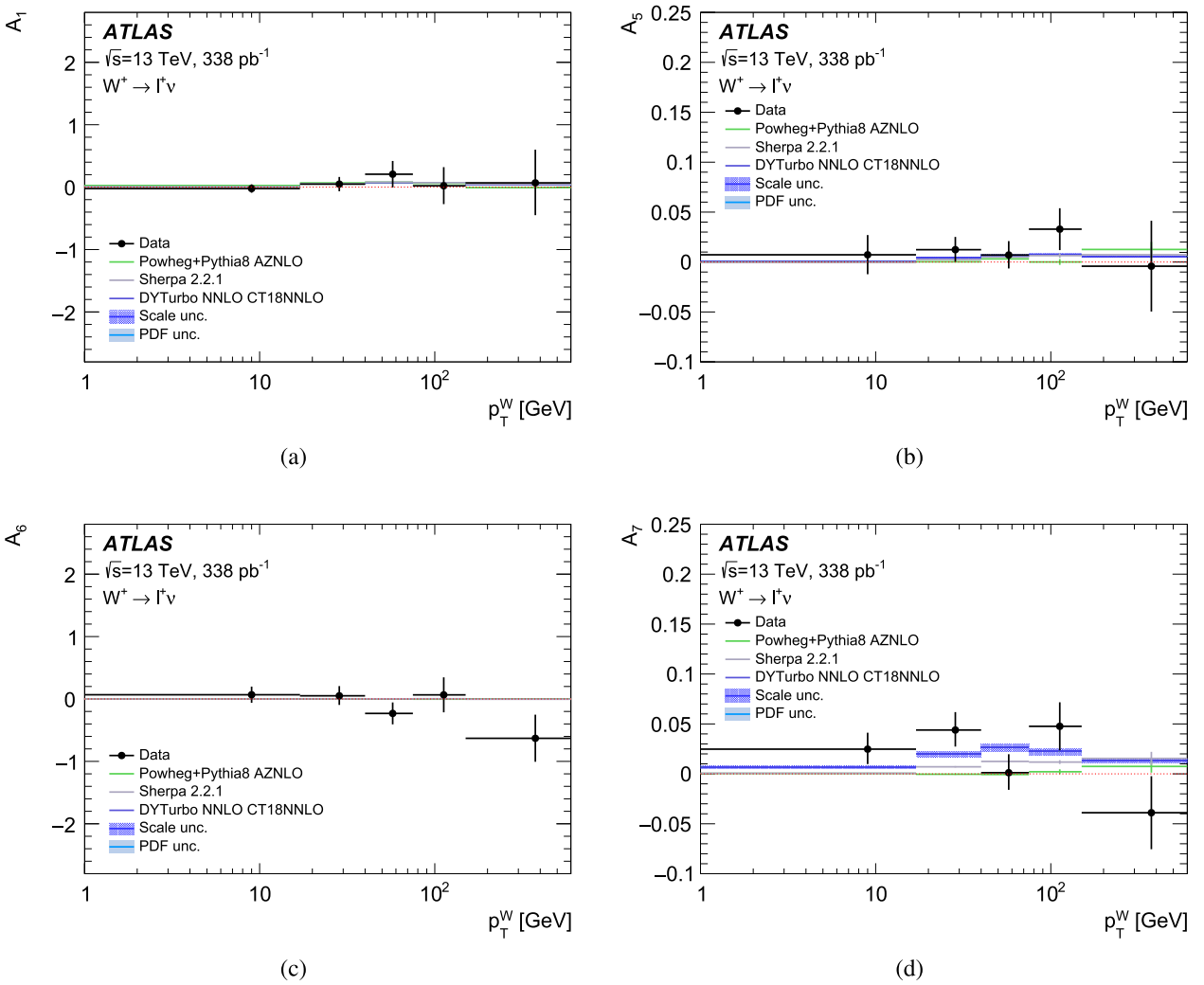

Fig. 15 The **a** A_1, **b** A_5, **c** A_6 and **d** A_7 coefficients extracted for the channel $W^+ \to \ell^+\nu$ as a function of p_{T}^W with comparison to the predictions from DYTURBO, POWHEG, and SHERPA. The errors represent the total uncertainty in the measurement. As described in the text, a post-fit rebinning is applied in which two adjacent bins are averaged, effectively reducing the number of bins by a factor of two to mitigate strong bin-to-bin anticorrelations induced by statistical fluctuations. The error bars for the predictions show the total uncertainty for DYTURBO, but only the statistical uncertainties for POWHEG+PYTHIA8 and SHERPA MC generators

$A_{1,5-7}$, these results are included for completeness. Despite their limited sensitivity, the extraction of these coefficients and of the Lam-Tung relation provides a useful consistency check and may inform future analyses with larger datasets. To improve the readability of the results, a post-fit rebinning procedure is applied, reducing the number of measurement bins by a factor of two. This step is motivated by the presence of strong bin-to-bin anticorrelations observed during the extraction of the A_i. The rebinning enhances the stability of the results and allows for a clearer interpretation of potential trends, even in regions dominated by statistical uncertainties. The measured $A_{1,5-7}$ coefficients are shown in Figs. 14 and 15. The A_7 coefficient is expected to be larger in W-boson production compared with Z-boson production due to the parity-violating nature of the weak interaction (see Refs. [85–87]). A slight deviation from zero is visible in the intermediate p_{T} range, though still limited by statistical uncertainties. The Lam-Tung relation, $A_0 - A_2 = 0$, is studied using the combined-fit results, and shown in Fig. 16 for W^- and W^+ production. Uncertainties in the measurements are derived from the full covariance matrix to account for correlations between A_0 and A_2. The data measurements lack the precision needed to probe potential deviations from zero, which are expected from calculations including higher-order diagrams.

As described in Sect. 3.2, the profile likelihood ratio fit is used to simultaneously extract the angular coefficients and the differential cross-sections in each measurement bin.

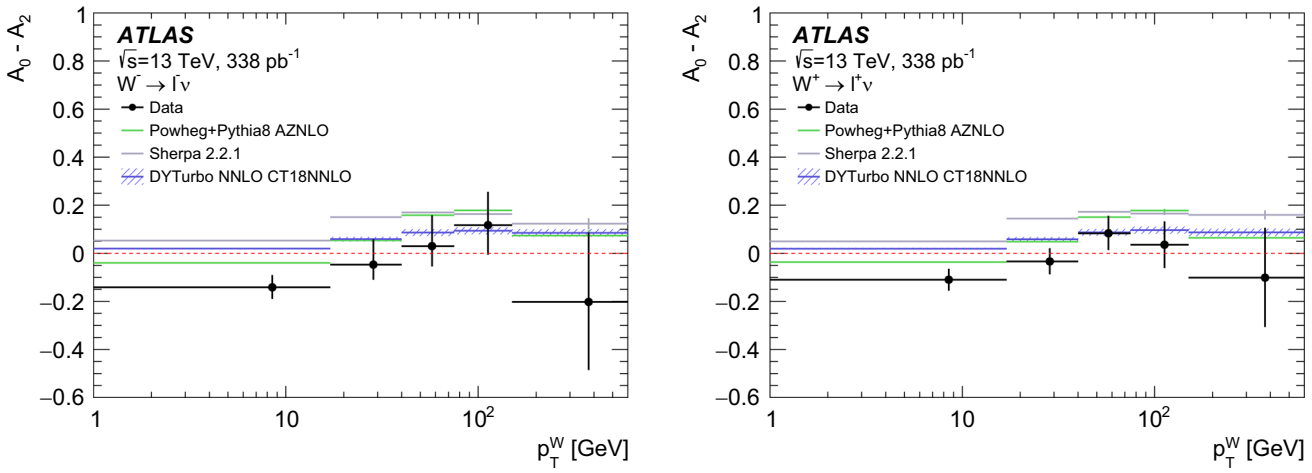

Fig. 16 Comparison between the measured values of $A_0 - A_2$ as function of p_{T}^W and predictions from the POWHEG and SHERPA event generators, as well as from DYTURBO for **a** W^- and **b** W^+. The error bars for the DYTURBO predictions show the total theory uncertainty. The data points are shown with their total uncertainties. As described in the text, a post-fit rebinning is applied in which two adjacent bins are averaged, effectively reducing the number of bins by a factor of two to mitigate strong bin-to-bin anticorrelations induced by statistical fluctuations

The resulting $\frac{d\sigma}{dp_T}$ within the full phase space of the decay leptons are shown in Fig. 17 for W^- and W^+ channels, together with the predicted values from POWHEG+PYTHIA8 and SHERPA 2.2.1 MC generators and the analytical predictions computed with the DYTURBO program. The predictions are computed by performing the resummation of logarithmically-enhanced contributions in the small transverse momentum region of the lepton pairs at NNLL accuracy and also include the corresponding finite-order QCD contributions at NNLO (corrections up to $\mathcal{O}(\alpha_s^2)$). Nonperturbative contributions to the initial-state partons transverse momentum are included in DYTURBO as in Ref. [88]. Theory uncertainties are estimated through up and down variations of the nominal factorisation, renormalisation, and resummation scales by a factor of two, excluding variations in opposite directions, and taking the envelope of all variations. The PDF uncertainties for the CT18NNLO PDF sets are estimated by calculating the variations for all eigenvectors or replicas and combining the results following the prescriptions.

The differential cross-sections are measured with a precision of 3% at low p_{T}^W. Owing to the threefold $(\cos\theta, \phi, p_{\mathrm{T}}^W)$ nature of the measurement and the statistical nature of its limitations, strong bin-to-bin anticorrelations of up to about 70% are observed. The DYTURBO resummed predictions show the best agreement across the full spectrum. The theory uncertainties at very low p_{T}^W are dominated by the PDF uncertainty but at higher p_{T}^W are dominated by the scale variations. The MC predictions describe the low-p_{T}^W region reasonably well. At higher transverse momenta, SHERPA 2.2.1 provides an overall good description, whereas POWHEG+PYTHIA8 shows worse agreement for $p_{\mathrm{T}}^W > 40\,\mathrm{GeV}$, as expected. Overall, the W^+ measurements show the largest deviation from the predictions.

7 Conclusions

This paper presents for the first time the measurement of the full set of angular coefficient for the W-boson and a differential measurement in p_{T}^W of absolute cross-sections within the full phase space of the decay leptons. Such a measurement is achieved by exploiting the methodology already developed and published for the extraction of the Z-boson angular coefficients. The twofold ambiguity in the reconstruction of the neutrino momenta in the CS frame and the corresponding ambiguity on the sign of $\cos\theta_{\mathrm{CS}}$ is solved on a statistical basis by imposing a simple m^W constraint. The measurement is performed using the data samples collected in dedicated low pile-up runs with the ATLAS detector at the LHC, corresponding to an integrated luminosity of $338\,\mathrm{pb}^{-1}$ at $\sqrt{s} = 13\,\mathrm{TeV}$. These low pile-up datasets offer a much improved resolution of the hadronic recoil compared with that from the nominal high pile-up Run 2 LHC proton–proton data, enabling the success of the challenging task of measuring neutrino-related observables. A profile likelihood fit extracts the eight angular coefficients and the corresponding unpolarised cross-section simultaneously as parameters of interest in each measurement bin in p_{T}^W space. The uncertainties in these measurements are mostly statistical in nature and the experimental and theory systematic uncertainties are at the percent level over most of the range.

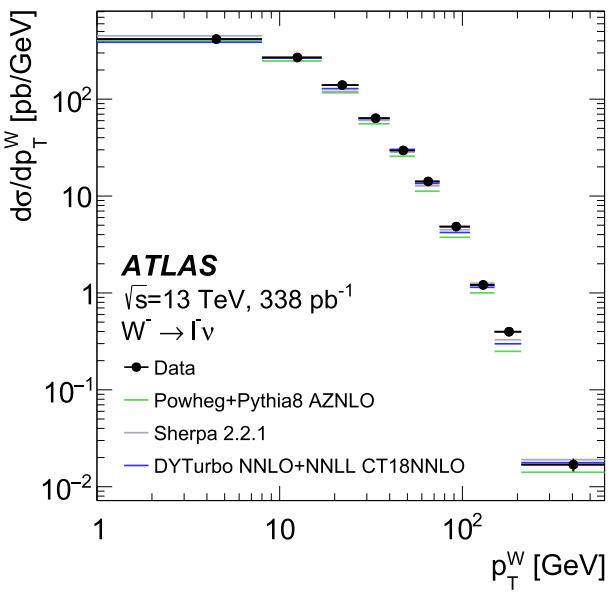

(a)

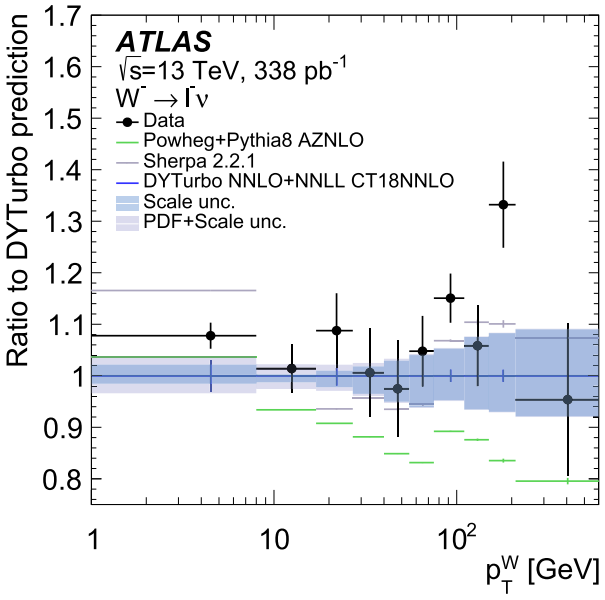

(b)

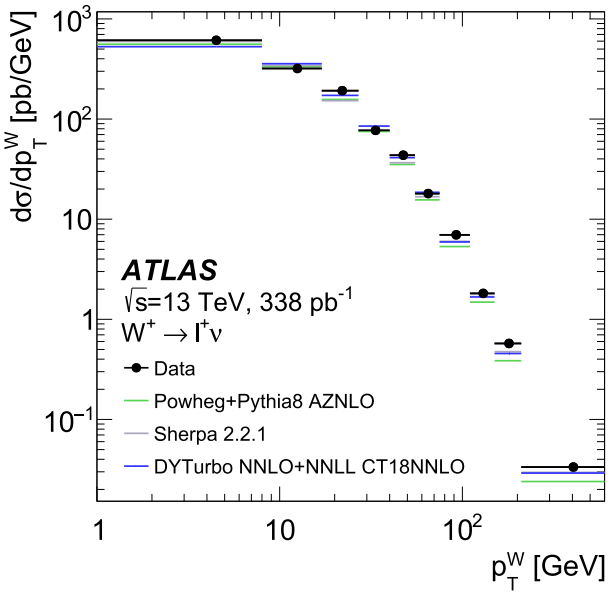

(c)

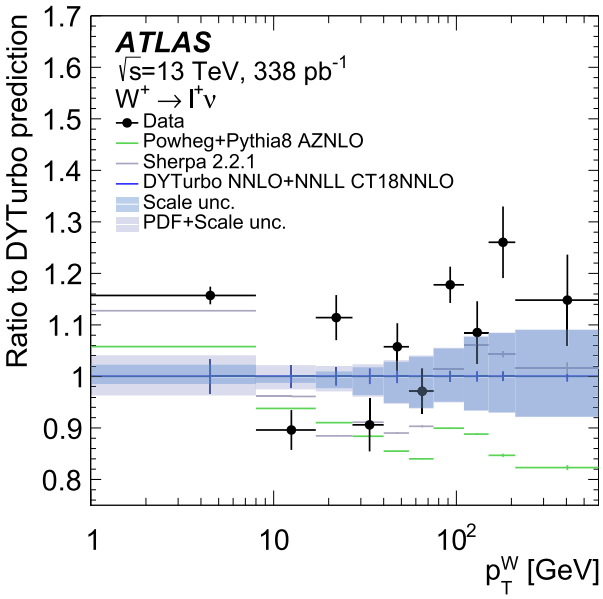

(d)

Fig. 17 Comparison of the measured absolute differential cross-sections $\frac{d\sigma}{dp_T}$ for **a** W^- and **c** W^+ bosons with predictions from POWHEG and SHERPA event generators, as well as from DYTURBO. The quoted cross-sections include the branching ratio to a single lepton flavour. Ratio of the measured $\frac{d\sigma}{dp_T}$ and the MC predictions to DYTURBO for **b** W^- and **d** W^+. Theory uncertainties in the DYTURBO predictions include variations of the renormalisation, factorisation, and resummation scales, as well as PDF uncertainties. The data points are shown with their total uncertainties

The angular coefficients $A_{0,2-4}$ measured for both W^- and W^+ bosons, are found to be significantly different from zero. These measurements are compared with DYTURBO predictions computed at $\mathcal{O}(\alpha_s^2)$ (NNLO). The $\frac{d\sigma}{dp_T}$ distributions, measured within the full phase space of the decay leptons, are also compared with DYTURBO predictions at NNLO, including transverse momentum resummation at NNLL accuracy in QCD and using various PDF sets. Overall, good agreement between the measurements and the theory predictions is observed.

Acknowledgements We thank CERN for the very successful operation of the LHC and its injectors, as well as the support staff at CERN and at our institutions worldwide without whom ATLAS could not be operated efficiently. The crucial computing support from all WLCG partners is acknowledged gratefully, in particular from CERN, the ATLAS Tier-1 facilities at TRIUMF/SFU (Canada), NDGF (Denmark, Norway, Sweden), CC-IN2P3 (France), KIT/GridKA (Germany), INFN-CNAF (Italy), NL-T1 (Netherlands), PIC (Spain), RAL (UK) and BNL (USA), the Tier-2 facilities worldwide and large non-WLCG resource providers. Major contributors of computing resources are listed in Ref. [89]. We gratefully acknowledge the support of ANPCyT, Argentina; YerPhI, Armenia; ARC, Australia; BMWFW and FWF, Austria; ANAS, Azerbaijan; CNPq and FAPESP, Brazil; NSERC, NRC and CFI, Canada; CERN; ANID, Chile; CAS, MOST and NSFC, China; Minciencias, Colombia; MEYS CR, Czech Republic; DNRF and DNSRC, Denmark; IN2P3-CNRS and CEA-DRF/IRFU, France; SRNSFG, Georgia; BMFTR, HGF and MPG, Germany; GSRI, Greece; RGC and Hong Kong SAR, China; ICHEP and Academy of Sciences and Humanities, Israel; INFN, Italy; MEXT and JSPS, Japan; CNRST, Morocco; NWO, Netherlands; RCN, Norway; MNiSW, Poland; FCT, Portugal; MNE/IFA, Romania; MSTDI, Serbia; MSSR, Slovakia; ARIS and MVZI, Slovenia; DSI/NRF, South Africa; MICIU/AEI, Spain; SRC and Wallenberg Foundation, Sweden; SERI, SNSF and Cantons of Bern and Geneva, Switzerland; NSTC, Taipei; TENMAK, Türkiye; STFC/UKRI, United Kingdom; DOE and NSF, United States of America. Individual groups and members have received support from BCKDF, CANARIE, CRC and DRAC, Canada; CERN-CZ, FORTE and PRIMUS, Czech Republic; COST, ERC, ERDF, Horizon 2020, ICSC-NextGenerationEU and Marie Skłodowska-Curie Actions, European Union; Investissements d'Avenir Labex, Investissements d'Avenir Idex and ANR, France; DFG and AvH Foundation, Germany; Herakleitos, Thales and Aristeia programmes co-financed by EU-ESF and the Greek NSRF, Greece; BSF-NSF and MINERVA, Israel; NCN and NAWA, Poland; La Caixa Banking Foundation, CERCA Programme Generalitat de Catalunya and PROMETEO and GenT Programmes Generalitat Valenciana, Spain; Göran Gustafssons Stiftelse, Sweden; The Royal Society and Leverhulme Trust, United Kingdom. In addition, individual members wish to acknowledge support from CERN: European Organization for Nuclear Research (CERN DOCT); Chile: Agencia Nacional de Investigación y Desarrollo (FONDECYT 1230812, FONDECYT 1240864, Fondecyt 3240661, Fondecyt Regular 1240721); China: Chinese Ministry of Science and Technology (MOST-2023YFA1605700, MOST-2023YFA1609300), National Natural Science Foundation of China (NSFC - 12175119, NSFC 12275265); Czech Republic: Czech Science Foundation (GACR - 24-11373S), Ministry of Education Youth and Sports (ERC-CZ-LL2327, FORTE CZ.02.01.01/00/22_008/0004632), PRIMUS Research Programme (PRIMUS/21/SCI/017); EU: H2020 European Research Council (ERC - 101002463); European Union: European Research Council (BARD No. 101116429, ERC - 948254, ERC 101089007), European Regional Development Fund (HE COFUND GA No.101081355, ERDF), European Union, Future Artificial Intelligence Research (FAIR-NextGenerationEU PE00000013), Italian Center for High Performance Computing, Big Data and Quantum Computing (ICSC, NextGenerationEU); France: Agence Nationale de la Recherche (ANR-21-CE31-0013, ANR-21-CE31-0022, ANR-22-EDIR-0002, ANR-24-CE31-0504-01); Germany: Baden-Württemberg Stiftung (BW Stiftung-Postdoc Eliteprogramme), Deutsche Forschungsgemeinschaft (DFG - 469666862, DFG - CR 312/5-2); China: Research Grants Council (GRF); Italy: Istituto Nazionale di Fisica Nucleare (ICSC, NextGenerationEU), Ministero dell'Università e della Ricerca (NextGenEU 153D23001490006 M4C2.1.1, NextGenEU I53D23000820006 M4C2.1.1, NextGenEU I53D23001490006 M4C2.1.1, SOE2024_0000023); Japan: Japan Society for the Promotion of Science (JSPS KAKENHI JP22H01227, JSPS KAKENHI JP22H04944, JSPS KAKENHI JP22KK0227, JSPS KAKENHI JP24K23939, JSPS KAKENHI JP24KK0251, JSPS KAKENHI JP25H00650, JSPS KAKENHI JP25H01291, JSPS KAKENHI JP25K01023); Norway: Research Council of Norway (RCN-314472); Poland: Ministry of Science and Higher Education (IDUB AGH, POB8, D4 no 9722), Polish National Science Centre (NCN 2021/42/E/ST2/00350, NCN OPUS 2023/51/B/ST2/02507, NCN UMO-2019/34/E/ST2/00393, UMO-2022/47/O/ST2/00148, UMO-2023/49/B/ST2/04085, UMO-2023/51/B/ST2/00920, UMO-2024/53/N/ST2/00869); Portugal: Foundation for Science and Technology (FCT); Spain: Generalitat Valenciana (ASFAE/2022/008), Ministry of Science and Innovation (MCIN & NextGenEU PCI2022-135018-2, MICIN & FEDER PID2021-125273 NB, RYC2019-028510-I, RYC2020-030254-I, RYC2021-031273-I, RYC2022-038164-I), Ministerio de Ciencia, Innovación y Universidades/Agencia Estatal de Investigación (PID2022-142604OB-C22); Sweden: Carl Trygger Foundation (Carl Trygger Foundation CTS 22:2312), Swedish Research Council (Swedish Research Council 2023-04654, VR 2021-03651, VR 2022-03845, VR 2022-04683, VR 2023-03403, VR 2024-05451), Knut and Alice Wallenberg Foundation (KAW 2018.0458, KAW 2022.0358, KAW 2023.0366); Switzerland: Swiss National Science Foundation (SNSF - PCEFP2_194658); United Kingdom: Royal Society (NIF-R1-231091); United States of America: U.S. Department of Energy (ECA DE-AC02-76SF00515), Neubauer Family Foundation.

Data Availability Statement This manuscript has no associated data. [Authors' comment: The public release of data supporting the findings of this article will follow the CERN Open Data Policy (https://cds.cern.ch/record/2745133). The values of relevant plots and tables associated with this article are stored in HEPData (https://www.hepdata.net/record/ins2970689).]

Code Availability Statement This manuscript has no associated code/software. [Authors' comment: The ATLAS Collaboration's Athena software, including the configuration of the event generators, is open source (http://gitlab.cern.ch/atlas/athena).]

Funded by SCOAP[3].

References

1. J.C. Collins, D.E. Soper, Angular distribution of dileptons in high-energy hadron collisions. Phys. Rev. D **16**, 2219 (1977). https://doi.org/10.1103/PhysRevD.16.2219
2. E. Mirkes, J. Ohnemus, W and Z polarization effects in hadronic collisions. Phys. Rev. D **50**, 5692 (1994). https://doi.org/10.1103/PhysRevD.50.5692. arXiv:hep-ph/9406381
3. E. Mirkes, Angular decay distribution of leptons from W-bosons at NLO in hadronic collisions. Nucl. Phys. B **387**, 3 (1992). https://doi.org/10.1016/0550-3213(92)90046-E
4. E. Mirkes, J. Ohnemus, Angular distributions of Drell–Yan lepton pairs at the Fermilab Tevatron: order α_s^2 corrections and Monte Carlo studies. Phys. Rev. D **51**, 4891 (1995). https://doi.org/10.1103/PhysRevD.51.4891. arXiv:hep-ph/9412289
5. E. Mirkes, J. Ohnemus, Polarization effects in Drell–Yan type processes $h_1 + h_2 \to (W, Z, \gamma^*, J/\psi) + X$. (1994). arXiv:hep-ph/9408402
6. ATLAS Collaboration, Measurement of the angular coefficients in Z-boson events using electron and muon pairs from data taken at $\sqrt{s} = 8$ TeV with the ATLAS detector. JHEP **08**, 159 (2016). https://doi.org/10.1007/JHEP08(2016)159. arXiv:1606.00689 [hep-ex]
7. ATLAS Collaboration, A precise measurement of the Z-boson double-differential transverse momentum and rapidity distributions in the full phase space of the decay leptons with the ATLAS experiment at $\sqrt{s} = 8$ TeV. Eur. Phys. J. C **84**, 315 (2024). https://doi.org/10.1140/epjc/s10052-024-12438-w. arXiv:2309.09318 [hep-ex]
8. LHCb Collaboration, First measurement of the $Z \to \mu^+\mu^-$ angular coefficients in the forward region of pp collisions at $\sqrt{s} = 13$ TeV. Phys. Rev. Lett. **129**, 091801 (2022). https://doi.org/10.1103/PhysRevLett.129.091801. arXiv:2203.01602 [hep-ex]
9. C.M.S. Collaboration, Angular coefficients of Z bosons produced in pp collisions at $\sqrt{s} = 8$ TeV and decaying to $\mu^+\mu^-$ as a function of transverse momentum and rapidity. Phys. Lett. B **750**, 154 (2015). https://doi.org/10.1016/j.physletb.2015.08.061. arXiv:1504.03512 [hep-ex]
10. L. Evans, P. Bryant, L.H.C. Machine, JINST **3**, S08001 (2008). https://doi.org/10.1088/1748-0221/3/08/S08001
11. CDF Collaboration, First measurement of the angular coefficients of Drell–Yan e^+e^- pairs in the Z mass region from $p\bar{p}$ Collisions at $\sqrt{s} = 1.96$ TeV. Phys. Rev. Lett. **106**, 241801 (2011). https://doi.org/10.1103/PhysRevLett.106.241801
12. D. Acosta et al., Measurement of the azimuthal angle distribution of leptons from W boson decays as a function of the W transverse momentum in $p\bar{p}$ collisions at $\sqrt{s} = 1.8$ TeV. Phys. Rev. D **73**, 052002 (2006). https://doi.org/10.1103/PhysRevD.73.052002. arXiv:hep-ex/0504020
13. ATLAS Collaboration, Measurement of the polarisation of W bosons produced with large transverse momentum in pp collisions at $\sqrt{s} = 7$ TeV with the ATLAS experiment. Eur. Phys. J. C **72**, 2001 (2012). https://doi.org/10.1103/PhysRevD.73.052002. arXiv:1203.2165 [hep-ex]
14. C.M.S. Collaboration, Measurement of the polarization of W bosons with large transverse momenta in W+Jets events at the LHC. Phys. Rev. Lett. **107**, 021802 (2011). https://doi.org/10.1103/PhysRevLett.107.021802. arXiv:1104.3829 [hep-ex]
15. C.M.S. Collaboration, Measurements of the W boson rapidity, helicity, double-differential cross sections, and charge asymmetry in pp collisions at $\sqrt{s} = 13$ TeV. Phys. Rev. D **102**, 092012 (2020). https://doi.org/10.1103/PhysRevD.102.092012. arXiv:2008.04174 [hep-ex]
16. M. Pellen, R. Poncelet, A. Popescu, T. Vitos, Angular coefficients in W + j production at the LHC with high precision. Eur. Phys. J. C (2022). https://doi.org/10.1140/epjc/s10052-022-10641-1. arXiv:2204.12394 [hep-ph]
17. ATLAS Collaboration, Measurement of the W-boson mass and width with the ATLAS detector using proton–proton collisions at $\sqrt{s} = 7$ TeV. Eur. Phys. J. C **84**, 1309 (2024). https://doi.org/10.1140/epjc/s10052-024-13190-x. arXiv:2403.15085 [hep-ex]
18. LHCb Collaboration, Measurement of the W boson mass. JHEP **01**, 036 (2022). https://doi.org/10.1007/JHEP01(2022)036. arXiv:2109.01113 [hep-ex]
19. CMS Collaboration, High-precision measurement of the W boson mass with the CMS experiment at the LHC. (2024). arXiv:2412.13872 [hep-ex]
20. M.A. Ebert, J.K.L. Michel, I.W. Stewart, F.J. Tackmann, Drell-Yan q_T resummation of fiducial power corrections at N^3LL. JHEP **04**, 102 (2021). https://doi.org/10.1007/JHEP04(2021)102. arXiv:2006.11382 [hep-ph]
21. A. Glazov, Defiducialization: providing experimental measurements for accurate fixed-order predictions. Eur. Phys. J. C **80**, 875 (2020). https://doi.org/10.1140/epjc/s10052-020-08435-4. arXiv:2001.02933 [hep-ex]
22. G.P. Salam, E. Slade, Cuts for two-body decays at colliders. JHEP **11**, 220 (2021). https://doi.org/10.1007/JHEP11(2021)220. arXiv:2106.08329 [hep-ph]
23. S. Alekhin, A. Kardos, S. Moch, Z. Trócsányi, Precision studies for Drell–Yan processes at NNLO. Eur. Phys. J. C **81**, 573 (2021). https://doi.org/10.1140/epjc/s10052-021-09361-9. arXiv:2104.02400 [hep-ph]
24. ATLAS Collaboration, Precise measurements of W- and Z-boson transverse momentum spectra with the ATLAS detector using pp collisions at $\sqrt{s} = 5.02$ TeV and 13 TeV. Eur. Phys. J. C **84**, 1126 (2024). https://doi.org/10.1140/epjc/s10052-024-13414-0. arXiv:2404.06204 [hep-ex]
25. ATLAS Collaboration, Measurement of $W^{\pm}$-boson differential cross-sections in proton–proton collisions with low pile-up data at $\sqrt{s} = 5.02$ TeV and 13 TeV with the ATLAS detector. Eur. Phys. J. C **85**, 729 (2025). https://doi.org/10.1140/epjc/s10052-025-14178-x. arXiv:2502.09403 [hep-ex]
26. ATLAS Collaboration, The ATLAS experiment at the CERN large hadron collider. JINST **3**, S08003 (2008). https://doi.org/10.1088/1748-0221/3/08/S08003
27. G. Avoni et al., The new LUCID-2 detector for luminosity measurement and monitoring in ATLAS. JINST **13**, P07017 (2018). https://doi.org/10.1088/1748-0221/13/07/P07017
28. ATLAS Collaboration, Performance of the ATLAS trigger system in, Eur. Phys. J. C **77**(2017), 317 (2015). https://doi.org/10.1140/epjc/s10052-017-4852-3. arXiv:1611.09661 [hep-ex]
29. ATLAS Collaboration, Software and computing for Run 3 of the ATLAS experiment at the LHC. Eur. Phys. J. C **85**, 234 (2025). https://doi.org/10.1140/epjc/s10052-024-13701-w. arXiv:2404.06335 [hep-ex]
30. C.S. Lam, W.-K. Tung, Systematic approach to inclusive lepton pair production in hadronic collisions. Phys. Rev. D **18**, 2447 (1978). https://doi.org/10.1103/PhysRevD.18.2447
31. C.S. Lam, W.-K. Tung, Structure function relations at large transverse momenta in lepton-pair production processes. Phys. Lett. B **80**, 228 (1979). https://doi.org/10.1016/0370-2693(79)90204-1
32. C.S. Lam, W.-K. Tung, Parton-model relation without quantum-chromodynamic modifications in lepton pair production. Phys. Rev. D **21**, 2712 (1980). https://doi.org/10.1103/PhysRevD.21.2712
33. E. Richter-Was, Z. Was, W production at LHC: lepton angular distributions and reference frames for probing hard QCD. Eur. Phys. J. C **77** (2017). https://doi.org/10.1140/epjc/s10052-017-4649-4. ISSN: 1434-6052
34. B.A. Betchart, R. Demina, A. Harel, Analytic solutions for neutrino momenta in decay of top quarks. Nucl. Instrum. Methods

A **736**, 169 (2014). https://doi.org/10.1016/j.nima.2013.10.039. arXiv:1305.1878 [hep-ph]
35. ATLAS Collaboration, Luminosity determination in pp collisions at $\sqrt{s} = 13$ TeV using the ATLAS detector at the LHC. Eur. Phys. J. C **83**, 982 (2023). https://doi.org/10.1140/epjc/s10052-023-11747-w. arXiv:2212.09379 [hep-ex]
36. S. Agostinelli et al., GEANT4 – a simulation toolkit. Nucl. Instrum. Methods A **506**, 250 (2003). https://doi.org/10.1016/S0168-9002(03)01368-8
37. ATLAS Collaboration, The ATLAS simulation infrastructure. Eur. Phys. J. C **70**, 823 (2010). https://doi.org/10.1140/epjc/s10052-010-1429-9. arXiv:1005.4568 [physics.ins-det]
38. T. Sjöstrand, S. Mrenna, P. Skands, A brief introduction to PYTHIA 8.1. Comput. Phys. Commun. **178**, 852 (2008). https://doi.org/10.1016/j.cpc.2008.01.036. arXiv:0710.3820 [hep-ph]
39. NNPDF Collaboration, R.D. Ball et al., Parton distributions with LHC data. Nucl. Phys. B **867**, 244 (2013). https://doi.org/10.1016/j.nuclphysb.2012.10.003. arXiv:1207.1303 [hep-ph]
40. ATLAS Collaboration, The Pythia 8 A3 tune description of ATLAS minimum bias and inelastic measurements incorporating the Donnachie–Landshoff diffractive model. ATL-PHYS-PUB-2016-017. 2016. https://cds.cern.ch/record/2206965
41. P. Nason, A new method for combining NLO QCD with shower Monte Carlo algorithms. JHEP **11**, 040 (2004). https://doi.org/10.1088/1126-6708/2004/11/040. arXiv:hep-ph/0409146
42. S. Frixione, P. Nason, C. Oleari, Matching NLO QCD computations with parton shower simulations: the POWHEG method. JHEP **11**, 070 (2007). https://doi.org/10.1088/1126-6708/2007/11/070. arXiv:0709.2092 [hep-ph]
43. S. Alioli, P. Nason, C. Oleari, E. Re, NLO vector-boson production matched with shower in POWHEG. JHEP **07**, 060 (2008). https://doi.org/10.1088/1126-6708/2008/07/060. arXiv:0805.4802 [hep-ph]
44. S. Alioli, P. Nason, C. Oleari, E. Re, A general framework for implementing NLO calculations in shower Monte Carlo programs: the POWHEG BOX. JHEP **06**, 043 (2010). https://doi.org/10.1007/JHEP06(2010)043. arXiv:1002.2581 [hep-ph]
45. H.-L. Lai et al., New parton distributions for collider physics. Phys. Rev. D **82**, 074024 (2010). https://doi.org/10.1103/PhysRevD.82.074024. arXiv:1007.2241 [hep-ph]
46. T. Sjöstrand et al., An introduction to PYTHIA 8.2. Comput. Phys. Commun. **191**, 159 (2015). https://doi.org/10.1016/j.cpc.2015.01.024. ISSN: 0010-4655
47. ATLAS Collaboration, Measurement of the Z/γ^* boson transverse momentum distribution in pp collisions at $\sqrt{s} = 7$ TeV with the ATLAS detector. JHEP **09**, 145 (2014). https://doi.org/10.1007/JHEP09(2014)145. arXiv:1406.3660 [hep-ex]
48. P. Golonka, Z. Was, PHOTOS Monte Carlo: a precision tool for QED corrections in Z and W decays. Eur. Phys. J. C **45**, 97 (2006). https://doi.org/10.1140/epjc/s2005-02396-4. arXiv:hep-ph/0506026
49. E. Bothmann et al., Event generation with Sherpa 2.2. SciPost Phys. **7**, 034 (2019). https://doi.org/10.21468/SciPostPhys.7.3.034. arXiv:1905.09127 [hep-ph]
50. NNPDF Collaboration, R.D. Ball et al., Parton distributions for the LHC run II. JHEP **04**, 040 (2015). https://doi.org/10.1007/JHEP04(2015)040. arXiv:1410.8849 [hep-ph]
51. T. Gleisberg, S. Höche, Comix, a new matrix element generator. JHEP **12**, 039 (2008). https://doi.org/10.1088/1126-6708/2008/12/039. arXiv:0808.3674 [hep-ph]
52. F. Buccioni et al., OpenLoops 2. Eur. Phys. J. C **79**, 866 (2019). https://doi.org/10.1140/epjc/s10052-019-7306-2. arXiv:1907.13071 [hep-ph]
53. F. Cascioli, P. Maierhöfer, S. Pozzorini, Scattering amplitudes with open loops. Phys. Rev. Lett. **108**, 111601 (2012). https://doi.org/10.1103/PhysRevLett.108.111601. arXiv:1111.5206 [hep-ph]
54. A. Denner, S. Dittmaier, L. Hofer, COLLIER: a Fortran-based complex one-loop library in extended regularizations. Comput. Phys. Commun. **212**, 220 (2017). https://doi.org/10.1016/j.cpc.2016.10.013. arXiv:1604.06792 [hep-ph]
55. S. Schumann, F. Krauss, A parton shower algorithm based on Catani–Seymour dipole factorisation. JHEP **03**, 038 (2008). https://doi.org/10.1088/1126-6708/2008/03/038. arXiv:0709.1027 [hep-ph]
56. S. Höche, F. Krauss, M. Schönherr, F. Siegert, A critical appraisal of NLO+PS matching methods. JHEP **09**, 049 (2012). https://doi.org/10.1007/JHEP09(2012)049. arXiv:1111.1220 [hep-ph]
57. S. Höche, F. Krauss, M. Schönherr, F. Siegert, QCD matrix elements + parton showers. The NLO case. JHEP **04**, 027 (2013). https://doi.org/10.1007/JHEP04(2013)027. arXiv:1207.5030 [hep-ph]
58. S. Catani, F. Krauss, B.R. Webber, R. Kuhn, QCD matrix elements + parton showers. JHEP **2001**, 063 (2002). https://doi.org/10.1088/1126-6708/2001/11/063. arXiv:hep-ph/0109231
59. S. Höche, F. Krauss, S. Schumann, F. Siegert, QCD matrix elements and truncated showers. JHEP **05**, 053 (2009). https://doi.org/10.1088/1126-6708/2009/05/053. arXiv:0903.1219 [hep-ph]
60. S. Camarda et al., DYTurbo: fast predictions for Drell–Yan processes. Eur. Phys. J. C **80**, 251 (2020). https://doi.org/10.1140/epjc/s10052-020-7757-5. arXiv:1910.07049 [hep-ph]
61. S. Camarda, L. Cieri, G. Ferrera, Drell–Yan lepton-pair production: q_T resummation at N^3LL accuracy and fiducial cross sections at N^3LO. Phys. Rev. D **104**, L111503 (2021). https://doi.org/10.1103/PhysRevD.104.L111503. arXiv:2103.04974 [hep-ph]
62. S. Camarda, L. Cieri, G. Ferrera, Fiducial perturbative power corrections within the q_T subtraction formalism. Eur. Phys. J. C **82**, 575 (2022). https://doi.org/10.1140/epjc/s10052-022-10510-x. arXiv:2111.14509 [hep-ph]
63. S. Camarda, L. Cieri, G. Ferrera, Drell–Yan lepton-pair production: q_T resummation at N4LL accuracy. Phys. Lett. B **845**, 138125 (2023). https://doi.org/10.1016/j.physletb.2023.138125. arXiv:2303.12781 [hep-ph]
64. L.A. Harland-Lang, A.D. Martin, P. Motylinski, R.S. Thorne, Parton distributions in the LHC era: MMHT 2014 PDFs. Eur. Phys. J. C **75**, 204 (2015). https://doi.org/10.1140/epjc/s10052-015-3397-6. arXiv:1412.3989 [hep-ph]
65. ATLAS Collaboration, Study of top-quark pair modelling and uncertainties using ATLAS measurements at $\sqrt{s} = 13$ TeV. ATL-PHYS-PUB-2020-023. 2020. https://cds.cern.ch/record/2730443
66. M. Beneke, P. Falgari, S. Klein, C. Schwinn, Hadronic top-quark pair production with NNLL threshold resummation. Nucl. Phys. B **855**, 695 (2012). https://doi.org/10.1016/j.nuclphysb.2011.10.021. arXiv:1109.1536 [hep-ph]
67. M. Cacciari, M. Czakon, M. Mangano, A. Mitov, P. Nason, Top-pair production at hadron colliders with next-to-next-to-leading logarithmic soft-gluon resummation. Phys. Lett. B **710**, 612 (2012). https://doi.org/10.1016/j.physletb.2012.03.013. arXiv:1111.5869 [hep-ph]
68. P. Bärnreuther, M. Czakon, A. Mitov, Percent-level-precision physics at the tevatron: next-to-next-to-leading order QCD corrections to $q\bar{q} \to t\bar{t} + X$. Phys. Rev. Lett. **109**, 132001 (2012). https://doi.org/10.1103/PhysRevLett.109.132001. arXiv:1204.5201 [hep-ph]
69. M. Czakon, A. Mitov, NNLO corrections to top-pair production at hadron colliders: the all-fermionic scattering channels. JHEP **12**, 054 (2012). https://doi.org/10.1007/JHEP12(2012)054. arXiv:1207.0236 [hep-ph]
70. M. Czakon, A. Mitov, NNLO corrections to top pair production at hadron colliders: the quark-gluon reaction. JHEP **01**, 080 (2013). https://doi.org/10.1007/JHEP01(2013)080. arXiv:1210.6832 [hep-ph]

71. M. Czakon, P. Fiedler, A. Mitov, Total top-quark pair-production cross section at hadron colliders through $O(\alpha_s^4)$. Phys. Rev. Lett. **110**, 252004 (2013). https://doi.org/10.1103/PhysRevLett.110.252004. arXiv:1303.6254 [hep-ph]
72. M. Czakon, A. Mitov, Top++: a program for the calculation of the top-pair cross-section at hadron colliders. Comput. Phys. Commun. **185**, 2930 (2014). https://doi.org/10.1016/j.cpc.2014.06.021. arXiv:1112.5675 [hep-ph]
73. ATLAS Collaboration, Multi-boson simulation for 13 TeV ATLAS analyses. ATL-PHYS-PUB-2017-005. 2017. https://cds.cern.ch/record/2261933
74. D.J. Lange, The EvtGen particle decay simulation package. Nucl. Instrum. Methods A **462**, 152 (2001). https://doi.org/10.1016/S0168-9002(01)00089-4
75. P. Skands, S. Carrazza, J. Rojo, Tuning PYTHIA 8.1: the Monash 2013 tune. Eur. Phys. J. C **74**, 3024 (2014). https://doi.org/10.1140/epjc/s10052-014-3024-y. arXiv:1404.5630 [hep-ph]
76. ATLAS Collaboration, Performance of electron and photon triggers in ATLAS during LHC Run 2. Eur. Phys. J. C **80**, 47 (2020). https://doi.org/10.1140/epjc/s10052-019-7500-2. arXiv:1909.00761 [hep-ex]
77. ATLAS Collaboration, Performance of the ATLAS muon triggers in Run 2. JINST **15**, P09015 (2020). https://doi.org/10.1088/1748-0221/15/09/p09015. arXiv:2004.13447 [physics.ins-det]
78. ATLAS Collaboration, Vertex reconstruction performance of the ATLAS detector at $\sqrt{s} = 13$ TeV. ATL-PHYS-PUB-2015-026. 2015. https://cds.cern.ch/record/2037717
79. ATLAS Collaboration, Electron and photon performance measurements with the ATLAS detector using the 2015–2017 LHC proton–proton collision data. JINST **14**, P12006 (2019). https://doi.org/10.1088/1748-0221/14/12/P12006. arXiv:1908.00005 [hep-ex]
80. ATLAS Collaboration, Muon reconstruction and identification efficiency in ATLAS using the full Run 2 pp collision data set at $\sqrt{s} = 13$ TeV. Eur. Phys. J. C **81**, 578 (2021). https://doi.org/10.1140/epjc/s10052-021-09233-2. arXiv:2012.00578 [hep-ex]
81. ATLAS Collaboration, Jet reconstruction and performance using particle flow with the ATLAS detector. Eur. Phys. J. C **77**, 466 (2017). https://doi.org/10.1140/epjc/s10052-017-5031-2. arXiv:1703.10485 [hep-ex]
82. ATLAS Collaboration, Jet energy scale and resolution measured in proton–proton collisions at $\sqrt{s} = 13$ TeV with the ATLAS detector. Eur. Phys. J. C **81**, 689 (2021). https://doi.org/10.1140/epjc/s10052-021-09402-3. arXiv:2007.02645 [hep-ex]
83. R. Gauld, A. Gehrmann-De Ridder, T. Gehrmann, E. Glover, A. Huss, Precise predictions for the angular coefficients in Z-boson production at the LHC. J. High Energy Phys. **2017**, 3 (2017). https://doi.org/10.1007/JHEP11(2017)003. ISSN: 1029-8479
84. T.-J. Hou et al., New CTEQ global analysis of quantum chromodynamics with high-precision data from the LHC. Phys. Rev. D **103**, 014013 (2021). https://doi.org/10.1103/PhysRevD.103.014013. arXiv:1912.10053 [hep-ph]
85. R. Frederix, K. Hagiwara, T. Yamada, H. Yokoya, T-odd asymmetry in W+jet events at the LHC. Phys. Rev. Lett. **113**, 152001 (2014). https://doi.org/10.1103/PhysRevLett.113.15200. arXiv:1407.1016 [hep-ph]
86. K. Hagiwara, K.-I. Hikasa, N. Kai, Parity-odd asymmetries in W-jet events at hadron colliders. Phys. Rev. Lett. **52**, 1076 (1984). https://doi.org/10.1103/PhysRevLett.52.1076
87. K. Hagiwara, K.-I. Hikasa, H. Yokoya, Parity-odd asymmetries in W-jet events at the Fermilab Tevatron. Phys. Rev. Lett. **97**, 221802 (2006). https://doi.org/10.1103/PhysRevLett.97.221802. arXiv:hep-ph/0604208
88. ATLAS Collaboration, Determination of the strong coupling constant α_s from transverse energy-energy correlations in multijet events at $\sqrt{s} = 8$ TeV using the ATLAS detector. Eur. Phys. J. C **77**, 872 (2017). https://doi.org/10.1140/epjc/s10052-017-5442-0. arXiv:1707.02562 [hep-ex]
89. ATLAS Collaboration, ATLAS computing acknowledgements. ATL-SOFT-PUB-2025-001. 2025. https://cds.cern.ch/record/2922210

ATLAS Collaboration[*]

G. Aad[104], E. Aakvaag[17], B. Abbott[123], S. Abdelhameed[119a], K. Abeling[55], N. J. Abicht[49], S. H. Abidi[30], M. Aboelela[45], A. Aboulhorma[36e], H. Abramowicz[157], Y. Abulaiti[120], B. S. Acharya[69a,69b,m], A. Ackermann[63a], C. Adam Bourdarios[4], L. Adamczyk[87a], S. V. Addepalli[149], M. J. Addison[103], J. Adelman[118], A. Adiguzel[22c], T. Adye[137], A. A. Affolder[139], Y. Afik[40], M. N. Agaras[13], A. Aggarwal[102], C. Agheorghiesei[28c], F. Ahmadov[39,ad], S. Ahuja[97], S. Ahuja[169], X. Ai[143b], G. Aielli[76a,76b], A. Aikot[169], M. Ait Tamlihat[36e], B. Aitbenchikh[36a], M. Akbiyik[102], T. P. A. Åkesson[100], A. V. Akimov[151], D. Akiyama[174], N. N. Akolkar[25], S. Aktas[172], G. L. Alberghi[24b], J. Albert[171], U. Alberti[20], P. Albicocco[53], G. L. Albouy[60], S. Alderweireldt[52], Z. L. Alegria[124], M. Aleksa[37], I. N. Aleksandrov[39], C. Alexa[28b], T. Alexopoulos[10], F. Alfonsi[24b], M. Algren[56], M. Alhroob[173], B. Ali[135], H. M. J. Ali[93,w], S. Ali[32], S. W. Alibocus[94], M. Aliev[34c], G. Alimonti[71a], W. Alkakhi[55], C. Allaire[66], B. M. M. Allbrooke[152], D. R. Allen[124], J. S. Allen[103], J. F. Allen[52], P. P. Allport[21], A. Aloisio[72a,72b], F. Alonso[92], C. Alpigiani[142], Z. M. K. Alsolami[93], A. Alvarez Fernandez[102], M. Alves Cardoso[56], M. G. Alviggi[72a,72b], M. Aly[103], Y. Amaral Coutinho[83b], A. Ambler[106], C. Amelung[37], M. Amerl[103], C. G. Ames[111], T. Amezza[130], D. Amidei[108], B. Amini[54], K. Amirie[161], A. Amirkhanov[39], S. P. Amor Dos Santos[133a], K. R. Amos[169], D. Amperiadou[158], S. An[84], C. Anastopoulos[145], T. Andeen[11], J. K. Anders[94], A. C. Anderson[59], A. Andreazza[71a,71b], S. Angelidakis[9], A. Angerami[42], A. V. Anisenkov[39], A. Annovi[74a], C. Antel[37], E. Antipov[151], M. Antonelli[53], F. Anulli[75a], M. Aoki[84], T. Aoki[159], M. A. Aparo[152], L. Aperio Bella[48], M. Apicella[31], C. Appelt[157], A. Apyan[27], M. Arampatzi[10], S. J. Arbiol Val[88], C. Arcangeletti[53], A. T. H. Arce[51], J-F. Arguin[110], S. Argyropoulos[158], J.-H. Arling[48], O. Arnaez[4], H. Arnold[151], G. Artoni[75a,75b], H. Asada[113], K. Asai[121], S. Asatryan[179], N. A. Asbah[37], R. A. Ashby Pickering[173], A. M. Aslam[97], K. Assamagan[30], R. Astalos[29a], K. S. V. Astrand[100], S. Atashi[165], R. J. Atkin[34a], H. Atmani[36f], P. A. Atmasiddha[131], K. Augsten[135], A. D. Auriol[41], V. A. Austrup[103], A. S. Avad[96], G. Avolio[37], K. Axiotis[56], A. Azzam[13], D. Babal[29b], H. Bachacou[138], K. Bachas[158,q], A. Bachiu[35], E. Bachmann[50], M. J. Backes[63a], A. Badea[40], T. M. Baer[108], P. Bagnaia[75a,75b], M. Bahmani[19], D. Bahner[54], K. Bai[126], J. T. Baines[137], L. Baines[96], O. K. Baker[178], E. Bakos[16], D. Bakshi Gupta[8], L. E. Balabram Filho[83b], V. Balakrishnan[123], R. Balasubramanian[4], E. M. Baldin[38], P. Balek[87a], E. Ballabene[24a,24b], F. Balli[138], L. M. Baltes[63a], W. K. Balunas[33], J. Balz[102], I. Bamwidhi[119b], E. Banas[88], M. Bandieramonte[132], A. Bandyopadhyay[25], S. Bansal[25], L. Barak[157], M. Barakat[48], E. L. Barberio[107], D. Barberis[18b], M. Barbero[104], M. Z. Barel[117], T. Barillari[112], M-S. Barisits[37], T. Barklow[149], P. Baron[136], D. A. Baron Moreno[103], A. Baroncelli[62], A. J. Barr[129], J. D. Barr[98], F. Barreiro[101], J. Barreiro Guimarães da Costa[14], M. G. Barros Teixeira[133a], S. Barsov[38], F. Bartels[63a], R. Bartoldus[149], A. E. Barton[93], P. Bartos[29a], M. Baselga[49], S. Bashiri[88], A. Bassalat[66,b], M. J. Basso[162a], S. Bataju[45], R. Bate[170], R. L. Bates[59], S. Batlamous[101], M. Battaglia[139], D. Battulga[19], M. Bauce[75a,75b], M. Bauer[79], P. Bauer[25], L. T. Bayer[48], L. T. Bazzano Hurrell[31], J. B. Beacham[112], T. Beau[130], J. Y. Beaucamp[92], P. H. Beauchemin[164], P. Bechtle[25], H. P. Beck[20,p], K. Becker[173], A. J. Beddall[82], V. A. Bednyakov[39], C. P. Bee[151], L. J. Beemster[16], M. Begalli[83d], M. Begel[30], J. K. Behr[48], J. F. Beirer[37], F. Beisiegel[25], M. Belfkir[119b], G. Bella[157], L. Bellagamba[24b], A. Bellerive[35], C. D. Bellgraph[68], P. Bellos[21], K. Beloborodov[38], I. Benaoumeur[21], D. Benchekroun[36a], F. Bendebba[36a], Y. Benhammou[157], K. C. Benkendorfer[61], L. Beresford[48], M. Beretta[53], E. Bergeaas Kuutmann[167], N. Berger[4], B. Bergmann[135], J. Beringer[18a], G. Bernardi[5], C. Bernius[149], F. U. Bernlochner[25], A. Berrocal Guardia[13], T. Berry[97], P. Berta[136], A. Berthold[50], A. Berti[133a], R. Bertrand[104], S. Bethke[112], A. Betti[75a,75b], A. J. Bevan[96], L. Bezio[56], N. K. Bhalla[54], S. Bharthuar[112], S. Bhatta[151], P. Bhattarai[149], Z. M. Bhatti[120], K. D. Bhide[54], V. S. Bhopatkar[124], R. M. Bianchi[132], G. Bianco[24a,24b], O. Biebel[111], M. Biglietti[77a], C. S. Billingsley[45], Y. Bimgdi[36f], M. Bindi[55], A. Bingham[177], A. Bingul[22b], C. Bini[75a,75b], G. A. Bird[33], M. Birman[175], M. Biros[136], S. Biryukov[152], T. Bisanz[49], E. Bisceglie[24a,24b], J. P. Biswal[137], D. Biswas[147], I. Bloch[48], A. Blue[59], U. Blumenschein[96], V. S. Bobrovnikov[39], L. Boccardo[57a,57b], M. Boehler[54], B. Boehm[172], D. Bogavac[13], A. G. Bogdanchikov[38], L. S. Boggia[130], V. Boisvert[97], P. Bokan[37], T. Bold[87a], M. Bomben[5], M. Bona[96], M. Boonekamp[138], A. G. Borbély[59], I. S. Bordulev[38], G. Borissov[93], D. Bortoletto[129], D. Boscherini[24b], M. Bosman[13], K. Bouaouda[36a], N. Bouchhar[169], L. Boudet[4], J. Boudreau[132], E. V. Bouhova-Thacker[93], D. Boumediene[41], R. Bouquet[57a,57b], A. Boveia[122], J. Boyd[37], D. Boye[30], I. R. Boyko[39], L. Bozianu[56], J. Bracinik[21], N. Brahimi[4], G. Brandt[177], O. Brandt[33], B. Brau[105],

J. E. Brau[126], R. Brener[175], L. Brenner[117], R. Brenner[167], S. Bressler[175], G. Brianti[78a,78b], D. Britton[59], D. Britzger[112], I. Brock[25], R. Brock[109], G. Brooijmans[42], A. J. Brooks[68], E. M. Brooks[162b], E. Brost[30], L. M. Brown[162a,171], L. E. Bruce[61], T. L. Bruckler[129], P. A. Bruckman de Renstrom[88], B. Brüers[48], A. Bruni[24b], G. Bruni[24b], D. Brunner[47a,47b], M. Bruschi[24b], N. Bruscino[75a,75b], T. Buanes[17], Q. Buat[142], D. Buchin[112], A. G. Buckley[59], O. Bulekov[82], B. A. Bullard[149], S. Burdin[94], C. D. Burgard[49], A. M. Burger[91], B. Burghgrave[8], O. Burlayenko[54], J. Burleson[168], J. C. Burzynski[148], E. L. Busch[42], V. Büscher[102], P. J. Bussey[59], O. But[25], J. M. Butler[26], C. M. Buttar[59], J. M. Butterworth[98], W. Buttinger[137], C. J. Buxo Vazquez[109], A. R. Buzykaev[39], S. Cabrera Urbán[169], L. Cadamuro[66], H. Cai[37], Y. Cai[24a,24b,114c], Y. Cai[114a], V. M. M. Cairo[37], O. Cakir[3a], N. Calace[37], P. Calafiura[18a], G. Calderini[130], P. Calfayan[35], L. Calic[100], G. Callea[59], L. P. Caloba[83b], D. Calvet[41], S. Calvet[41], R. Camacho Toro[130], S. Camarda[37], D. Camarero Munoz[27], P. Camarri[76a,76b], C. Camincher[171], M. Campanelli[98], A. Camplani[43], V. Canale[72a,72b], A. C. Canbay[3a], E. Canonero[97], J. Cantero[169], Y. Cao[168], F. Capocasa[27], M. Capua[44a,44b], A. Carbone[71a,71b], R. Cardarelli[76a], J. C. J. Cardenas[8], M. P. Cardiff[27], G. Carducci[44a,44b], T. Carli[37], G. Carlino[72a], J. I. Carlotto[13], B. T. Carlson[132,r], E. M. Carlson[171], J. Carmignani[94], L. Carminati[71a,71b], A. Carnelli[4], M. Carnesale[37], S. Caron[116], E. Carquin[140g], I. B. Carr[107], S. Carrá[73a,73b], G. Carratta[24a,24b], C. Carrion Martinez[169], A. M. Carroll[126], M. P. Casado[13,h], P. Casolaro[72a,72b], M. Caspar[48], W. R. Castiglioni[40], F. L. Castillo[4], L. Castillo Garcia[13], V. Castillo Gimenez[169], N. F. Castro[133a,133e], A. Catinaccio[37], J. R. Catmore[128], T. Cavaliere[4], V. Cavaliere[30], L. J. Caviedes Betancourt[23b], E. Celebi[82], S. Cella[37], V. Cepaitis[56], K. Cerny[125], A. S. Cerqueira[83a], A. Cerri[74a,am], L. Cerrito[76a,76b], F. Cerutti[18a], B. Cervato[71a,71b], A. Cervelli[24b], G. Cesarini[53], S. A. Cetin[82], P. M. Chabrillat[130], R. Chakkappai[66], S. Chakraborty[173], A. Chambers[61], J. Chan[18a], W. Y. Chan[159], J. D. Chapman[33], E. Chapon[138], B. Chargeishvili[155b], D. G. Charlton[21], C. Chauhan[136], Y. Che[114a], S. Chekanov[6], G. A. Chelkov[39,a], B. Chen[157], B. Chen[171], H. Chen[114a], H. Chen[30], J. Chen[144a], J. Chen[148], M. Chen[129], S. Chen[89], S. J. Chen[114a], X. Chen[144a], X. Chen[15,ah], Z. Chen[62], C. L. Cheng[176], H. C. Cheng[64a], S. Cheong[149], A. Cheplakov[39], E. Cherepanova[117], R. Cherkaoui El Moursli[36e], E. Cheu[7], K. Cheung[65], L. Chevalier[138], V. Chiarella[53], G. Chiarelli[74a], G. Chiodini[70a], A. S. Chisholm[21], A. Chitan[28b], M. Chitishvili[169], M. V. Chizhov[39,s], K. Choi[11], Y. Chou[142], E. Y. S. Chow[116], K. L. Chu[175], M. C. Chu[64a], X. Chu[14,114c], Z. Chubinidze[53], J. Chudoba[134], J. J. Chwastowski[88], D. Cieri[112], K. M. Ciesla[87a], V. Cindro[95], A. Ciocio[18a], F. Cirotto[72a,72b], Z. H. Citron[175], M. Citterio[71a], D. A. Ciubotaru[28b], A. Clark[56], P. J. Clark[52], N. Clarke Hall[98], C. Clarry[161], S. E. Clawson[48], C. Clement[47a,47b], L. Clissa[24a,24b], Y. Coadou[104], M. Cobal[69a,69c], A. Coccaro[57b], R. F. Coelho Barrue[133a], R. Coelho Lopes De Sa[105], S. Coelli[71a], L. S. Colangeli[161], B. Cole[42], P. Collado Soto[101], J. Collot[60], R. Coluccia[70a,70b], P. Conde Muiño[133a,133g], M. P. Connell[34c], S. H. Connell[34c], E. I. Conroy[129], M. Contreras Cossio[11], F. Conventi[72a,aj], A. M. Cooper-Sarkar[129], L. Corazzina[75a,75b], F. A. Corchia[24a,24b], A. Cordeiro Oudot Choi[142], L. D. Corpe[41], M. Corradi[75a,75b], F. Corriveau[106,ab], A. Cortes-Gonzalez[159], M. J. Costa[169], F. Costanza[4], D. Costanzo[145], J. Couthures[4], G. Cowan[97], K. Cranmer[176], L. Cremer[49], D. Cremonini[24a,24b], S. Crépé-Renaudin[60], F. Crescioli[130], T. Cresta[73a,73b], M. Cristinziani[147], M. Cristoforetti[78a,78b], E. Critelli[98], V. Croft[117], G. Crosetti[44a,44b], A. Cueto[101], H. Cui[98], Z. Cui[7], B. M. Cunnett[152], W. R. Cunningham[59], F. Curcio[169], J. R. Curran[52], M. J. Da Cunha Sargedas De Sousa[57a,57b], J. V. Da Fonseca Pinto[83b], C. Da Via[103], W. Dabrowski[87a], T. Dado[37], S. Dahbi[154], T. Dai[108], D. Dal Santo[20], C. Dallapiccola[105], M. Dam[43], G. D'amen[30], V. D'Amico[111], J. R. Dandoy[35], M. D'Andrea[57a,57b], D. Dannheim[37], G. D'anniballe[74a,74b], M. Danninger[148], V. Dao[151], G. Darbo[57b], S. J. Das[30], F. Dattola[48], S. D'Auria[71a,71b], A. D'Avanzo[72a,72b], T. Davidek[136], J. Davidson[173], I. Dawson[96], K. De[8], C. De Almeida Rossi[161], R. De Asmundis[72a], N. De Biase[48], S. De Castro[24a,24b], N. De Groot[116], P. de Jong[117], H. De la Torre[118], A. De Maria[114a], A. De Salvo[75a], U. De Sanctis[76a,76b], F. De Santis[70a,70b], A. De Santo[152], J. B. De Vivie De Regie[60], J. Debevc[95], D. V. Dedovich[39], J. Degens[94], A. M. Deiana[45], J. Del Peso[101], L. Delagrange[130], F. Deliot[138], C. M. Delitzsch[49], M. Della Pietra[72a,72b], D. Della Volpe[56], A. Dell'Acqua[37], L. Dell'Asta[71a,71b], M. Delmastro[4], C. C. Delogu[57a,57b], P. A. Delsart[60], S. Demers[178], M. Demichev[39], S. P. Denisov[38], H. Denizli[22a,l], L. D'Eramo[41], D. Derendarz[88], F. Derue[130], P. Dervan[94,*], A. M. Desai[1], K. Desch[25], F. A. Di Bello[57a,57b], A. Di Ciaccio[76a,76b], L. Di Ciaccio[4], A. Di Domenico[75a,75b], C. Di Donato[72a,72b], A. Di Girolamo[37], G. Di Gregorio[62], A. Di Luca[78a,78b], B. Di Micco[77a,77b], R. Di Nardo[77a,77b], K. F. Di Petrillo[40], M. Diamantopoulou[35], F. A. Dias[117], M. A. Diaz[140a,140b], A. R. Didenko[39], M. Didenko[169], S. D. Diefenbacher[18a], E. B. Diehl[108],

S. Díez Cornell[48], C. Diez Pardos[147], C. Dimitriadi[150], A. Dimitrievska[21], A. Dimri[151], Y. Ding[62], J. Dingfelder[25], T. Dingley[129], I-M. Dinu[28b], S. J. Dittmeier[63b], F. Dittus[37], M. Divisek[136], B. Dixit[94], F. Djama[104], T. Djobava[155b], C. Doglioni[100,103], A. Dohnalova[29a], Z. Dolezal[136], K. Domijan[87a], K. M. Dona[40], M. Donadelli[83d], B. Dong[109], J. Donini[41], A. D'Onofrio[72a,72b], M. D'Onofrio[94], J. Dopke[137], A. Doria[72a], N. Dos Santos Fernandes[133a], I. A. Dos Santos Luz[83e], P. Dougan[103], M. T. Dova[92], A. T. Doyle[59], M. P. Drescher[55], E. Dreyer[175], I. Drivas-koulouris[10], M. Drnevich[120], D. Du[62], T. A. du Pree[117], Z. Duan[114a], M. Dubau[4], F. Dubinin[39], M. Dubovsky[29a], E. Duchovni[175], G. Duckeck[111], P. K. Duckett[98], O. A. Ducu[28b], D. Duda[52], A. Dudarev[37], M. M. Dudek[88], E. R. Duden[27], M. D'uffizi[103], L. Duflot[66], M. Dührssen[37], I. Duminica[28g], A. E. Dumitriu[28b], M. Dunford[63a], K. Dunne[47a,47b], A. Duperrin[104], H. Duran Yildiz[3a], A. Durglishvili[155b], G. I. Dyckes[18a], M. Dyndal[87a], B. S. Dziedzic[37], Z. O. Earnshaw[152], G. H. Eberwein[129], B. Eckerova[29a], S. Eggebrecht[55], E. Egidio Purcino De Souza[83e], G. Eigen[17], K. Einsweiler[18a], T. Ekelof[167], P. A. Ekman[100], S. El Farkh[36b], Y. El Ghazali[62], H. El Jarrari[34j], A. El Moussaouy[36a], D. Elitez[37], M. Ellert[167], F. Ellinghaus[177], T. A. Elliot[97], N. Ellis[37], J. Elmsheuser[30], M. Elsawy[119a], M. Elsing[37], D. Emeliyanov[137], Y. Enari[84], S. Epari[110], D. Ernani Martins Neto[88], F. Ernst[37], M. Escalier[66], C. Escobar[169], E. Etzion[157], G. Evans[133a,133b], H. Evans[68], L. S. Evans[48], A. Ezhilov[38], S. Ezzarqtouni[36a], F. Fabbri[24a,24b], L. Fabbri[24a,24b], G. Facini[98], V. Fadeyev[139], R. M. Fakhrutdinov[38], D. Fakoudis[102], S. Falciano[75a], L. F. Falda Ulhoa Coelho[133a], F. Fallavollita[112], G. Falsetti[44a,44b], J. Faltova[136], C. Fan[168], K. Y. Fan[64b], Y. Fan[14], Y. Fang[14,114c], M. Fanti[71a,71b], M. Faraj[69a,69b], Z. Farazpay[99], A. Farbin[8], A. Farilla[77a], K. Farman[154], T. Farooque[109], J. N. Farr[178], M. S. Farrington[61], S. M. Farrington[52,137], F. Fassi[36e], D. Fassouliotis[9], L. Fayard[66], P. Federic[136], P. Federicova[134], O. L. Fedin[38,a], M. Feickert[176], L. Feligioni[104], D. E. Fellers[18a], C. Feng[143a], Y. Feng[14], Z. Feng[117], M. J. Fenton[165], L. Ferencz[48], B. Fernandez Barbadillo[93], P. Fernandez Martinez[67], M. J. V. Fernoux[104], J. Ferrando[93], A. Ferrari[167], P. Ferrari[116,117], R. Ferrari[73a], D. Ferrere[56], C. Ferretti[108], M. P. Fewell[1], D. Fiacco[75a,75b], F. Fiedler[102], P. Fiedler[135], S. Filimonov[39], M. S. Filip[28b,t], A. Filipčič[95], E. K. Filmer[162a], F. Filthaut[116], M. C. N. Fiolhais[133a,133c,c], L. Fiorini[169], W. C. Fisher[109], T. Fitschen[103], P. M. Fitzhugh[138], I. Fleck[147], P. Fleischmann[108], T. Flick[177], M. Flores[34d,ag], L. R. Flores Castillo[64a], L. Flores Sanz De Acedo[37], F. M. Follega[78a,78b], N. Fomin[33], J. H. Foo[161], A. Formica[138], A. C. Forti[103], E. Fortin[37], A. W. Fortman[18a], L. Foster[18a], L. Fountas[9,i], D. Fournier[66], H. Fox[93], P. Francavilla[74a,74b], S. Francescato[61], S. Franchellucci[56], M. Franchini[24a,24b], S. Franchino[63a], D. Francis[37], L. Franco[116], L. Franconi[48], M. Franklin[61], G. Frattari[27], Y. Y. Frid[157], J. Friend[59], N. Fritzsche[37], A. Froch[56], D. Froidevaux[37], J. A. Frost[137], Y. Fu[109], S. Fuenzalida Garrido[140g], M. Fujimoto[151], K. Y. Fung[64a], E. Furtado De Simas Filho[83e], M. Furukawa[159], J. Fuster[169], A. Gaa[55], A. Gabrielli[24a,24b], A. Gabrielli[161], P. Gadow[37], G. Gagliardi[57a,57b], L. G. Gagnon[18a], S. Gaid[85b], S. Galantzan[157], J. Gallagher[1], E. J. Gallas[129], A. L. Gallen[167], B. J. Gallop[137], K. K. Gan[122], S. Ganguly[159], Y. Gao[52], A. Garabaglu[142], F. M. Garay Walls[140a,140b], C. García[169], A. Garcia Alonso[117], A. G. Garcia Caffaro[178], J. E. García Navarro[169], M. A. Garcia Ruiz[23b], M. Garcia-Sciveres[18a], G. L. Gardner[131], R. W. Gardner[40], N. Garelli[164], R. B. Garg[149], J. M. Gargan[33], C. A. Garner[161], C. M. Garvey[34a], V. K. Gassmann[164], G. Gaudio[73a], V. Gautam[13], P. Gauzzi[75a,75b], J. Gavranovic[95], I. L. Gavrilenko[133a], A. Gavrilyuk[38], C. Gay[170], G. Gaycken[126], E. N. Gazis[10], A. Gekow[122], C. Gemme[57b], M. H. Genest[60], A. D. Gentry[115], S. George[97], T. Geralis[46], A. A. Gerwin[123], P. Gessinger-Befurt[37], M. E. Geyik[177], M. Ghani[173], K. Ghorbanian[96], A. Ghosal[147], A. Ghosh[165], A. Ghosh[7], B. Giacobbe[24b], S. Giagu[75a,75b], T. Giani[117], A. Giannini[62], S. M. Gibson[97], M. Gignac[139], D. T. Gil[87b], A. K. Gilbert[87a], B. J. Gilbert[42], D. Gillberg[35], G. Gilles[117], D. M. Gingrich[2,ai], M. P. Giordani[69a,69c], P. F. Giraud[138], G. Giugliarelli[69a,69c], D. Giugni[71a], F. Giuli[76a,76b], I. Gkialas[9,i], L. K. Gladilin[38], C. Glasman[101], M. Glazewska[20], R. M. Gleason[165], G. Glemža[48], M. Glisic[126], I. Gnesi[44b], Y. Go[30], M. Goblirsch-Kolb[37], B. Gocke[49], D. Godin[110], B. Gokturk[22a], S. Goldfarb[107], T. Golling[56], M. G. D. Gololo[34c], D. Golubkov[38], J. P. Gombas[109], A. Gomes[133a,133b], G. Gomes Da Silva[147], A. J. Gomez Delegido[37], R. Gonçalo[133a], L. Gonella[21], A. Gongadze[155c], F. Gonnella[21], J. L. Gonski[149], R. Y. González Andana[52], S. González de la Hoz[169], M. V. Gonzalez Rodrigues[48], R. Gonzalez Suarez[167], S. Gonzalez-Sevilla[56], L. Goossens[37], B. Gorini[37], E. Gorini[70a,70b], A. Gorišek[95], T. C. Gosart[131], A. T. Goshaw[51], M. I. Gostkin[39], S. Goswami[124], C. A. Gottardo[37], S. A. Gotz[111], M. Gouighri[36b], A. G. Goussiou[142], N. Govender[34c], R. P. Grabarczyk[129], I. Grabowska-Bold[87a], K. Graham[35], E. Gramstad[128], S. Grancagnolo[70a,70b], C. M. Grant[1], P. M. Gravila[28f], F. G. Gravili[70a,70b], H. M. Gray[18a], M. Greco[112], M. J. Green[1], C. Grefe[25], A. S. Grefsrud[17], I. M. Gregor[48],

K. T. Greif[165], P. Grenier[149], S. G. Grewe[112], A. A. Grillo[139], K. Grimm[32], S. Grinstein[13,x], J.-F. Grivaz[66], E. Gross[175], J. Grosse-Knetter[55], L. Guan[108], G. Guerrieri[37], R. Guevara[128], R. Gugel[102], J. A. M. Guhit[108], A. Guida[19], E. Guilloton[173], S. Guindon[37], F. Guo[14,114c], J. Guo[144a], L. Guo[48], L. Guo[114b,v], Y. Guo[108], Y. Guo[42], A. Gupta[49], R. Gupta[132], S. Gupta[27], S. Gurbuz[25], S. S. Gurdasani[48], G. Gustavino[75a,75b], P. Gutierrez[123], L. F. Gutierrez Zagazeta[131], M. Gutsche[50], C. Gutschow[98], C. Gwenlan[129], C. B. Gwilliam[94], E. S. Haaland[128], A. Haas[120], M. Habedank[59], C. Haber[18a], H. K. Hadavand[8], A. Haddad[41], A. Hadef[50], A. I. Hagan[93], J. J. Hahn[147], E. H. Haines[98], M. Haleem[172], J. Haley[124], G. D. Hallewell[104], J. A. Hallford[48], K. Hamano[171], H. Hamdaoui[167], M. Hamer[25], S. E. D. Hammoud[66], E. J. Hampshire[97], J. Han[143a], L. Han[114a], L. Han[62], S. Han[14], K. Hanagaki[84], M. Hance[139], D. A. Hangal[42], H. Hanif[148], M. D. Hank[131], J. B. Hansen[43], P. H. Hansen[43], T. Harenberg[177], S. Harkusha[179], M. L. Harris[105], Y. T. Harris[25], J. Harrison[13], N. M. Harrison[122], P. F. Harrison[173], M. L. E. Hart[98], N. M. Hartman[112], N. M. Hartmann[111], R. Z. Hasan[97,137], Y. Hasegawa[146], F. Haslbeck[129], S. Hassan[17], R. Hauser[109], M. Haviernik[136], C. M. Hawkes[21], R. J. Hawkings[37], Y. Hayashi[159], D. Hayden[109], C. Hayes[108], R. L. Hayes[117], C. P. Hays[129], J. M. Hays[96], H. S. Hayward[94], M. He[14,114c], Y. He[48], Y. He[98], N. B. Heatley[96], V. Hedberg[100], J. Heilman[35], S. Heim[48], T. Heim[18a], J. J. Heinrich[126], L. Heinrich[112], J. Hejbal[134], M. Helbig[50], A. Held[176], S. Hellesund[17], C. M. Helling[170], S. Hellman[47a,47b], A. M. Henriques Correia[37], H. Herde[100], Y. Hernández Jiménez[151], L. M. Herrmann[25], T. Herrmann[50], G. Herten[54], R. Hertenberger[111], L. Hervas[37], M. E. Hesping[102], N. P. Hessey[162a], J. Hessler[112], M. Hidaoui[36b], N. Hidic[136], E. Hill[161], T. S. Hillersoy[17], S. J. Hillier[21], J. R. Hinds[109], F. Hinterkeuser[25], M. Hirose[127], S. Hirose[163], D. Hirschbuehl[177], T. G. Hitchings[103], B. Hiti[95], J. Hobbs[151], R. Hobincu[28e], N. Hod[175], A. M. Hodges[168], M. C. Hodgkinson[145], B. H. Hodkinson[129], A. Hoecker[37], D. D. Hofer[108], J. Hofer[169], J. Hofner[102], M. Holzbock[37], L. B. A. H. Hommels[33], V. Homsak[129], B. P. Honan[103], J. J. Hong[68], T. M. Hong[132], B. H. Hooberman[168], W. H. Hopkins[6], M. C. Hoppesch[168], Y. Horii[113], M. E. Horstmann[112], S. Hou[154], M. R. Housenga[168], J. Howarth[59], J. Hoya[6], M. Hrabovsky[125], T. Hryn'ova[4], P. J. Hsu[65], S.-C. Hsu[142], T. Hsu[66], M. Hu[18a], Q. Hu[62], S. Huang[33], X. Huang[14,114c], Y. Huang[136], Y. Huang[114b], Y. Huang[14], Z. Huang[66], Z. Hubacek[135], F. Huegging[25], T. B. Huffman[129], M. Hufnagel Maranha De Faria[83a], C. A. Hugli[48], M. Huhtinen[37], S. K. Huiberts[128], R. Hulsken[106], C. E. Hultquist[18a], D. L. Humphreys[105], N. Huseynov[12], J. Huston[109], J. Huth[61], L. Huth[48], R. Hyneman[7], G. Iacobucci[56], G. Iakovidis[30], L. Iconomidou-Fayard[66], J. P. Iddon[37], P. Iengo[72a,72b], Y. Iiyama[159], T. Iizawa[159], Y. Ikegami[84], D. Iliadis[158], N. Ilic[161], H. Imam[36a], G. Inacio Goncalves[83d], S. A. Infante Cabanas[140c], T. Ingebretsen Carlson[47a,47b], J. M. Inglis[96], G. Introzzi[73a,73b], M. Iodice[77a], V. Ippolito[75a,75b], R. K. Irwin[94], M. Ishino[159], W. Islam[176], C. Issever[19], S. Istin[22a,ao], K. Itabashi[127], H. Ito[174], R. Iuppa[78a,78b], A. Ivina[175], V. Izzo[72a], P. Jacka[135], P. Jackson[1], R. M. Jacobs[48], P. Jain[48], K. Jakobs[54], T. Jakoubek[175], J. Jamieson[59], W. Jang[159], S. Jankovych[136], M. Javurkova[105], P. Jawahar[103], L. Jeanty[126], J. Jejelava[155a,ae], P. Jenni[54,f], C. E. Jessiman[35], C. Jia[143a], H. Jia[170], J. Jia[151], X. Jia[112,114c], Z. Jia[114a], C. Jiang[52], Q. Jiang[64b], S. Jiggins[48], M. Jimenez Ortega[169], J. Jimenez Pena[13], S. Jin[114a], A. Jinaru[28b], O. Jinnouchi[141], P. Johansson[145], K. A. Johns[7], J. W. Johnson[139], F. A. Jolly[48], D. M. Jones[152], E. Jones[48], K. S. Jones[8], P. Jones[33], R. W. L. Jones[93], T. J. Jones[94], H. L. Joos[55], R. Joshi[122], J. Jovicevic[16], X. Ju[18a], J. J. Junggeburth[37], T. Junkermann[63a], A. Juste Rozas[13,x], M. K. Juzek[88], S. Kabana[140f], A. Kaczmarska[88], S. A. Kadir[149], M. Kado[112], H. Kagan[122], M. Kagan[149], A. Kahn[131], C. Kahra[102], T. Kaji[159], E. Kajomovitz[156], N. Kakati[175], N. Kakoty[13], I. Kalaitzidou[54], S. Kandel[8], N. Kanellos[10], N. J. Kang[139], D. Kar[34j], E. Karentzos[25], K. Karki[8], O. Karkout[117], S. N. Karpov[39], Z. M. Karpova[39], V. Kartvelishvili[93,155b], A. N. Karyukhin[38], E. Kasimi[158], J. Katzy[48], S. Kaur[35], K. Kawade[146], M. P. Kawale[123], C. Kawamoto[89], T. Kawamoto[62], E. F. Kay[37], S. Kazakos[109], V. F. Kazanin[38], J. M. Keaveney[34a], R. Keeler[171], G. V. Kehris[61], J. S. Keller[35], J. M. Kelly[171], J. J. Kempster[152], O. Kepka[134], J. Kerr[162b], B. P. Kerridge[137], B. P. Kerševan[95], L. Keszeghova[29a], R. A. Khan[132], A. Khanov[124], A. G. Kharlamov[38], T. Kharlamova[38], E. E. Khoda[142], M. Kholodenko[133a], T. J. Khoo[19], G. Khoriauli[172], Y. Khoulaki[36a], Y. A. R. Khwaira[130], B. Kibirige[34j], D. Kim[6], D. W. Kim[18b], Y. K. Kim[40], N. Kimura[98], M. K. Kingston[55], A. Kirchhoff[55], C. Kirfel[25], F. Kirfel[25], J. Kirk[137], A. E. Kiryunin[112], S. Kita[163], O. Kivernyk[25], M. Klassen[164], C. Klein[35], L. Klein[172], M. H. Klein[45], S. B. Klein[56], U. Klein[94], A. Klimentov[30], T. Klioutchnikova[37], P. Kluit[117], S. Kluth[112], E. Kneringer[79], T. M. Knight[161], A. Knue[49], M. Kobel[50], D. Kobylianskii[175], S. F. Koch[129], M. Kocian[149], P. Kodyš[136], D. M. Koeck[126], T. Koffas[35], O. Kolay[50], I. Koletsou[4], T. Komarek[88], K. Köneke[55], A. X. Y. Kong[1], T. Kono[121],

N. Konstantinidis[98], P. Kontaxakis[56], B. Konya[100], R. Kopeliansky[42], S. Koperny[87a], R. Koppenhofer[54], K. Korcyl[88], K. Kordas[158,d], A. Korn[98], S. Korn[55], I. Korolkov[13], N. Korotkova[38], B. Kortman[117], O. Kortner[112], S. Kortner[112], W. H. Kostecka[118], M. Kostov[29a], V. V. Kostyukhin[147], A. Kotsokechagia[37], A. Kotwal[51], A. Koulouris[37], A. Kourkoumeli-Charalampidi[73a,73b], C. Kourkoumelis[9], E. Kourlitis[112], O. Kovanda[126], R. Kowalewski[171], W. Kozanecki[126], A. S. Kozhin[38], V. A. Kramarenko[38], G. Kramberger[95], P. Kramer[25], M. W. Krasny[130], A. Krasznahorkay[105], A. C. Kraus[118], J. W. Kraus[177], J. A. Kremer[48], N. B. Krengel[147], T. Kresse[50], L. Kretschmann[177], J. Kretzschmar[94], P. Krieger[161], K. Krizka[21], K. Kroeninger[49], H. Kroha[112], J. Kroll[134], J. Kroll[131], K. S. Krowpman[109], U. Kruchonak[39], H. Krüger[25], N. Krumnack[81], M. C. Kruse[51], O. Kuchinskaia[39], S. Kuday[3a], S. Kuehn[37], R. Kuesters[54], T. Kuhl[48], V. Kukhtin[39], Y. Kulchitsky[39], S. Kuleshov[140b,140d], J. Kull[1], E. V. Kumar[111], M. Kumar[34j], N. Kumari[48], P. Kumari[162b], A. Kupco[134], A. Kupich[38], O. Kuprash[54], H. Kurashige[86], L. L. Kurchaninov[162a], O. Kurdysh[4], A. Kurova[38], M. Kuze[141], A. K. Kvam[105], J. Kvita[125], N. G. Kyriacou[142], M. Laassiri[30], C. Lacasta[169], F. Lacava[75a,75b], H. Lacker[19], D. Lacour[130], N. N. Lad[98], E. Ladygin[39], A. Lafarge[41], B. Laforge[130], T. Lagouri[178], F. Z. Lahbabi[36a], S. Lai[37,55], W. S. Lai[98], J. E. Lambert[171], S. Lammers[68], W. Lampl[7], C. Lampoudis[158,d], G. Lamprinoudis[172], A. N. Lancaster[118], E. Lançon[30], U. Landgraf[54], M. P. J. Landon[96], V. S. Lang[54], A. J. Lankford[165], F. Lanni[37], K. Lantzsch[25], A. Lanza[73a], M. Lanzac Berrocal[169], J. F. Laporte[138], T. Lari[71a], D. Larsen[17], L. Larson[11], F. Lasagni Manghi[24b], M. Lassnig[37], S. D. Lawlor[145], R. Lazaridou[165], M. Lazzaroni[71a,71b], E. T. T. Le[165], H. D. M. Le[109], E. M. Le Boulicaut[178], L. T. Le Pottier[18a], B. Leban[24a,24b], F. Ledroit-Guillon[60], T. F. Lee[162b], L. L. Leeuw[34c], M. Lefebvre[171], C. Leggett[18a], G. Lehmann Miotto[37], M. Leigh[56], W. A. Leight[105], W. Leinonen[116], A. Leisos[158,u], M. A. L. Leite[83c], C. E. Leitgeb[19], R. Leitner[136], K. J. C. Leney[45], T. Lenz[25], S. Leone[74a], C. Leonidopoulos[52], A. Leopold[150], J. LePage Bourbonnais[35], R. Les[109], C. G. Lester[33], M. Levchenko[38], J. Levêque[4], L. J. Levinson[175], G. Levrini[24a,24b], M. P. Lewicki[88], C. Lewis[142], D. J. Lewis[4], L. Lewitt[145], A. Li[30], B. Li[143a], C. Li[108], C-Q. Li[112], H. Li[143a], H. Li[103], H. Li[15], H. Li[62], H. Li[143a], J. Li[144a], K. Li[14], L. Li[144a], R. Li[178], S. Li[14,114c], S. Li[144a,144b], T. Li[5], X. Li[106], Y. Li[14], Z. Li[159], Z. Li[14,114c], Z. Li[62], S. Liang[14,114c], Z. Liang[14], M. Liberatore[138], B. Liberti[76a], G. B. Libotte[83d], K. Lie[64c], J. Lieber Marin[83e], H. Lien[68], H. Lin[108], S. F. Lin[151], L. Linden[111], R. E. Lindley[7], J. H. Lindon[37], J. Ling[61], E. Lipeles[131], A. Lipniacka[17], A. Lister[170], J. D. Little[68], B. Liu[14], B. X. Liu[114b], D. Liu[144b], D. Liu[139], E. H. L. Liu[21], J. K. K. Liu[120], K. Liu[144b], K. Liu[144a,144b], M. Liu[62], M. Y. Liu[62], P. Liu[14], Q. Liu[149], S. Liu[151], X. Liu[62], X. Liu[143a], Y. Liu[114b,114c], Y. Liu[168], Y. L. Liu[143a], Y. W. Liu[62], Z. Liu[66,k], S. L. Lloyd[96], E. M. Lobodzinska[48], P. Loch[7], E. Lodhi[161], K. Lohwasser[145], E. Loiacono[48], J. D. Lomas[21], J. D. Long[42], I. Longarini[165], R. Longo[168], A. Lopez Solis[13], N. A. Lopez-canelas[7], N. Lorenzo Martinez[4], A. M. Lory[111], M. Losada[119a], G. Löschcke Centeno[4], X. Lou[47a,47b], X. Lou[14,114c], A. Lounis[66], P. A. Love[93], M. Lu[66], S. Lu[131], Y. J. Lu[154], H. J. Lubatti[142], C. Luci[75a,75b], F. L. Lucio Alves[114a], F. Luehring[68], B. S. Lunday[131], O. Lundberg[150], J. Lunde[37], N. A. Luongo[6], M. S. Lutz[37], A. B. Lux[26], D. Lynn[30], R. Lysak[134], V. Lysenko[135], E. Lytken[100], V. Lyubushkin[39], T. Lyubushkina[39], M. M. Lyukova[151], H. Ma[30], K. Ma[62], L. L. Ma[143a], W. Ma[62], Y. Ma[124], J. C. MacDonald[102], P. C. Machado De Abreu Farias[83e], D. Macina[37], R. Madar[41], T. Madula[98], J. Maeda[86], T. Maeno[30], P. T. Mafa[34c,j], H. Maguire[145], M. Maheshwari[33], V. Maiboroda[66], A. Maio[133a,133b,133d], K. Maj[87a], O. Majersky[48], S. Majewski[126], R. Makhmanazarov[38], N. Makovec[66], V. Maksimovic[16], B. Malaescu[130], J. Malamant[128], Pa. Malecki[88], V. P. Maleev[38], F. Malek[60,o], M. Mali[95], D. Malito[97], U. Mallik[80,*], A. Maloizel[5], S. Maltezos[10], A. Malvezzi Lopes[83d], S. Malyukov[39], J. Mamuzic[95], G. Mancini[53], M. N. Mancini[27], G. Manco[73a,73b], J. P. Mandalia[96], S. S. Mandarry[152], I. Mandić[95], L. Manhaes de Andrade Filho[83a], I. M. Maniatis[175], J. Manjarres Ramos[91], D. C. Mankad[175], A. Mann[111], T. Manoussos[37], M. N. Mantinan[40], S. Manzoni[37], L. Mao[144a], X. Mapekula[34c], A. Marantis[158], R. R. Marcelo Gregorio[96], G. Marchiori[5], C. Marcon[71a], E. Maricic[16], M. Marinescu[48], S. Marium[48], M. Marjanovic[123], A. Markhoos[54], M. Markovitch[66], M. K. Maroun[105], M. C. Marr[148], G. T. Marsden[103], E. J. Marshall[93], Z. Marshall[18a], S. Marti-Garcia[169], J. Martin[98], T. A. Martin[137], V. J. Martin[52], B. Martin dit Latour[17], L. Martinelli[75a,75b], M. Martinez[13,x], P. Martinez Agullo[169], V. I. Martinez Outschoorn[105], P. Martinez Suarez[37], S. Martin-Haugh[137], G. Martinovicova[136], V. S. Martoiu[28b], A. C. Martyniuk[98], A. Marzin[37], D. Mascione[78a,78b], L. Masetti[102], J. Masik[103], A. L. Maslennikov[39], S. L. Mason[42], P. Massarotti[72a,72b], P. Mastrandrea[74a,74b], A. Mastroberardino[44a,44b], T. Masubuchi[127], T. T. Mathew[126], J. Matousek[136], D. M. Mattern[49], K. Mauer[48], J. Maurer[28b], T. Maurin[59], A. J. Maury[66], B. Maček[95], C. Mavungu Tsava[104], D. A. Maximov[38], A. E. May[103], E. Mayer[41],

R. Mazini[34j], I. Maznas[118], S. M. Mazza[139], E. Mazzeo[37], J. P. Mc Gowan[171], S. P. Mc Kee[108], C. A. Mc Lean[6], C. C. McCracken[170], E. F. McDonald[107], A. E. McDougall[117], L. F. Mcelhinney[93], J. A. Mcfayden[152], R. P. McGovern[131], R. P. Mckenzie[34j], T. C. Mclachlan[48], D. J. Mclaughlin[98], S. J. McMahon[137], C. M. Mcpartland[94], R. A. McPherson[171,ab], S. Mehlhase[111], A. Mehta[94], D. Melini[169], B. R. Mellado Garcia[34j], A. H. Melo[55], F. Meloni[48], A. M. Mendes Jacques Da Costa[103], L. Meng[93], S. Menke[112], M. Mentink[37], E. Meoni[44a,44b], G. Mercado[118], S. Merianos[158], C. Merlassino[69a,69c], C. Meroni[71a,71b], J. Metcalfe[6], A. S. Mete[6], E. Meuser[102], C. Meyer[68], J-P. Meyer[138], Y. Miao[114a], R. P. Middleton[137], M. Mihovilovic[66], L. Mijović[52], G. Mikenberg[175], M. Mikestikova[134], M. Mikuž[95], H. Mildner[102], A. Milic[37], D. W. Miller[40], E. H. Miller[149], A. Milov[175], D. A. Milstead[47a,47b], T. Min[114a], A. A. Minaenko[38], I. A. Minashvili[155b], A. I. Mincer[120], B. Mindur[87a], M. Mineev[39], Y. Mino[89], L. M. Mir[13], M. Miralles Lopez[59], M. Mironova[18a], M. Missio[41], A. Mitra[173], V. A. Mitsou[169], Y. Mitsumori[113], O. Miu[161], P. S. Miyagawa[96], T. Mkrtchyan[37], M. Mlinarevic[98], T. Mlinarevic[98], M. Mlynarikova[136], L. Mlynarska[87a], C. Mo[144a], S. Mobius[20], M. H. Mohamed Farook[115], S. Mohapatra[42], M. F. Mohd Soberi[52], S. Mohiuddin[124], G. Mokgatitswane[34j], L. Moleri[175], U. Molinatti[129], L. G. Mollier[20], B. Mondal[134], S. Mondal[135], K. Mönig[48], E. Monnier[104], L. Monsonis Romero[169], J. Montejo Berlingen[13], A. Montella[47a,47b], M. Montella[122], F. Montereali[77a,77b], F. Monticelli[92], S. Monzani[69a,69c], A. Morancho Tarda[43], N. Morange[66], A. L. Moreira De Carvalho[48], M. Moreno Llácer[169], C. Moreno Martinez[56], J. M. Moreno Perez[23b], P. Morettini[57b], S. Morgenstern[37], M. Morii[61], M. Morinaga[159], M. Moritsu[90], F. Morodei[75a,75b], P. Moschovakos[37], B. Moser[54], M. Mosidze[155b], T. Moskalets[45], P. Moskvitina[116], J. Moss[32], P. Moszkowicz[87a], T. Motta Quirino[83d], A. Moussa[36d], Y. Moyal[175], H. Moyano Gomez[13], E. J. W. Moyse[105], T. G. Mroz[88], S. Muanza[104], M. Mucha[25], J. Mueller[132], G. A. Mullier[167], A. J. Mullin[33], J. J. Mullin[51], A. C. Mullins[45], A. E. Mulski[61], D. P. Mungo[161], D. Munoz Perez[169], F. J. Munoz Sanchez[103], W. J. Murray[137,173], M. Muškinja[95], C. Mwewa[48], A. G. Myagkov[38,a], A. J. Myers[8], G. Myers[108], M. Myska[135], B. P. Nachman[149], K. Nagai[129], K. Nagano[84], R. Nagasaka[159], J. L. Nagle[30,al], E. Nagy[104], A. M. Nairz[37], Y. Nakahama[84], K. Nakamura[84], K. Nakkalil[5], A. Nandi[63b], H. Nanjo[127], E. A. Narayanan[45], Y. Narukawa[159], I. Naryshkin[38], L. Nasella[71a,71b], S. Nasri[119b], C. Nass[25], G. Navarro[23a], A. Nayaz[19], P. Y. Nechaeva[38], S. Nechaeva[24a,24b], F. Nechansky[134], L. Nedic[129], T. J. Neep[21], A. Negri[73a,73b], M. Negrini[24b], C. Nellist[117], C. Nelson[106], K. Nelson[108], S. Nemecek[134], M. Nessi[37,g], M. S. Neubauer[168], J. Newell[94], P. R. Newman[21], Y. W. Y. Ng[168], B. Ngair[119a], H. D. N. Nguyen[110], J. D. Nichols[123], R. B. Nickerson[129], R. Nicolaidou[138], J. Nielsen[139], M. Niemeyer[55], J. Niermann[37], N. Nikiforou[37], V. Nikolaenko[38,a], I. Nikolic-Audit[130], P. Nilsson[30], I. Ninca[48], G. Ninio[157], A. Nisati[75a], R. Nisius[112], N. Nitika[175], E. K. Nkadimeng[34b], T. Nobe[159], D. Noll[149], T. Nommensen[153], M. B. Norfolk[145], B. J. Norman[35], L. C. Nosler[18a], M. Noury[36a], J. Novak[95], T. Novak[95], R. Novotny[135], L. Nozka[125], K. Ntekas[165], D. Ntounis[149], N. M. J. Nunes De Moura Junior[83b], J. Ocariz[130], I. Ochoa[133a], S. Oerdek[48,y], J. T. Offermann[40], A. Ogrodnik[88], A. Oh[103], C. C. Ohm[150], H. Oide[84], M. L. Ojeda[37], Y. Okumura[159], L. F. Oleiro Seabra[133a], I. Oleksiyuk[56], G. Oliveira Correa[13], D. Oliveira Damazio[30], J. L. Oliver[1], R. Omar[68], Ö. O. Öncel[54], A. P. O'Neill[20], Y. Onoda[141], A. Onofre[133a,133e,e], P. U. E. Onyisi[11], M. J. Oreglia[40], D. Orestano[77a,77b], R. Orlandini[77a,77b], R. S. Orr[161], L. M. Osojnak[42], Y. Osumi[113], G. Otero y Garzon[31], H. Otono[90], M. Ouchrif[36d], F. Ould-Saada[128], T. Ovsiannikova[142], M. Owen[59], R. E. Owen[137], V. E. Ozcan[22a], F. Ozturk[88], N. Ozturk[8], S. Ozturk[82], H. A. Pacey[129], K. Pachal[162a], A. Pacheco Pages[13], C. Padilla Aranda[13], G. Padovano[75a,75b], S. Pagan Griso[18a], J. Pampel[25], J. Pan[178], D. K. Panchal[11], C. E. Pandini[60], J. G. Panduro Vazquez[137], H. D. Pandya[1], H. Pang[138], P. Pani[48], G. Panizzo[69a,69c], L. Panwar[130], L. Paolozzi[56], S. Parajuli[168], A. Paramonov[6], C. Paraskevopoulos[53], D. Paredes Hernandez[64b], S. R. Paredes Saenz[52], A. Pareti[73a,73b], K. R. Park[42], T. H. Park[112], F. Parodi[57a,57b], J. A. Parsons[42], U. Parzefall[54], B. Pascual Dias[41], L. Pascual Dominguez[101], E. Pasqualucci[75a], S. Passaggio[57b], F. Pastore[97], P. Patel[88], U. M. Patel[51], J. R. Pater[103], T. Pauly[37], F. Pauwels[136], C. I. Pazos[164], M. Pedersen[128], R. Pedro[133a], S. V. Peleganchuk[38], O. Penc[134], S. Peng[15], G. D. Penn[178], K. E. Penski[111], M. Penzin[38], B. S. Peralva[83d], A. P. Pereira Peixoto[142], L. Pereira Sanchez[149], D. V. Perepelitsa[30,al], G. Perera[105], E. Perez Codina[37], M. Perganti[10], H. Pernegger[37], S. Perrella[75a,75b], K. Peters[48], R. F. Y. Peters[103], B. A. Petersen[37], T. C. Petersen[43], E. Petit[104], V. Petousis[135], A. R. Petri[71a,71b], C. Petridou[158,d], T. Petru[136], M. Pettee[18a], A. Petukhov[82], K. Petukhova[37], R. Pezoa[140g], L. Pezzotti[24a,24b], G. Pezzullo[178], L. Pfaffenbichler[37], A. J. Pfleger[79], T. M. Pham[176], T. Pham[107], P. W. Phillips[137], G. Piacquadio[151],

E. Pianori[18a], F. Piazza[126], R. Piegaia[31], D. Pietreanu[28b], A. D. Pilkington[103], M. Pinamonti[69a,69c], J. L. Pinfold[2], G. Pinheiro Matos[42], B. C. Pinheiro Pereira[133a], J. Pinol Bel[13], A. E. Pinto Pinoargote[130], L. Pintucci[69a,69c], K. M. Piper[152], A. Pirttikoski[56], D. A. Pizzi[35], L. Pizzimento[64b], A. Plebani[33], M.-A. Pleier[30], V. Pleskot[136], E. Plotnikova[39], G. Poddar[96], R. Poettgen[100], L. Poggioli[130], S. Polacek[136], G. Polesello[73a], A. Poley[148], A. Polini[24b], C. S. Pollard[173], Z. B. Pollock[122], E. Pompa Pacchi[123], N. I. Pond[98], D. Ponomarenko[68], L. Pontecorvo[37], S. Popa[28a], G. A. Popeneciu[28d], A. Poreba[37], D. M. Portillo Quintero[162a], S. Pospisil[135], M. A. Postill[145], P. Postolache[28c], K. Potamianos[173], P. A. Potepa[87a], I. N. Potrap[39], C. J. Potter[33], H. Potti[153], J. Poveda[169], M. E. Pozo Astigarraga[37], R. Pozzi[37], A. Prades Ibanez[76a,76b], S. R. Pradhan[145], J. Pretel[171], D. Price[103], M. Primavera[70a], L. Primomo[69a,69c], M. A. Principe Martin[101], R. Privara[125], T. Procter[87b], M. L. Proffitt[142], N. Proklova[131], K. Prokofiev[64c], G. Proto[112], J. Proudfoot[6], M. Przybycien[87a], W. W. Przygoda[87b], A. Psallidas[46], J. E. Puddefoot[145], D. Pudzha[53], H. I. Purnell[1], D. Pyatiizbyantseva[116], J. Qian[108], R. Qian[109], D. Qichen[129], Y. Qin[13], T. Qiu[52], A. Quadt[55], M. Queitsch-Maitland[103], G. Quetant[56], R. P. Quinn[170], G. Rabanal Bolanos[61], D. Rafanoharana[112], F. Raffaeli[76a,76b], F. Ragusa[71a,71b], J. L. Rainbolt[40], S. Rajagopalan[30], E. Ramakoti[39], L. Rambelli[57a,57b], I. A. Ramirez-Berend[35], K. Ran[108,114c], D. S. Rankin[131], N. P. Rapheeha[34j], H. Rasheed[28b], A. Rastogi[18a], S. Rave[102], S. Ravera[57a,57b], B. Ravina[37], I. Ravinovich[175], M. Raymond[37], A. L. Read[128], N. P. Readioff[145], D. M. Rebuzzi[73a,73b], A. S. Reed[59], K. Reeves[27], D. Reikher[37], A. Rej[49], C. Rembser[37], H. Ren[62], M. Renda[28b], F. Renner[48], A. G. Rennie[59], M. Repik[56], A. L. Rescia[57a,57b], S. Resconi[71a], M. Ressegotti[57a,57b], S. Rettie[117], W. F. Rettie[35], M. M. Revering[33], E. Reynolds[18a], O. L. Rezanova[39], P. Reznicek[136], H. Riani[36d], N. Ribaric[51], B. Ricci[69a,69c], E. Ricci[78a,78b], R. Richter[112], S. Richter[47a,47b], E. Richter-Was[87b], M. Ridel[130], S. Ridouani[36d], P. Rieck[120], P. Riedler[37], E. M. Riefel[47a,47b], J. O. Rieger[117], M. Rijssenbeek[151], M. Rimoldi[37], L. Rinaldi[24a,24b], P. Rincke[55,167], G. Ripellino[167], I. Riu[13], J. C. Rivera Vergara[171], F. Rizatdinova[124], E. Rizvi[96], B. R. Roberts[18a], S. S. Roberts[139], D. Robinson[33], A. Robson[59], A. Rocchi[76a,76b], C. Roda[74a,74b], F. A. Rodriguez[118], S. Rodriguez Bosca[37], Y. Rodriguez Garcia[23a], A. M. Rodríguez Vera[118], S. Roe[37], J. T. Roemer[37], O. Røhne[128], R. A. Rojas[37], C. P. A. Roland[130], A. Romaniouk[79], E. Romano[73a,73b], M. Romano[24b], A. C. Romero Hernandez[168], N. Rompotis[94], L. Roos[130], S. Rosati[75a], B. J. Rosser[40], E. Rossi[129], E. Rossi[72a,72b], L. P. Rossi[61], L. Rossini[54], R. Rosten[122], M. Rotaru[28b], R. Roth[37], D. Rousseau[66], D. Rousso[48], S. Roy-Garand[161], A. Rozanov[104], Z. M. A. Rozario[59], Y. Rozen[156], A. Rubio Jimenez[169], V. H. Ruelas Rivera[19], T. A. Ruggeri[1], A. Ruggiero[129], A. Ruiz-Martinez[169], A. Rummler[37], G. B. Rupnik Boero[37], Z. Rurikova[54], N. A. Rusakovich[39], S. Ruscelli[49], H. L. Russell[171], G. Russo[75a,75b], J. P. Rutherfoord[7], S. Rutherford Colmenares[33], M. Rybar[136], P. Rybczynski[87a], A. Ryzhov[45], J. A. Sabater Iglesias[56], H.F-W. Sadrozinski[139], F. Safai Tehrani[75a], S. Saha[1], M. Sahinsoy[82], B. Sahoo[175], A. Saibel[169], B. T. Saifuddin[123], M. Saimpert[138], G. T. Saito[83c], M. Saito[159], T. Saito[159], A. Sala[71a,71b], A. Salnikov[149], J. Salt[169], A. Salvador Salas[157], F. Salvatore[152], A. Salzburger[37], D. Sammel[54], E. Sampson[93], D. Sampsonidis[158,d], D. Sampsonidou[126], M. A. A. Samy[59], J. Sánchez[169], V. Sanchez Sebastian[169], H. Sandaker[128], C. O. Sander[48], J. A. Sandesara[176], M. Sandhoff[177], C. Sandoval[23b], L. Sanfilippo[63a], D. P. C. Sankey[137], T. Sano[89], A. Sansoni[53], M. Santana Queiroz[18b], L. Santi[37], C. Santoni[41], H. Santos[133a,133b], A. Santra[175], E. Sanzani[24a,24b], K. A. Saoucha[85b], J. G. Saraiva[133a,133d], J. Sardain[7], O. Sasaki[84], K. Sato[163], C. Sauer[37], E. Sauvan[4], P. Savard[161,ai], R. Sawada[159], C. Sawyer[137], L. Sawyer[99], A. M. Sayed[27], C. Sbarra[24b], A. Sbrizzi[24a,24b], T. Scanlon[98], J. Schaarschmidt[142], U. Schäfer[102], A. C. Schaffer[45,66], D. Schaile[111], R. D. Schamberger[151], C. Scharf[19], M. M. Schefer[20], V. A. Schegelsky[38], D. Scheirich[136], M. Schernau[140f], C. Scheulen[56], C. Schiavi[57a,57b], M. Schioppa[44a,44b], B. Schlag[149], S. Schlenker[37], J. Schmeing[177], E. Schmidt[112], M. A. Schmidt[177], K. Schmieden[25], C. Schmitt[102], N. Schmitt[102], S. Schmitt[48], N. A. Schneider[111], L. Schoeffel[138], A. Schoening[63b], P. G. Scholer[35], E. Schopf[147], M. Schott[25], S. Schramm[56], T. Schroer[56], H-C. Schultz-Coulon[63a], M. Schumacher[54], B. A. Schumm[139], Ph. Schune[138], H. R. Schwartz[7], A. Schwartzman[149], T. A. Schwarz[108], Ph. Schwemling[138], R. Schwienhorst[109], F. G. Sciacca[20], A. Sciandra[30], G. Sciolla[27], F. Scuri[74a], C. D. Sebastiani[37], K. Sedlaczek[118], S. C. Seidel[115], A. Seiden[139], B. D. Seidlitz[42], C. Seitz[48], J. M. Seixas[83b], G. Sekhniaidze[72a], L. Selem[60], N. Semprini-Cesari[24a,24b], A. Semushin[179], D. Sengupta[56], V. Senthilkumar[169], L. Serin[66], M. Sessa[72a,72b], H. Severini[123], F. Sforza[57a,57b], A. Sfyrla[56], Q. Sha[14], H. Shaddix[118], A. H. Shah[33], R. Shaheen[150], J. D. Shahinian[131], M. Shamim[37], L. Y. Shan[14], M. Shapiro[18a], A. Sharma[37], A. S. Sharma[170], P. Sharma[30], P. B. Shatalov[38], K. Shaw[152], S. M. Shaw[103],

Q. Shen[14], D. J. Sheppard[148], P. Sherwood[98], L. Shi[98], X. Shi[14], S. Shimizu[84], I. P. J. Shipsey[129,*], S. Shirabe[90], M. Shiyakova[39,z], M. J. Shochet[40], D. R. Shope[128], B. Shrestha[123], S. Shrestha[122,an], I. Shreyber[39], M. J. Shroff[171], P. Sicho[134], A. M. Sickles[168], E. Sideras Haddad[34j,166], A. C. Sidley[117], A. Sidoti[24b], F. Siegert[50], Dj. Sijacki[16], F. Sili[62], J. M. Silva[52], I. Silva Ferreira[83b], M. V. Silva Oliveira[30], S. B. Silverstein[47a], S. Simion[66], R. Simoniello[37], E. L. Simpson[103], H. Simpson[152], L. R. Simpson[6], S. Simsek[82], S. Sindhu[55], P. Sinervo[161], S. N. Singh[27], S. Singh[30], S. Sinha[48], S. Sinha[103], M. Sioli[24b,24a], K. Sioulas[9], I. Siral[37], E. Sitnikova[48], J. Sjölin[47a,47b], A. Skaf[55], E. Skorda[21], P. Skubic[123], M. Slawinska[88], I. Slazyk[17], I. Sliusar[128], V. Smakhtin[175], B. H. Smart[137], S.Yu. Smirnov[140b], Y. Smirnov[82], L. N. Smirnova[38,a], O. Smirnova[100], A. C. Smith[42], D. R. Smith[165], J. L. Smith[103], M. B. Smith[35], R. Smith[149], H. Smitmanns[102], M. Smizanska[93], K. Smolek[135], P. Smolyanskiy[135], A. A. Snesarev[39], H. L. Snoek[117], S. Snyder[30], R. Sobie[171,ab], A. Soffer[157], C. A. Solans Sanchez[37], E.Yu. Soldatov[39], U. Soldevila[169], A. A. Solodkov[34j], S. Solomon[27], A. Soloshenko[39], K. Solovieva[54], O. V. Solovyanov[41], P. Sommer[50], A. Sonay[13], A. Sopczak[135], A. L. Sopio[52], F. Sopkova[29b], J. D. Sorenson[115], I. R. Sotarriva Alvarez[141], V. Sothilingam[63a], O. J. Soto Sandoval[140c,140b], S. Sottocornola[68], R. Soualah[85a], Z. Soumaimi[36e], D. South[48], N. Soybelman[175], S. Spagnolo[70a,70b], M. Spalla[112], D. Sperlich[54], B. Spisso[72a,72b], D. P. Spiteri[59], L. Splendori[104], M. Spousta[136], E. J. Staats[35], R. Stamen[63a], E. Stanecka[88], W. Stanek-Maslouska[48], M. V. Stange[50], B. Stanislaus[18a], M. M. Stanitzki[48], E. A. Starchenko[38], G. H. Stark[139], J. Stark[91], P. Staroba[134], P. Starovoitov[85b], R. Staszewski[88], C. Stauch[111], G. Stavropoulos[46], A. Steffl[37], A. Stein[102], P. Steinberg[30], B. Stelzer[148,162a], H. J. Stelzer[132], O. Stelzer[162a], H. Stenzel[58], T. J. Stevenson[152], G. A. Stewart[37], J. R. Stewart[124], G. Stoicea[28b], M. Stolarski[133a], S. Stonjek[112], A. Straessner[50], J. Strandberg[150], S. Strandberg[47a,47b], M. Stratmann[177], M. Strauss[123], T. Strebler[104], P. Strizenec[29b], R. Ströhmer[172], D. M. Strom[126], R. Stroynowski[45], A. Strubig[47a,47b], S. A. Stucci[30], B. Stugu[17], J. Stupak[123], N. A. Styles[48], D. Su[149], S. Su[62], X. Su[62], D. Suchy[29a], A. D. Sudhakar Ponnu[55], K. Sugizaki[131], V. V. Sulin[38], D. M. S. Sultan[129], L. Sultanaliyeva[25], S. Sultansoy[3b], S. Sun[176], W. Sun[14], N. Sur[100], M. R. Sutton[152], M. Svatos[134], P. N. Swallow[33], M. Swiatlowski[162a], A. Swoboda[37], I. Sykora[29a], M. Sykora[136], T. Sykora[136], D. Ta[102], K. Tackmann[48,y], A. Taffard[165], R. Tafirout[162a], Y. Takubo[84], M. Talby[104], A. A. Talyshev[38], K. C. Tam[64b], N. M. Tamir[157], A. Tanaka[159], J. Tanaka[159], R. Tanaka[66], M. Tanasini[151], Z. Tao[170], S. Tapia Araya[140g], S. Tapprogge[102], A. Tarek Abouelfadl Mohamed[37], S. Tarem[156], K. Tariq[14], G. Tarna[37], G. F. Tartarelli[71a], M. J. Tartarin[91], P. Tas[136], M. Tasevsky[134], E. Tassi[44b,44a], A. C. Tate[168], Y. Tayalati[36e,aa], G. N. Taylor[107], W. Taylor[162b], R. J. Taylor Vara[169], A. S. Tegetmeier[91], P. Teixeira-Dias[97], J. J. Teoh[161], K. Terashi[159], J. Terron[101], S. Terzo[13], M. Testa[53], R. J. Teuscher[161,ab], A. Thaler[79], O. Theiner[56], T. Theveneaux-Pelzer[104], D. W. Thomas[97], J. P. Thomas[21], E. A. Thompson[18a], P. D. Thompson[21], E. Thomson[131], R. E. Thornberry[45], C. Tian[62], Y. Tian[56], V. Tikhomirov[82], Yu.A. Tikhonov[39], S. Timoshenko[38], D. Timoshyn[136], E. X. L. Ting[1], P. Tipton[178], A. Tishelman-Charny[30], K. Todome[141], S. Todorova-Nova[136], L. Toffolin[69a,69c], M. Togawa[84], J. Tojo[90], S. Tokár[29a], O. Toldaiev[68], G. Tolkachev[104], M. Tomoto[84], L. Tompkins[149,n], E. Torrence[126], H. Torres[91], D. I. Torres Arza[140g], E. Torró Pastor[169], M. Toscani[31], C. Tosciri[40], M. Tost[11], D. R. Tovey[145], T. Trefzger[172], P. M. Tricarico[13], A. Tricoli[30], I. M. Trigger[162a], S. Trincaz-Duvoid[130], D. A. Trischuk[171], A. Tropina[39], D. Truncali[76a,76b], L. Truong[34c], M. Trzebinski[88], A. Trzupek[88], F. Tsai[151], M. Tsai[108], A. Tsiamis[158], P. V. Tsiareshka[39], S. Tsigaridas[162a], A. Tsirigotis[158,u], V. Tsiskaridze[155a], E. G. Tskhadadze[155a], Y. Tsujikawa[89], I. I. Tsukerman[38], V. Tsulaia[18a], S. Tsuno[84], K. Tsuri[121], D. Tsybychev[151], Y. Tu[64b], A. Tudorache[28b], V. Tudorache[28b], S. B. Tuncay[129], S. Turchikhin[57a,57b], I. Turk Cakir[3a], R. Turra[71a], T. Turtuvshin[39,ac], P. M. Tuts[42], S. Tzamarias[158,d], Y. Uematsu[84], F. Ukegawa[163], P. A. Ulloa Poblete[140c,140b], E. N. Umaka[30], G. Unal[37], A. Undrus[30], G. Unel[165], J. Urban[29b], P. Urrejola[140e], G. Usai[8], R. Ushioda[160], M. Usman[110], F. Ustuner[52], Z. Uysal[82], V. Vacek[135], B. Vachon[106], T. Vafeiadis[37], A. Vaitkus[98], C. Valderanis[111], E. Valdes Santurio[47a,47b], M. Valente[37], S. Valentinetti[24b,24a], A. Valero[169], E. Valiente Moreno[169], A. Vallier[91], J. A. Valls Ferrer[169], D. R. Van Arneman[117], A. Van Der Graaf[49], H. Z. Van Der Schyf[34j], P. Van Gemmeren[6], M. Van Rijnbach[37], S. Van Stroud[98], I. Van Vulpen[117], P. Vana[136], M. Vanadia[76a,76b], U. M. Vande Voorde[150], W. Vandelli[37], E. R. Vandewall[149], D. Vannicola[157], L. Vannoli[53], R. Vari[75a], M. Varma[178], E. W. Varnes[7], C. Varni[118], D. Varouchas[66], L. Varriale[169], K. E. Varvell[153], M. E. Vasile[28b], L. Vaslin[84], M. D. Vassilev[149], A. Vasyukov[39], L. M. Vaughan[124], R. Vavricka[136], T. Vazquez Schroeder[13], J. Veatch[32], V. Vecchio[103], M. J. Veen[105], I. Veliscek[30], I. Velkovska[95], L. M. Veloce[161], F. Veloso[133a,133c], A. G. Veltman[52], S. Veneziano[75a], A. Ventura[70a,70b], A. Verbytskyi[112],

M. Verducci[74a,74b], C. Vergis[96], M. Verissimo De Araujo[83b], W. Verkerke[117], J. C. Vermeulen[117], C. Vernieri[149], M. Vessella[165], M. C. Vetterli[148,ai], A. Vgenopoulos[102], N. Viaux Maira[140g,af], T. Vickey[145], O. E. Vickey Boeriu[145], G. H. A. Viehhauser[129], L. Vigani[63b], M. Vigl[112], M. Villa[24a,24b], M. Villaplana Perez[169], E. M. Villhauer[40], E. Vilucchi[53], M. Vincent[169], M. G. Vincter[35], A. Visibile[117], A. Visive[117], C. Vittori[37], I. Vivarelli[24b,24a], M. I. Vivas Albornoz[48], E. Voevodina[112], F. Vogel[111], J. C. Voigt[50], P. Vokac[135], Yu. Volkotrub[87b], L. Vomberg[25], E. Von Toerne[25], B. Vormwald[37], K. Vorobev[51], M. Vos[169], K. Voss[147], M. Vozak[37], L. Vozdecky[123], N. Vranjes[16], M. Vranjes Milosavljevic[16], M. Vreeswijk[117], N. K. Vu[144b,144a], R. Vuillermet[37], O. Vujinovic[102], I. Vukotic[40], I. K. Vyas[35], J. F. Wack[33], S. Wada[163], C. Wagner[149], J. M. Wagner[18a], W. Wagner[177], S. Wahdan[177], H. Wahlberg[92], C. H. Waits[123], J. Walder[137], R. Walker[111], K. Walkingshaw Pass[59], W. Walkowiak[147], A. Wall[131], E. J. Wallin[100], T. Wamorkar[18a], K. Wandall-Christensen[169], A. Wang[62], A. Z. Wang[139], C. Wang[102], C. Wang[11], H. Wang[18a], J. Wang[64c], P. Wang[103], P. Wang[98], R. Wang[61], R. Wang[6], S. M. Wang[154], S. Wang[14], T. Wang[116], T. Wang[62], W. T. Wang[129], W. Wang[14], X. Wang[168], X. Wang[144a], X. Wang[48], Y. Wang[151], Y. Wang[62], Z. Wang[108], Z. Wang[144b], Z. Wang[108], C. Wanotayaroj[84], A. Warburton[106], A. L. Warnerbring[147], S. Waterhouse[97], A. T. Watson[21], H. Watson[52], M. F. Watson[21], E. Watton[37], G. Watts[142], B. M. Waugh[98], J. M. Webb[54], C. Weber[30], H. A. Weber[19], M. S. Weber[20], S. M. Weber[63a], C. Wei[62], Y. Wei[54], A. R. Weidberg[129], E. J. Weik[120], J. Weingarten[49], C. Weiser[54], C. J. Wells[48], T. Wenaus[30], T. Wengler[37], N. S. Wenke[112], N. Wermes[25], M. Wessels[63a], A. M. Wharton[93], A. S. White[61], A. White[8], M. J. White[1], D. Whiteson[165], L. Wickremasinghe[127], W. Wiedenmann[176], M. Wielers[137], R. Wierda[150], C. Wiglesworth[43], H. G. Wilkens[37], J. J. H. Wilkinson[33], D. M. Williams[42], H. H. Williams[131], S. Williams[33], S. Willocq[105], B. J. Wilson[103], D. J. Wilson[103], P. J. Windischhofer[40], F. I. Winkel[31], F. Winklmeier[126], B. T. Winter[54], M. Wittgen[149], M. Wobisch[99], T. Wojtkowski[60], Z. Wolffs[117], J. Wollrath[37], M. W. Wolter[88], H. Wolters[133a,133c], M. C. Wong[139], E. L. Woodward[42], S. D. Worm[48], B. K. Wosiek[88], K. W. Woźniak[88], S. Wozniewski[55], K. Wraight[59], C. Wu[161], C. Wu[21], J. Wu[159], M. Wu[114b], M. Wu[116], S. L. Wu[176], S. Wu[14,ak], X. Wu[62], Y. Q. Wu[161], Y. Wu[62], Z. Wu[4], Z. Wu[114a], J. Wuerzinger[112], T. R. Wyatt[103], B. M. Wynne[52], S. Xella[43], L. Xia[114a], M. Xie[62], A. Xiong[126], D. Xu[14], H. Xu[62], L. Xu[62], R. Xu[131], T. Xu[108], Y. Xu[142], Z. Xu[52], R. Xue[132], B. Yabsley[153], S. Yacoob[34a], Y. Yamaguchi[84], E. Yamashita[159], H. Yamauchi[163], T. Yamazaki[18a], Y. Yamazaki[86], S. Yan[59], Z. Yan[105], H. J. Yang[144a,144b], H. T. Yang[62], S. Yang[62], T. Yang[64c], X. Yang[37], X. Yang[14], Y. Yang[159], Y. Yang[62], W-M. Yao[18a], C. L. Yardley[152], J. Ye[14], S. Ye[30], X. Ye[62], Y. Yeh[98], I. Yeletskikh[39], B. Yeo[18b], M. R. Yexley[98], T. P. Yildirim[129], K. Yorita[174], C. J. S. Young[37], C. Young[149], N. D. Young[126], Y. Yu[62], J. Yuan[14,114c,ak], M. Yuan[108], R. Yuan[144b], L. Yue[98], M. Zaazoua[62], B. Zabinski[88], I. Zahir[36a], A. Zaio[57a,57b], Z. K. Zak[88], T. Zakareishvili[169], S. Zambito[56], J. A. Zamora Saa[140d], J. Zang[159], R. Zanzottera[71a,71b], O. Zaplatilek[135], C. Zeitnitz[177], H. Zeng[14], D. T. Zenger Jr[27], O. Zenin[38], T. Ženiš[29a], S. Zenz[96], D. Zerwas[66], M. Zhai[14,114c], D. F. Zhang[145], G. Zhang[14,ak], J. Zhang[143a], J. Zhang[6], L. Zhang[62], L. Zhang[114a], P. Zhang[14,114c], R. Zhang[114a], S. Zhang[91], T. Zhang[159], Y. Zhang[142], Y. Zhang[98], Y. Zhang[62], Y. Zhang[114a], Z. Zhang[18a], Z. Zhang[143a], Z. Zhang[66], H. Zhao[142], T. Zhao[143a], Y. Zhao[35], Z. Zhao[62], Z. Zhao[62], A. Zhemchugov[39], J. Zheng[114a], K. Zheng[168], X. Zheng[62], Z. Zheng[149], D. Zhong[168], B. Zhou[108], H. Zhou[7], N. Zhou[144a], Y. Zhou[15], Y. Zhou[114a], Y. Zhou[7], J. Zhu[108], X. Zhu[144b], Y. Zhu[144a], Y. Zhu[62], X. Zhuang[14], K. Zhukov[68], N. I. Zimine[39], J. Zinsser[63b], M. Ziolkowski[147], L. Živković[16], A. Zoccoli[24b,24a], K. Zoch[61], A. Zografos[37], T. G. Zorbas[145], O. Zormpa[46], L. Zwalinski[37]

[1] Department of Physics, University of Adelaide, Adelaide, Australia
[2] Department of Physics, University of Alberta, Edmonton, AB, Canada
[3] [(a)]Department of Physics, Ankara University, Ankara, Türkiye; [(b)]Division of Physics, TOBB University of Economics and Technology, Ankara, Türkiye
[4] LAPP, Université Savoie Mont Blanc, CNRS/IN2P3, Annecy, France
[5] APC, Université Paris Cité, CNRS/IN2P3, Paris, France
[6] High Energy Physics Division, Argonne National Laboratory, Argonne, IL, USA
[7] Department of Physics, University of Arizona, Tucson, AZ, USA
[8] Department of Physics, University of Texas at Arlington, Arlington, TX, USA
[9] Physics Department, National and Kapodistrian University of Athens, Athens, Greece
[10] Physics Department, National Technical University of Athens, Zografou, Greece

[11] Department of Physics, University of Texas at Austin, Austin, TX, USA
[12] Institute of Physics, Azerbaijan Academy of Sciences, Baku, Azerbaijan
[13] Institut de Física d'Altes Energies (IFAE), Barcelona Institute of Science and Technology, Barcelona, Spain
[14] Institute of High Energy Physics, Chinese Academy of Sciences, Beijing, China
[15] Physics Department, Tsinghua University, Beijing, China
[16] Institute of Physics, University of Belgrade, Belgrade, Serbia
[17] Department for Physics and Technology, University of Bergen, Bergen, Norway
[18] [(a)]Physics Division, Lawrence Berkeley National Laboratory, Berkeley, CA, USA; [(b)]University of California, Berkeley, CA, USA
[19] Institut für Physik, Humboldt Universität zu Berlin, Berlin, Germany
[20] Albert Einstein Center for Fundamental Physics and Laboratory for High Energy Physics, University of Bern, Bern, Switzerland
[21] School of Physics and Astronomy, University of Birmingham, Birmingham, UK
[22] [(a)]Department of Physics, Bogazici University, Istanbul, Türkiye; [(b)]Department of Physics Engineering, Gaziantep University, Gaziantep, Türkiye; [(c)]Department of Physics, Istanbul University, Istanbul, Türkiye
[23] [(a)]Facultad de Ciencias y Centro de Investigaciónes, Universidad Antonio Nariño, Bogotá, Colombia; [(b)]Departamento de Física, Universidad Nacional de Colombia, Bogotá, Colombia
[24] [(a)]Dipartimento di Fisica e Astronomia A. Righi, Università di Bologna, Bologna, Italy; [(b)]INFN Sezione di Bologna, Bologna, Italy
[25] Physikalisches Institut, Universität Bonn, Bonn, Germany
[26] Department of Physics, Boston University, Boston, MA, USA
[27] Department of Physics, Brandeis University, Waltham, MA, USA
[28] [(a)]Transilvania University of Brasov, Brasov, Romania; [(b)]Horia Hulubei National Institute of Physics and Nuclear Engineering, Bucharest, Romania; [(c)]Department of Physics, Alexandru Ioan Cuza University of Iasi, Iasi, Romania; [(d)]National Institute for Research and Development of Isotopic and Molecular Technologies, Physics Department, Cluj-Napoca, Romania; [(e)]National University of Science and Technology Politechnica, Bucharest, Romania; [(f)]West University in Timisoara, Timisoara, Romania; [(g)]Faculty of Physics, University of Bucharest, Bucharest, Romania
[29] [(a)]Faculty of Mathematics, Physics and Informatics, Comenius University, Bratislava, Slovak Republic; [(b)]Department of Subnuclear Physics, Institute of Experimental Physics of the Slovak Academy of Sciences, Kosice, Slovak Republic
[30] Physics Department, Brookhaven National Laboratory, Upton, NY, USA
[31] Universidad de Buenos Aires, Facultad de Ciencias Exactas y Naturales, Departamento de Física, y CONICET, Instituto de Física de Buenos Aires (IFIBA), Buenos Aires, Argentina
[32] California State University, CA, USA
[33] Cavendish Laboratory, University of Cambridge, Cambridge, UK
[34] [(a)]Department of Physics, University of Cape Town, Cape Town, South Africa; [(b)]iThemba Labs, Western Cape, South Africa; [(c)]Department of Mechanical Engineering Science, University of Johannesburg, Johannesburg, South Africa; [(d)]National Institute of Physics, University of the Philippines Diliman (Philippines), South Africa ; [(e)]Department of Physics, Stellenbosch University, Matieland, South Africa; [(f)]University of KwaZulu-Natal, School of Agriculture and Science, Mathematics, Westville, South Africa; [(g)]University of South Africa, Department of Physics, Pretoria, South Africa; [(h)]University of Pretoria, Department of Mechanical and Aeronautical Engineering, Pretoria, South Africa; [(i)]University of Zululand, KwaDlangezwa, South Africa; [(j)]School of Physics, University of the Witwatersrand, Johannesburg, South Africa
[35] Department of Physics, Carleton University, Ottawa, ON, Canada
[36] [(a)]Faculté des Sciences Ain Chock, Université Hassan II de Casablanca, Morocco; [(b)]Faculté des Sciences, Université Ibn-Tofail, Kénitra, Morocco; [(c)]Faculté des Sciences Semlalia, Université Cadi Ayyad, LPHEA-Marrakech, Marrakesh, Morocco; [(d)]LPMR, Faculté des Sciences, Université Mohamed Premier, Oujda, Morocco; [(e)]Faculté des sciences, Université Mohammed V, Rabat, Morocco; [(f)]Institute of Applied Physics, Mohammed VI Polytechnic University, Ben Guerir, Morocco
[37] CERN, Geneva, Switzerland
[38] Affiliated with an Institute Formerly Covered by a Cooperation Agreement with CERN, Geneva, Switzerland
[39] Affiliated with an International Laboratory Covered by a Cooperation Agreement with CERN, Geneva, Switzerland
[40] Enrico Fermi Institute, University of Chicago, Chicago, IL, USA

[41] LPC, Université Clermont Auvergne, CNRS/IN2P3, Clermont-Ferrand, France
[42] Nevis Laboratory, Columbia University, Irvington, NY, USA
[43] Niels Bohr Institute, University of Copenhagen, Copenhagen, Denmark
[44] [(a)]Dipartimento di Fisica, Università della Calabria, Rende, Italy; [(b)]INFN Gruppo Collegato di Cosenza, Laboratori Nazionali di Frascati, Frascati, Italy
[45] Physics Department, Southern Methodist University, Dallas, TX, USA
[46] National Centre for Scientific Research "Demokritos", Agia Paraskevi, Greece
[47] [(a)]Department of Physics, Stockholm University, Stockholm, Sweden; [(b)]Oskar Klein Centre, Stockholm, Sweden
[48] Deutsches Elektronen-Synchrotron DESY, Hamburg and Zeuthen, Germany
[49] Fakultät Physik, Technische Universität Dortmund, Dortmund, Germany
[50] Institut für Kern- und Teilchenphysik, Technische Universität Dresden, Dresden, Germany
[51] Department of Physics, Duke University, Durham, NC, USA
[52] SUPA - School of Physics and Astronomy, University of Edinburgh, Edinburgh, UK
[53] INFN e Laboratori Nazionali di Frascati, Frascati, Italy
[54] Physikalisches Institut, Albert-Ludwigs-Universität Freiburg, Freiburg, Germany
[55] II. Physikalisches Institut, Georg-August-Universität Göttingen, Göttingen, Germany
[56] Département de Physique Nucléaire et Corpusculaire, Université de Genève, Geneva, Switzerland
[57] [(a)]Dipartimento di Fisica, Università di Genova, Genoa, Italy; [(b)]INFN Sezione di Genova, Genoa, Italy
[58] II. Physikalisches Institut, Justus-Liebig-Universität Giessen, Giessen, Germany
[59] SUPA - School of Physics and Astronomy, University of Glasgow, Glasgow, UK
[60] LPSC, Université Grenoble Alpes, CNRS/IN2P3, Grenoble INP, Grenoble, France
[61] Laboratory for Particle Physics and Cosmology, Harvard University, Cambridge, MA, USA
[62] Department of Modern Physics and State Key Laboratory of Particle Detection and Electronics, University of Science and Technology of China, Hefei, China
[63] [(a)]Kirchhoff-Institut für Physik, Ruprecht-Karls-Universität Heidelberg, Heidelberg, Germany; [(b)]Physikalisches Institut, Ruprecht-Karls-Universität Heidelberg, Heidelberg, Germany
[64] [(a)]Department of Physics, Chinese University of Hong Kong, Shatin, N.T., Hong Kong, China; [(b)]Department of Physics, University of Hong Kong, Pok Fu Lam, Hong Kong, China; [(c)]Department of Physics and Institute for Advanced Study, Hong Kong University of Science and Technology, Clear Water Bay, Kowloon, Hong Kong, China
[65] Department of Physics, National Tsing Hua University, Hsinchu, Taiwan
[66] IJCLab, Université Paris-Saclay, CNRS/IN2P3, 91405, Orsay, France
[67] Centro Nacional de Microelectrónica (IMB-CNM-CSIC), Barcelona, Spain
[68] Department of Physics, Indiana University, Bloomington, IN, USA
[69] [(a)]INFN Gruppo Collegato di Udine, Sezione di Trieste, Udine, Italy; [(b)]ICTP, Trieste, Italy; [(c)]Dipartimento Politecnico di Ingegneria e Architettura, Università di Udine, Udine, Italy
[70] [(a)]INFN Sezione di Lecce, Lecce, Italy; [(b)]Dipartimento di Matematica e Fisica, Università del Salento, Lecce, Italy
[71] [(a)]INFN Sezione di Milano, Milan, Italy; [(b)]Dipartimento di Fisica, Università di Milano, Milan, Italy
[72] [(a)]INFN Sezione di Napoli, Naples, Italy; [(b)]Dipartimento di Fisica, Università di Napoli, Naples, Italy
[73] [(a)]INFN Sezione di Pavia, Pavia, Italy; [(b)]Dipartimento di Fisica, Università di Pavia, Pavia, Italy
[74] [(a)]INFN Sezione di Pisa, Pisa, Italy; [(b)]Dipartimento di Fisica E. Fermi, Università di Pisa, Pisa, Italy
[75] [(a)]INFN Sezione di Roma, Rome, Italy; [(b)]Dipartimento di Fisica, Sapienza Università di Roma, Rome, Italy
[76] [(a)]INFN Sezione di Roma Tor Vergata, Rome, Italy; [(b)]Dipartimento di Fisica, Università di Roma Tor Vergata, Rome, Italy
[77] [(a)]INFN Sezione di Roma Tre, Rome, Italy; [(b)]Dipartimento di Matematica e Fisica, Università Roma Tre, Rome, Italy
[78] [(a)]INFN-TIFPA, Povo, Italy; [(b)]Università degli Studi di Trento, Trento, Italy
[79] Universität Innsbruck, Department of Astro and Particle Physics, Innsbruck, Austria
[80] University of Iowa, Iowa City, IA, USA
[81] Department of Physics and Astronomy, Iowa State University, Ames, IA, USA
[82] Istinye University, Sariyer, Istanbul, Türkiye
[83] [(a)]Departamento de Engenharia Elétrica, Universidade Federal de Juiz de Fora (UFJF), Juiz de Fora, Brazil; [(b)]Universidade Federal do Rio De Janeiro COPPE/EE/IF, Rio de Janeiro, Brazil; [(c)]Instituto de Física, Universidade de São Paulo, São Paulo, Brazil; [(d)]Rio de Janeiro State University, Rio de Janeiro, Brazil; [(e)]Federal University of Bahia, Bahia, Brazil

[84] KEK, High Energy Accelerator Research Organization, Tsukuba, Japan
[85] [(a)]Khalifa University of Science and Technology, Abu Dhabi, United Arab Emirates; [(b)]University of Sharjah, Sharjah, United Arab Emirates
[86] Graduate School of Science, Kobe University, Kobe, Japan
[87] [(a)]Faculty of Physics and Applied Computer Science, AGH University of Krakow, Krakow, Poland; [(b)]Marian Smoluchowski Institute of Physics, Jagiellonian University, Krakow, Poland
[88] Institute of Nuclear Physics Polish Academy of Sciences, Krakow, Poland
[89] Faculty of Science, Kyoto University, Kyoto, Japan
[90] Research Center for Advanced Particle Physics and Department of Physics, Kyushu University, Fukuoka , Japan
[91] L2IT, Université de Toulouse, CNRS/IN2P3, UPS, Toulouse, France
[92] Instituto de Física La Plata, Universidad Nacional de La Plata and CONICET, La Plata, Argentina
[93] Physics Department, Lancaster University, Lancaster, UK
[94] Oliver Lodge Laboratory, University of Liverpool, Liverpool, UK
[95] Department of Experimental Particle Physics, Jožef Stefan Institute and Department of Physics, University of Ljubljana, Ljubljana, Slovenia
[96] Department of Physics and Astronomy, Queen Mary University of London, London, UK
[97] Department of Physics, Royal Holloway University of London, Egham, UK
[98] Department of Physics and Astronomy, University College London, London, UK
[99] Louisiana Tech University, Ruston, LA, USA
[100] Fysiska institutionen, Lunds universitet, Lund, Sweden
[101] Departamento de Física Teorica C-15 and CIAFF, Universidad Autónoma de Madrid, Madrid, Spain
[102] Institut für Physik, Universität Mainz, Mainz, Germany
[103] School of Physics and Astronomy, University of Manchester, Manchester, UK
[104] CPPM, Aix-Marseille Université, CNRS/IN2P3, Marseille, France
[105] Department of Physics, University of Massachusetts, Amherst, MA, USA
[106] Department of Physics, McGill University, Montreal, QC, Canada
[107] School of Physics, University of Melbourne, Melbourne, VIC, Australia
[108] Department of Physics, University of Michigan, Ann Arbor, MI, USA
[109] Department of Physics and Astronomy, Michigan State University, East Lansing, MI, USA
[110] Group of Particle Physics, University of Montreal, Montreal, QC, Canada
[111] Fakultät für Physik, Ludwig-Maximilians-Universität München, München, Germany
[112] Max-Planck-Institut für Physik (Werner-Heisenberg-Institut), München, Germany
[113] Graduate School of Science and Kobayashi-Maskawa Institute, Nagoya University, Nagoya, Japan
[114] [(a)]Department of Physics, Nanjing University, Nanjing, China; [(b)]School of Science, Shenzhen Campus of Sun Yat-sen University, Guangzhou, China; [(c)]University of Chinese Academy of Science (UCAS), Beijing, China
[115] Department of Physics and Astronomy, University of New Mexico, Albuquerque, NM, USA
[116] Institute for Mathematics, Astrophysics and Particle Physics, Radboud University/Nikhef, Nijmegen, The Netherlands
[117] Nikhef National Institute for Subatomic Physics and University of Amsterdam, Amsterdam, The Netherlands
[118] Department of Physics, Northern Illinois University, DeKalb, IL, USA
[119] [(a)]New York University Abu Dhabi, Abu Dhabi, United Arab Emirates; [(b)]United Arab Emirates University, Al Ain, United Arab Emirates
[120] Department of Physics, New York University, New York, NY, USA
[121] Ochanomizu University, Otsuka, Bunkyo-ku, Tokyo, Japan
[122] Ohio State University, Columbus, OH, USA
[123] Homer L. Dodge Department of Physics and Astronomy, University of Oklahoma, Norman, OK, USA
[124] Department of Physics, Oklahoma State University, Stillwater, OK, USA
[125] Palacký University, Joint Laboratory of Optics, Olomouc, Czech Republic
[126] Institute for Fundamental Science, University of Oregon, Eugene, OR, USA
[127] Graduate School of Science, University of Osaka, Osaka, Japan
[128] Department of Physics, University of Oslo, Oslo, Norway
[129] Department of Physics, Oxford University, Oxford, UK
[130] LPNHE, Sorbonne Université, Université Paris Cité, CNRS/IN2P3, Paris, France
[131] Department of Physics, University of Pennsylvania, Philadelphia, PA, USA

[132] Department of Physics and Astronomy, University of Pittsburgh, Pittsburgh, PA, USA
[133] [(a)]Laboratório de Instrumentação e Física Experimental de Partículas - LIP, Lisbon, Portugal; [(b)]Departamento de Física, Faculdade de Ciências, Universidade de Lisboa, Lisbon, Portugal; [(c)]Departamento de Física, Universidade de Coimbra, Coimbra, Portugal; [(d)]Centro de Física Nuclear da Universidade de Lisboa, Lisbon, Portugal; [(e)]Departamento de Física, Escola de Ciências, Universidade do Minho, Braga, Portugal; [(f)]Departamento de Física Teórica y del Cosmos, Universidad de Granada, Granada (Spain), Portugal; [(g)]Departamento de Física, Instituto Superior Técnico, Universidade de Lisboa, Lisbon, Portugal
[134] Institute of Physics of the Czech Academy of Sciences, Prague, Czech Republic
[135] Czech Technical University in Prague, Prague, Czech Republic
[136] Faculty of Mathematics and Physics, Charles University, Prague, Czech Republic
[137] Particle Physics Department, Rutherford Appleton Laboratory, Didcot, UK
[138] IRFU, CEA, Université Paris-Saclay, Gif-sur-Yvette, France
[139] Santa Cruz Institute for Particle Physics, University of California Santa Cruz, Santa Cruz, CA, USA
[140] [(a)]Departamento de Física, Pontificia Universidad Católica de Chile, Santiago, Chile; [(b)]Millennium Institute for Subatomic physics at high energy frontier (SAPHIR), Santiago, Chile; [(c)]Instituto de Investigación Multidisciplinario en Ciencia y Tecnología y Departamento de Física, Universidad de La Serena, La Serena, Chile; [(d)]Universidad Andres Bello, Department of Physics, Santiago, Chile; [(e)]Universidad San Sebastian, Recoleta, Chile; [(f)]Instituto de Alta Investigación, Universidad de Tarapacá, Arica, Chile; [(g)]Departamento de Física, Universidad Técnica Federico Santa María, Valparaíso, Chile
[141] Department of Physics, Institute of Science, Tokyo, Japan
[142] Department of Physics, University of Washington, Seattle, WA, USA
[143] [(a)]Institute of Frontier and Interdisciplinary Science and Key Laboratory of Particle Physics and Particle Irradiation (MOE), Shandong University, Qingdao, China; [(b)]School of Physics, Zhengzhou University, Zhengzhou, China
[144] [(a)]State Key Laboratory of Dark Matter Physics, School of Physics and Astronomy, Shanghai Jiao Tong University, Key Laboratory for Particle Astrophysics and Cosmology (MOE), SKLPPC, Shanghai, China; [(b)]State Key Laboratory of Dark Matter Physics, Tsung-Dao Lee Institute, Shanghai Jiao Tong University, Shanghai, China
[145] Department of Physics and Astronomy, University of Sheffield, Sheffield, UK
[146] Department of Physics, Shinshu University, Nagano, Japan
[147] Department Physik, Universität Siegen, Siegen, Germany
[148] Department of Physics, Simon Fraser University, Burnaby, BC, Canada
[149] SLAC National Accelerator Laboratory, Stanford, CA, USA
[150] Department of Physics, Royal Institute of Technology, Stockholm, Sweden
[151] Departments of Physics and Astronomy, Stony Brook University, Stony Brook, NY, USA
[152] Department of Physics and Astronomy, University of Sussex, Brighton, UK
[153] School of Physics, University of Sydney, Sydney, Australia
[154] Institute of Physics, Academia Sinica, Taipei, Taiwan
[155] [(a)]E. Andronikashvili Institute of Physics, Iv. Javakhishvili Tbilisi State University, Tbilisi, Georgia; [(b)]High Energy Physics Institute, Tbilisi State University, Tbilisi, Georgia; [(c)]University of Georgia, Tbilisi, Georgia
[156] Department of Physics, Technion, Israel Institute of Technology, Haifa, Israel
[157] Raymond and Beverly Sackler School of Physics and Astronomy, Tel Aviv University, Tel Aviv, Israel
[158] Department of Physics, Aristotle University of Thessaloniki, Thessaloniki, Greece
[159] International Center for Elementary Particle Physics and Department of Physics, University of Tokyo, Tokyo, Japan
[160] Graduate School of Science and Technology, Tokyo Metropolitan University, Tokyo, Japan
[161] Department of Physics, University of Toronto, Toronto, ON, Canada
[162] [(a)]TRIUMF, Vancouver, BC, Canada; [(b)]Department of Physics and Astronomy, York University, Toronto, ON, Canada
[163] Division of Physics and Tomonaga Center for the History of the Universe, Faculty of Pure and Applied Sciences, University of Tsukuba, Tsukuba, Japan
[164] Department of Physics and Astronomy, Tufts University, Medford, MA, USA
[165] Department of Physics and Astronomy, University of California Irvine, Irvine, CA, USA
[166] University of West Attica, Athens, Greece
[167] Department of Physics and Astronomy, University of Uppsala, Uppsala, Sweden
[168] Department of Physics, University of Illinois, Urbana, IL, USA
[169] Instituto de Física Corpuscular (IFIC), Centro Mixto Universidad de Valencia - CSIC, Valencia, Spain

[170] Department of Physics, University of British Columbia, Vancouver, BC, Canada
[171] Department of Physics and Astronomy, University of Victoria, Victoria, BC, Canada
[172] Fakultät für Physik und Astronomie, Julius-Maximilians-Universität Würzburg, Würzburg, Germany
[173] Department of Physics, University of Warwick, Coventry, UK
[174] Waseda University, Tokyo, Japan
[175] Department of Particle Physics and Astrophysics, Weizmann Institute of Science, Rehovot, Israel
[176] Department of Physics, University of Wisconsin, Madison, WI, USA
[177] Fakultät für Mathematik und Naturwissenschaften, Fachgruppe Physik, Bergische Universität Wuppertal, Wuppertal, Germany
[178] Department of Physics, Yale University, New Haven, CT, USA
[179] Yerevan Physics Institute, Yerevan, Armenia

[a] Also at Affiliated with an Institute Formerly Covered by a Cooperation Agreement with CERN, Geneva, Switzerland
[b] Also at An-Najah National University, Nablus, Palestine
[c] Also at Borough of Manhattan Community College, City University of New York, New York, NY, USA
[d] Also at Center for Interdisciplinary Research and Innovation (CIRI-AUTH), Thessaloniki, Greece
[e] Also at Centre of Physics of the Universities of Minho and Porto (CF-UM-UP), Braga, Portugal
[f] Also at CERN, Geneva, Switzerland
[g] Also at Département de Physique Nucléaire et Corpusculaire, Université de Genève, Geneva, Switzerland
[h] Also at Departament de Fisica de la Universitat Autonoma de Barcelona, Barcelona, Spain
[i] Also at Department of Financial and Management Engineering, University of the Aegean, Chios, Greece
[j] Also at Department of Mathematical Sciences, University of South Africa, Johannesburg, South Africa
[k] Also at Department of Modern Physics and State Key Laboratory of Particle Detection and Electronics, University of Science and Technology of China, Hefei, China
[l] Also at Department of Physics, Bolu Abant Izzet Baysal University, Bolu, Türkiye
[m] Also at Department of Physics, King's College London, London, UK
[n] Also at Department of Physics, Stanford University, Stanford, CA, USA
[o] Also at Department of Physics, Stellenbosch University, Stellenbosch, South Africa
[p] Also at Department of Physics, University of Fribourg, Fribourg, Switzerland
[q] Also at Department of Physics, University of Thessaly, Volos, Greece
[r] Also at Department of Physics, Westmont College, Santa Barbara, USA
[s] Also at Faculty of Physics, Sofia University, 'St. Kliment Ohridski', Sofia, Bulgaria
[t] Also at Faculty of Physics, University of Bucharest, Bucharest, Romania
[u] Also at Hellenic Open University, Patras, Greece
[v] Also at Henan University, Kaifeng, China
[w] Also at Imam Mohammad Ibn Saud Islamic University, Riyadh, Saudi Arabia
[x] Also at Institucio Catalana de Recerca i Estudis Avancats, ICREA, Barcelona, Spain
[y] Also at Institut für Experimentalphysik, Universität Hamburg, Hamburg, Germany
[z] Also at Institute for Nuclear Research and Nuclear Energy (INRNE) of the Bulgarian Academy of Sciences, Sofia, Bulgaria
[aa] Also at Institute of Applied Physics, Mohammed VI Polytechnic University, Ben Guerir, Morocco
[ab] Also at Institute of Particle Physics (IPP), Canada
[ac] Also at Institute of Physics and Technology, Mongolian Academy of Sciences, Ulaanbaatar, Mongolia
[ad] Also at Institute of Physics, Azerbaijan Academy of Sciences, Baku, Azerbaijan
[ae] Also at Institute of Theoretical Physics, Ilia State University, Tbilisi, Georgia
[af] Also at Millennium Institute for Subatomic physics at high energy frontier (SAPHIR), Santiago, Chile
[ag] Also at National Institute of Physics, University of the Philippines Diliman (Philippines), Quezon City, Philippines
[ah] Also at The Collaborative Innovation Center of Quantum Matter (CICQM), Beijing, China
[ai] Also at TRIUMF, Vancouver, BC, Canada
[aj] Also at Università di Napoli Parthenope, Naples, Italy
[ak] Also at University of Chinese Academy of Sciences (UCAS), Beijing, China
[al] Also at University of Colorado Boulder, Department of Physics, Colorado, USA
[am] Also at University of Siena, Siena, Italy

[an] Also at Washington College, Chestertown, MD, USA
[ao] Also at Yeditepe University, Physics Department, Istanbul, Türkiye
*Deceased